DESIGN OF ADVANCED REVERSE OSMOSIS AND NANOFILTRATION MEMBRANES FOR WATER PURIFICATION

BY

CHAOYI BA

DISSERTATION

Submitted in partial fulfillment of the requirements
for the degree of Doctor of Philosophy in Materials Science and Engineering
in the Graduate College of the
University of Illinois at Urbana-Champaign, 2010

Urbana, Illinois

Doctoral Committee:

Professor James Economy, Chair
Professor Phillip H. Geil
Associate Professor Jian Ku Shang
Assistant Professor Jianjun Cheng

ABSTRACT

Most commercially available reverse osmosis (RO) and nanofiltration (NF) membranes are based on the thin film composite (TFC) aromatic polyamide membranes. However, they have several disadvantages including low resistance to fouling, low chemical and thermal stabilities and limited chlorine tolerance. To address these problems, advanced RO/NF membranes are being developed from polyimides for water and wastewater treatments. The following three projects have resulted from my research.

(1) Positively charged and solvent resistant NF membranes. The use of solvent resistant membranes to facilitate small molecule separations has been a long standing industry goal of the chemical and pharmaceutical industries. We developed a solvent resistant membrane by chemically cross-linking of polyimide membrane using polyethylenimine. This membrane showed excellent stability in almost all organic solvents. In addition, this membrane was positively charged due to the amine groups remaining on the surface. As a result, high efficiency (> 95%) and selectivity for multivalent heavy metal removal was achieved.

(2) Fouling resistant NF membranes. Antifouling membranes are highly desired for "all" applications because fouling will lead to higher energy demand, increase of cleaning and corresponding down time and reduced life-time of the membrane elements. For fouling prevention, we designed a new membrane system using a coating technique to modify membrane surface properties to avoid adsorption of foulants like humic acid. A layer of water-soluble polymer such as polyvinyl alcohol (PVA), polyacrylic acid (PAA), polyvinyl sulfate (PVS) or sulfonated poly(ether ether ketone) (SPEEK), was adsorbed onto the surface of a positively charged membrane. The resultant membranes have a smooth and almost neutrally charged surface which

showed better fouling resistance than both the positively charged NF membranes and commercially available negatively charged NTR-7450 membrane. In addition, these membranes showed high efficiency for removal of multivalent ions (> 95% for both cations and anions). Therefore, these antifouling surfaces can be potentially used for water softening, water desalination and wastewater treatment in a membrane bioreactor (MBR) process.

(3) Thermally stable RO membranes. Commercial RO membranes cannot be used at temperature higher than 45°C due to the use of polysulfone substrate, which often limits their applications in industries. We successfully developed polyimides as the membrane substrate for thermally stable RO membranes due to their high thermal resistance. The polyimide-based composite polyamide membranes showed desalination performance comparable to the commercial TFC membrane. However, the key advantage of the polyimide-based membrane is its high thermal stability. As the feed temperature increased from 25^{o}C to 95^{o}C, the water flux increased 5 - 6 times while the salt rejection almost kept constant. This membrane appears to provide a unique solution for hot water desalination and also a feasible way to improve the water productivity by increasing the operating temperature without any drop in salt rejection.

To my family for their love and support …

ACKNOWLEDGEMENTS

I would like to express my sincere thanks to my advisor, Professor James Economy, not only for his guidance, inspiration, support and encouragement in every stage of my Ph.D study, but also for providing me with an excellent atmosphere and giving me trust and freedom to carry out the research. His vision, optimistic attitude, enthusiasm and continual pursuing for scientific and industrial challenges have provided me with lifetime benefits. It is the experience in Professor James Economy's group that strengthens my interests in research.

I am so grateful to Prof. Philip Geil, Prof. Jianjun Cheng and Prof. Jian-Ku Shang in my thesis committee for reading my thesis in their busy schedule.

Many thanks to Economy research group members, especially Dr. Chunqing Liu, Dr. Zhongren Yue and Jim Langer, for their help and friendship inside and outside school.

I would like to specially thank Dr. David Ladner in the Department of Civil and Environmental Engineering at UIUC who cooperated with me on the antifouling work. This research would not be possible without his help.

I would like to express my gratitude to the business office personnel, Jay Menacher, Debbie Kluge, Judy Brewer, Betsy Struck, Michelle Malloch, Peggy Wells, Cindy Brya and Bryan Kieft for all their help through all these years.

I would like to thank Vania Petrova, Scott MacLaren, Rick Haasch, and Julio Soares for the training of facilities in Frederick Seitz Materials Research Laboratory.

I would also like to thank our sponsor - the WaterCAMPWS, a Science and Technology Center of Advanced Materials for the Purification of Water with Systems under the National Science Foundation agreement number CTS-0120978. In the center, I learned a lot of research in the field of water purification.

Lastly, I would like to thank my parents for their endless love, sacrifice, support, understanding and encouragement since I was born. I would like to thank my wife, Ting Liu. She was always there cheering me up and standing by my side. I would like to thank my son whose birth brings more happiness to my life. I need to thank my parents-in-law for taking care of my son during my research.

TABLE OF CONTENTS

LIST OF FIGURES

LIST OF TABLES

CHAPTER 1

INTRODUCTION

1.1 Reverse osmosis (RO) and nanofiltration (NF) membranes – materials, structure and limits

The reverse osmosis process which uses polymeric membranes to achieve selective mass transport has become the simplest and most efficient technique to desalt the seawater and brackish water [1]. The desalination performance of a RO membrane depends largely on the membrane material and the membrane structure [2]. An industrially useful RO membrane must exhibit several characteristics such as high water flux, high salt rejection, mechanical stability, tolerance to temperature variation, resistance to fouling, and low cost. So far, a number of polymer materials such as cellulose acetates [3], polyamides [4, 5, 6], crosslinked poly (furfuryl alcohol) [7] and sulfonated polyethersulfone [8] have been used to make RO membranes. Of these, the following two have been the most successful.

Cellulose acetate (CA) was the first high-performance RO membrane material discovered. A typical CA membrane exhibits a flux of 0.9 $m^3m^{-2}day^{-1}$ at 425 psi and an average NaCl rejection of 97.5% from a 2000 mg/L NaCl feed solution. The main advantage of CA is its low price and hydrophilic nature which makes it less prone to fouling. CA also has a good chlorine resistance up to 5 ppm. Thus, today, CA membranes still maintain a small fraction of the market. However, an inherent weakness of CA is that it can be eaten by microorganisms. It also slowly hydrolyzes over time and is generally not used above 35^oC [9].

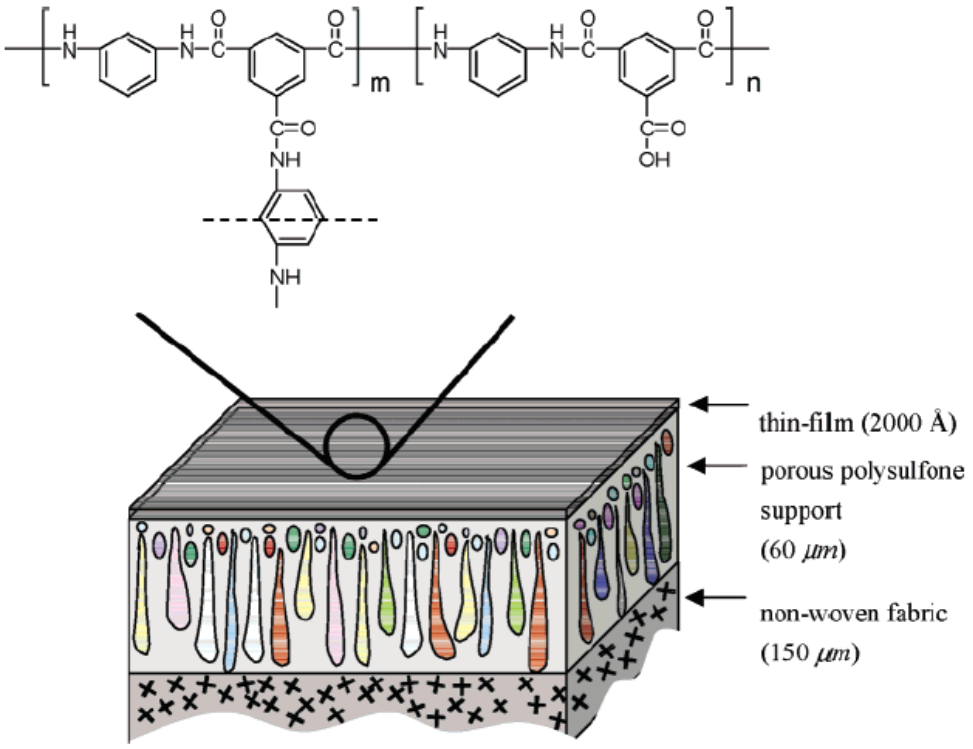

Figure 1.1 Schematic of thin-film-composite (TFC) RO membrane and the chemical structure of the aromatic polyamide thin-film layer [10].

A more successful, commercially available RO membrane for desalination is the *thin film composite (TFC) aromatic polyamide membrane*. Since it appeared around 1980, the TFC membranes have dominated the water desalination market because they show both high flux and very high salt rejection. A typical membrane exhibits a NaCl rejection of 99.5 % and a flux of 1.2 $m^3/m^2 \cdot$day for a feed solution of 35,000 mg/L NaCl at 800 psi [9]. A typical composite reverse osmosis membrane as commercially produced today is shown schematically in Figure 1.1 [10]**.** A base layer of a woven or a nonwoven fabric is overcoated with a layer of an anisotropic microporous polymer (usually polysulfone). The surface of the microporous support is coated with an ultrathin layer of a crosslinked aromatic polyamide. The porous support provides mechanical strength, whereas the separation is performed by the thin polyamide top-layer [2]. Still aromatic polyamides have several disadvantages including:

1) Low resistance to fouling. Membrane fouling (scale, silt, biofouling, organic fouling etc.) is the main cause of permeate flux decline and loss of water quality.

2) Limited oxidant tolerance due to the existence of secondary amides and electron-rich aromatic rings [11]. Chlorine is commonly used to kill bacteria in water. However, membrane selectivity is rapidly and permanently lost once exposed to feed water containing more than a few ppb levels of chlorine or hypochlorite disinfectants, which means that additional pre-treatment steps to remove chlorine must be taken before feed water is exposed to polyamide TFC membranes. Thus, today, the world is still waiting for a good composite membrane for RO and NF, which can tolerate about 20 ppm chlorine or hypochlorite.

3) Low chemical and thermal stabilities. They could hardly be used at temperature higher than 50^{o}C. They are also hardly used in non-aqueous systems because the substrate material, polysulfone, can be attacked by many organic solvents [12, 13]. It should be noted that hot wastewater from the food, chemical and petroleum processing industries are discharged directly and the energy loss is estimated at 1-2% of the total energy consumption in the US annually.

Nanofiltration (NF) has often been described as a process between ultrafiltration and reverse osmosis. Commonly, NF membranes are negatively charged so that they can efficiently reject multivalent anions such as sulfate and phosphate. The rejection to monovalent ions such as sodium chloride varies from 20% to 80% depending on the feed concentration and the material and manufacture of the membranes. NF also rejects uncharged, dissolved materials with a molecular weight cut-off (MWCO) of 200 – 1000 Dalton. The operating pressure for NF is considerably lower than the one for RO, which reduces the operating cost significantly. Industrial applications of nanofiltration are quite common in the food and dairy sector, in chemical processing,

in the pulp and paper industry, and in textiles, although the chief application continues to be in the treatment of fresh, process and waste waters. Membrane materials for NF include polyethersulfone, polyamides and cellulose derivatives. These materials, however, quickly lose their stability in contact with organic solvents. They are also subject to scaling and fouling and have low stability at high temperatures and pH extremes [2].

Therefore, the development of advanced membranes with higher thermal and chemical resistance as well as anti-fouling properties is critically required for water purification.

1.2 Membrane formation

So far, two different techniques have been adopted for the development of polymeric RO membranes, namely (i) the phase inversion method for asymmetric membranes and (ii) the interfacial polymerization technique for composite membranes [14].

Phase inversion is a process in which a polymer in solution is converted to a solid in a controlled manner. The change in phase can be initiated in a number of ways, such as solvent evaporation, thermal precipitation, immersion precipitation and vapor precipitation [15]. In this study, immersion precipitation has been used for membrane preparation and will be discussed here briefly.

In general, a polymer solution is cast as a film on a support (glass plate or non-woven fabric) with a casting knife. Then this film is immersed into a coagulation bath containing a non-solvent. Rapid exchange of solvent and non-solvent occurs with a consequently rapid phase separation and solidification at the interface. Once the skin forms, counter-diffusion of the solvent and non-solvent decreases and a highly porous, open substructure is developed.

The membrane morphology and performance are strongly influenced by the characteristics of the casting solution, such as the polymer concentration, the intrinsic viscosity and the composition. The introduction of a third component as an additive into the casting solution has been an effective way to improve the membrane performance. This additive may have several effects on the membrane formation process. For example, the viscosity of the polymer solution will be changed. Smid et al. [16] found that the minimal skin thickness of the membrane is reduced when a higher intrinsic viscosity of the polymer is used, leading to a decrease in membrane resistance and an increase in water flux through the membrane. Also, specific interactions between polymer and additive, solvent and additive, coagulant and additive, can be induced. The diffusion rate of solvent and non-solvent may be altered as well. Thus, the membrane development is mostly an empirical process and the membrane performance is usually optimized based on trial-and-error procedures.

Interfacial polymerization has been employed to prepare a thin layer of cross-linked polyamide depositing on a substrate ultrafiltration membrane. The performance of the membrane is mainly determined by the monomers used in the interfacial polymerization. Even small changes in the monomer's structure can strongly influence the membrane properties. So far, the best results were obtained using trimesoyl chloride and *m*-phenylene-diamine as monomers [2]. The membrane performance and morphology is dependent on several synthesis conditions, such as concentration of reactants, reaction time and post treatments of the resulting films [17]. Moreover, the surface roughness and pore dimension of the substrate membrane also have significant effects on the formation of the interfacial film. Generally, a smooth surface may favor the formation of a thick defect-free active layer. The resultant composite membrane will give high salt rejection and low flux. On the other

hand, a rough surface may result in a thin active layer with some defects. So the composite membrane may have higher flux with a little sacrifice of salt rejection [18, 19, 20].

1.3 Surface modification of membranes

Surface modification has commonly been used to further improve membrane performance of the prepared membranes. According to Zeman and Zydney, almost 50% of all MF and UF membranes marketed by 1996 were surface modified. However, the additive used and procedures followed in commercial membrane manufacture remain industrial secrets [21, 22]. By physical and/or chemical modification, membrane chemistry, morphology and pore structure may be altered resulting in improved selectivity and permeability. Many techniques can be used for this purpose and will be briefly summarized below.

1. Surface functionalization. Functional groups can be introduced to the membrane surface by plasma treatment or classical organic reactions like sulfonation. For example, by oxygen plasma treatment, aromatic polyamide RO membranes showed improved hydrophilicity and permeability due to the formation of carboxyl groups [23]. Similar results were observed by low-temperature H_2O or CO_2 plasma treatment of polymers such as polysulfone (PSf), polyethersulfone (PES), polyethylene (PE), polyamide (PA), poly-phenylene ether (PPE), poly(methyl methacrylate) (PMMA), etc. [24, 25, 26]. Sulfonic goups can be introduced to polymer membranes by direct reaction of cross-linked membranes based on polystyrene with concentrated sulfuric acid [27] or by blending polysulfone with sulfonated polysulfone [28]. Both water flux and salt rejection were thus increased. Polyacrylonitrile (PAN) membranes could be treated with NaOH or 3-(dimethylamino) propyl amine which correspondingly generated carboxylic or amine groups

respectively. The resultant membranes were either negatively or positively charged depending on the functional groups and their performance to various salts varied significantly [29, 30].

2. Cross-linking. Membranes are often prepared from soluble polymers by phase inversion method. Their solvent resistance is usually low and can be improved by cross-linking. Several strategies have been reported in the literature including reaction with di- or tri-functional molecules, hydrolysis by base treatment and UV or ion-beam irradiation. For example, a membrane prepared from poly(acrylonitrile-co-glycidyl methacrylate) (PANGMA) with a defined epoxide content was cross-linked by ammonolysis reaction yielding an extraordinary solvent-resistant and autoclavable membrane [31]. The PAN membranes became resistant to all common organic solvents including DMF, DMSO, and NMP after hydrolysis by NaOH, which provides a candidate material for either the selective layer or the supporting layer for a solvent resistant composite membrane [32]. Polyimide membranes were modified by immersing the films in the diamine/methanol solution for a stipulated period of time [33]. A series of linear aliphatic cross-linking diamine reagents (ethylenediamine, propane-1,3-diamine, and butane-1,4-diamine) were used. This study demonstrated for the first time that diamine crosslinked membranes possess high separation performance and provide impressive separation efficiency for H_2/CO_2 separation. Membrane surfaces can also be modified both chemically and physically when they are exposed to high energy particles. UV/ozone irradiation can break most C-C bonds and also can induce chain scission and cross-linking on polymer surface [34]. A commercial sulfonated polysulfone membrane was modified by ion-beam irradiation [35]. During modification, some of the sulfonic groups on the surface of the membrane were broken, which resulted in cross-linking of the polymer. These

changes modified the surface morphology of the membrane, and also decreased the negative charge of the membrane. It was observed that fouling of the modified membrane was significantly less severe than that of the virgin membrane [22].

3. Grafting. Most membrane materials such as polysulfone, polyethersulfone, polypropylene, polyamide and polyvinylidenefluoride (PVDF) are hydrophobic [36]. Although these membranes have excellent thermal, chemical and mechanical stabilities, they are easily susceptible to fouling, i.e., nonspecific adsorption of solutes on the membrane surface and pores resulting in severe flux decline [21, 36]. Therefore the most important purpose of surface modification of membranes is the improvement of membrane fouling resistance. A common strategy is to graft a layer of hydrophilic polymer on the membrane. Hydrophilic surfaces have proven to be less susceptible for fouling and are often reversible [37, 38, 39, 40]. For example, hydrophilic polyethylene glycol (PEG) chains have often been grafted on commercial polyamide membranes for fouling improvement [41, 42]. Other grafting monomers include acrylic acid (AA) [43], N-vinyl pyrrolidone [44], N,N-dimethylaminoethyl methacrylate (DMAEMA) [45], and 2-acrylamido-2-methyl-1-propanesulfonic acid (AMPS) [46]. The grafting techniques may include UV photoinitiation [44, 46], redox initiation [43, 45], and plasma initiation [22, 47].

4. Coating. In grafting, hydrophilic species are covalently bonded to the membrane surface. Membrane properties are therefore permanently changed and long term stability of the membranes may be decreased [48]. In coating, however, the chemistry of the initial membranes is retained and a new layer of hydrophilic film bearing the antifouling property is coated on top of the membrane surface via hydrophobic interactions, hydrogen bonding, van der Waals attractions, and electrostatic interactions [48]. Two coating techniques have been frequently applied,

namely dip coating and dynamic coating. In dip coating, the membrane is dipped into the coating solution and the polymer material is then adsorbed on the membrane surface [49, 50]. Dynamic coating can be carried out in dead-end or cross-flow modes. The membranes are loaded in a filtration cell with the surface facing the coating solution. Then the coating solution is circulated under pressure resulting in the in-situ formation of a layer of polymer film on the membrane surface [51]. Poly(vinyl alcohol) (PVA) has been widely used as a coating material for commercial polyamide membranes to improve their fouling resistance [52, 53]. To increase the chemical, thermal and mechanical stability of PVA, cross-linking was often conducted by reacting with aldehydes, anhydrides or diisocyanates etc. [54, 55, 56]. In recent years, polyelectrolytes have been used as coating materials to modify membrane charge and hydrophilicity [57]. Such coatings can be multilayer [58] or monolayer [59] and show high resistance to common organic foulants like proteins and humic substances. If the fouling still occurs, membrane cleaning can be easily applied to regenerate the membranes [57, 59].

1.4 Polyimide (PI) materials

Polyimides are the product of a reaction between a dianhydride and a diamine to produce a soluble polyamic acid, which is thermally or chemically converted to a polyimide by the loss of water. Typically, polyimides are excellent in thermal stability due to the stiff aromatic backbones. They are also resistant to a number of solvents such as aromatics, aliphatics, chlorinated hydrocarbons, ketones, esters and alcohols. Although polyimides are sensitive to alkalinity, they should be impervious to the pH encountered in natural feed waters for desalination.

Most polyimides are infusible and insoluble and thus any products, including membranes, need to be processed from polyamic acid solution. For example,

Kapton™ polyimide film is processed from polyamic acid utilizing two monomers pyromellitic dianhydride (PMDA) and 4,4′-oxydianiline (ODA). The PMDA/ODA polyimide has a very high glass transition temperature of approximately 400 ^{o}C and excellent resistance to most nonoxidizing acids at room temperature and almost all organic solvents [**60**]. Their thermal resistance allows separations to be performed for a long time at elevated temperatures [61]. Still, there are some soluble polyimides such as Lenzing P84 prepared from 3,3′,4,4′-benzophenone tetracarboxylic dianhydride with 80% toluenediisocynate and 20% methylphenylenediisocyanate (BTDA-TDI/MDI) with a glass transition temperature of 315 ^{o}C. Apparently, soluble polyimides have good processability for membrane development.

A unique feature of polyimides is their chemical reaction with amines, which results in the opening of some of the imide functions to form ortho-diamide functions. This reaction can be used to introduce functional groups onto the polyimide membrane surface by choosing suitable amines. In particular, by reacting with multifunctional amines (di- or higher functional), PIs can be cross-linked so that the PI membranes would show improved separation efficiency and solvent resistance. [62, 63].

1.5 Objectives and organization of this research

The goals of this project are to develop novel RO and nanofiltration (NF) membranes for desalination and water purification, which will greatly outperform current state-of-the-art RO/NF membrane systems. During the past 5 years, my research has been focusing on the development of positively charged and solvent resistant NF membranes, antifouling NF membranes, and thermally stable RO membranes. Polyimide materials were used for all the projects.

In chapter 2, we described the preparation and characterization of positively charged NF membranes by chemical modification of the P84 copolyimide asymmetric membranes using branched polyethylenimine (PEI). Optimized membrane performance was shown to be 50.9 ± 5.1% salt rejection to a 2.0 g/L NaCl solution with a flux of 1.2 ± 0.1 m^3m^{-2} day^{-1} at 13.8 bar and room temperature. The rejection sequence of $CaCl_2$ > NaCl > Na_2SO_4 indicates a positive charge at the membrane surface, which may be attributed to amine groups remaining after the reaction between PEI and polyimide. Upon modification, the pores of the membranes were filled with PEI molecules so as to cause the membranes to exhibit nanofiltration properties. The PEI-modified polyimide membranes likely have a highly cross-linked structure which makes these membranes stable in various operating environments including high temperature (100 °C), organic solvents, and mild acid and base (2 ≤ pH ≤ 10). These membranes showed efficient removal of multivalent heavy metal ions (> 95%) and may potentially be used for treatment of industrial wastewater.

In Chapter 3, a coating technique was applied to prepare an antifouling nanofiltration membrane. The positively charged membranes as described in Chapter 2 had low fouling resistance because of the strong adsorption of common foulants via electrostatic attraction. In order to avoid fouling, a layer of water-soluble polymers was adsorbed onto the membrane surface in a dynamic manner. With such coatings, membrane surface properties such as hydrophilicity, roughness and charge were modified to give improved resistance to fouling. Depending on the coating materials, the coating layer may be erasable or inerasable. For example, the neutral polymer polyvinyl alcohol (PVA) may be adsorbed onto the membrane surface by hydrogen bonding. Such interaction becomes weakened during acid cleaning so that the PVA layer can be detached. Thus, if membrane fouling occurs, the PVA layer and attached

foulants can be removed by acid cleaning to refresh the membrane. Negatively charged polymers such as polyacrylic acid (PAA) and polyvinyl sulfate (PVS) can be adsorbed onto the membrane surface by electrostatic force. Such strong interactions made the coating layers stable during acid cleaning. However, these coating layers permit removal of the foulants by a simple treatment with acid.

In Chapter 4, we attempted to apply the antifouling NF membranes as designed in Chapter 3 in a membrane bioreactor (MBR) process. One approach involved the use of partially PEI modified P84 copolyimide membranes with improved toughness to develop a series of membranes with various surface properties and separation capabilities. Another approach dealt with a nearly neutrally charged NF membrane developed by adsorption of a layer of negatively charged sulfonated poly(ether ether ketone) (SPEEK) onto the surface of a PEI modified PMDA-ODA polyimide membrane with positive surface charge. It was found that surface charge had significant influence on multivalent ion rejection and fouling resistance. The neutrally charged membrane could remove multivalent ions (both cations and anions) more efficiently (> 95%) than monovalent ions (80%) due to the size effect; a rejection sequence of $CaCl_2 \approx MgSO_4 \approx Na_2SO_4 >$ NaCl was observed. When using bovine serum albumin (BSA), humic acid and sodium alginate as the model foulants, the neutrally charged membrane exhibited much better fouling resistance than both the positively and negatively charged membranes. This result suggests that the foulants would less likely deposit onto a neutral membrane due to the elimination of the charge interaction between the membrane and the foulants. In addition, the neutrally charged NF membrane showed better resistance to activated sludge than the commercial NTR-7450 membrane, which indicates this membrane may be potentially applied in the MBR process.

In Chapter 5, we developed a thermally stable RO membrane using PMDA/ODA polyimide as a substrate and polyamide as the selective top layer. This substrate membrane was prepared by immersion precipitation of a casting solution composed of 15% polyamic acid (PAA) and 24% $ZnCl_2$ additive. Zinc ions were able to interact with the carboxylic groups of PAA forming an ionic cross-linking structure which facilitated the formation of a membrane with improved surface properties, mechanical strength and permeability. The PAA membranes were chemically imidized by a mixture of acetic anhydride and triethylamine at 100 ˚C to prevent pore collapse. Composite membranes were developed via interfacial polymerization of *m*-phenylenediamine (MPDA) and trimesoyl chloride (TMC) on the polyimide membranes. These composite membranes showed 98% rejection to 2.0 g/L NaCl solution with a permeation flux of 1.1 $m^3m^{-2}day^{-1}$ at 55.2 bar and room temperature. This composite membrane demonstrated good thermal stability. As the test temperature increased from 25 ˚C to 95 ˚C, the permeated flux of 2.0 g/L NaCl solution increased 5 - 6 times from 0.74 $m^3m^{-2}day^{-1}$ to 3.95 $m^3m^{-2}day^{-1}$ with a stable rejection rate when the pressure was fixed at 27.6 bar.

In summary, my research involves membrane preparation, characterization and application. The advanced membranes we have developed can greatly improve the separation capability of the commercial RO/NF membranes for desalination, water softening, heavy metal removal and organic removal, etc. They can also withstand harsh environments including organic solvents, high temperatures, and foulants. These membranes appear to display great commercial value. Future research can be conducted on the fundamental study of the antifouling mechanisms and the application in water purification or wastewater treatment in an MBR process.

1.6 References

[1] G. Belfort, Synthetic Membrane Processes: Fundamentals and Water Applications, Academic Press, Orlando, Florida, 1984.

[2] R.J. Petersen, Composite reverse osmosis and nanofiltration membranes, *J. Membr. Sci.* 1993, 83, 81.

[3] S. Loeb, S. Sourirajan, Sea water demineralization by means of an osmotic membrane, in *Saline Water Conversion II, R.F. Gould (ed.)*", *Advances in Chemistry Series Number 38,* American Chemical Society, Washington, DC, (1963) 117.

[4] J.E. Cadotte, Evaluation of composite reverse osmosis membrane, in *Materials Science of Synthetic Membranes, D.R.Lloyd (ed.), ACS Symposium Series Number 269,* American Chemical Society, Washington, DC, (1985)

[5] R.E. Larson, J.E. Cadotte, R.J. Petersen, The FT-30 seawater reverse osmosis membrane-element test results, *Desalination* 38 (1981) 473.

[6] J.E. Cadotte, Interfacially synthesized reverse osmosis membrane, *US Patents* 4277344 (1981).

[7] M. Kurihara, N. Harumiya, N. Kannamaru, T. Tonomura, M. Nakasatomi, Development of the PEC-1000 composite membrane for single stage sea water desalination and the concentration of dilute aqueous solutions containing valuable materials, *Desalination* 38 (1981) 449.

[8] A.K. Ghosh, V. Ramachandhran, M.S. Hanra, B.M. Misra, Synthesis, characterization, and performance of sulfonated polyethersulfone nanofiltration membranes, *J. Macromol. Sci. Pure Appl. Chem.* A39 (3) (2002) 199.

[9] R. W. Baker, Membrane Technology and Applications, 2nd ed., John Wiley & Sons, Ltd., Chichester, 2004.

[10] S.H. Kim, S.-Y. Kwak, T. Suzuki, Positron annihilation spectroscopic evidence to demonstrate the flux-enhancement mechanism in morphology-controlled thin-film-composite (TFC) membrane, *Environ. Sci. Technol.* 39 (2005) 1764.

[11] J. Glater, S. Hong, M. Elimelech, The search for a chlorine-resistant reverse osmosis membrane, *Desalination* 95 (1994) 325.

[12] M.J.H. Snow, D. de Winter, R. Buckingham, J. Campbell, J. Wagner, New techniques for extreme conditions: high temperature reverse osmosis and nanofiltration, *Desalination* 105 (1996) 57.

[13] M. Manttari, A. Pihlajamaki, E. Kaipainen, M. Nystrom, Effect of temperature and membrane pre-treatment by pressure on the filtration properties of nanofiltration membranes, *Desalination* 145 (2002) 81.

[14] I. Pinnau, B.D.Freeman, Formation and modification of polymeric membranes, I. Pinnau, B.D. Freeman, Eds., *ACS Symposium Series 744,* American Chemical Society, Washington D.C., 2000, 1.

[15] M.H.V. Mulder, Basic Principles of Memrane Technology, Kluwer, London, 1996.

[16] J. Smid, J.H.M. Albers, A.P.M. Kusters, The formation of asymmetric hollow fiber membranes for gas separation, using PPE of different intrinsic viscosities, *J. Membr. Sci.* 64 (1991) 121.

[17] C. Wu, S. Zhang, D. Yang, J. Wei, C. Yan, X. Jian, Preparation, characterization and application in wastewater treatment of a novel thermal stable composite membrane, *J. Membr. Sci.* 279 (2006) 238.

[18] P.S. Singh, S.V. Joshi, J.J. Trivedi, C.V. Devmurari, A.P. Rao, P.K. Ghosh, Probing the structural variations of thin film composite RO membranes obtained by coating polyamide over polysulfone membranes of different pore dimensions, *J. Membr. Sci.* 278 (2006) 19.

[19] N.-W. Oh, J. Jegal, K.-H. Lee, Preparation and Characterization of nanofiltration composite membranes using polyacrylonitrile (PAN). II. preparation and characterization of polyamide composite membranes, *J. Appl. Polym. Sci.* 80 (2001) 2729.

[20] M. Hirose, H. Ito, Y. Kamiyama, Effect of skin layer surface structures on the flux behaviour of RO membranes, *J. Membr. Sci.* 121 (1996) 209.

[21] L.J. Zeman, A.L. Zydney, Microfiltration and Ultrafiltration: Principles and Applications, Marcel Dekker, New York, 1996.

[22] K.C. Khulbe, C. Feng, T. Matsuura, The art of surface modification of synthetic polymeric membranes, *J. Appl. Polym. Sci.* 115 (2010) 855.

[23] S. Wu, J. Xing, C. Zheng, G. Xu, G. Zheng, J. Xu, Plasma modification of aromatic polyamide reverse osmosis composite membrane surface, *J. Appl. Polym. Sci.* 64 (1997) 1923.

[24] M.L. Steen, A.C. Jordan, E.R. Fisher, Hydrophilic modification of polymeric membranes by low temperature H2O plasma treatment, *J. Membr. Sci.* 204 (2002) 341.

[25] S. Pal, S.K. Ghatak, S. De, S. DasGupta, Characterization of CO2 plasma treated polymeric membranes and quantification of flux enhancement, *J. Membr. Sci.* 323 (2008) 1.

[26] J.M. Grace, L.J. Gerenser, Plasma treatment of polymers, *J. Dispersion Sci. Technol.* 24 (2003) 305.

[27] H. Byun, R. Burford, A. Fane, Sulfonation of cross-linked asymmetric membranes based on polystyrene and divinylbenzene, *J. Appl. Polym. Sci.* 39 (1990) 2293.

[28] A. Nabe, E. Staude, G. Belfort, Surface modification of polysulfone ultrafiltration membranes and fouling by BSA solutions, *J. Membr. Sci.* 133 (1997) 57.

[29] J. Wang, Z. Yue, J. Economy, Novel method to make a continuous micro-mesopore membrane with tailored surface chemistry for use in nanofiltration, *J. Membr. Sci.* 308 (2008) 191.

[30] J.Wang, Z. Yue, J.S. Ince, J. Economy, Preparation of nanofiltration membranes from polyacrylonitrile ultrafiltration membranes, *J. Membr. Sci.* 286 (2006) 333.

[31] H.-G. Hicke, I. Lehmanna, G. Malsch, M. Ulbricht, M. Becker, Preparation and characterization of a novel solvent-resistant and autoclavable polymer membrane, *J. Membr. Sci.* 198 (2002) 187.

[32] J. Wang, Z. Yue, J. Economy, Solvent resistant hydrolyzed polyacrylonitrile membranes, *Sep. Sci. Technol.* 44 (2009) 2827.

[33] T.-S. Chung, L. Shao, P.S. Tin, Surface modification of polyimide membranes by diamines for H2 and CO2 separation, *Macromol. Rapid Commun.* 27 (2006) 998.

[34] K. Fujimoto, Y. Takebayashi, H. Inoue, Y. Ikada, Ozone-induced graft polymerization onto polymer surface, *J Polym Sci Part A: Polym Chem* 31 (1993) 1035.

[35] R. Chennaamsetty, I. Escobar, X. Xu, Characterization of commercial water treatment membranes modified via ion beam irradiation, *Desalination* 188 (2006) 203.

[36] N. Hilal, O.O. Ogunbiyi, N.J. Miles, R. Nigmatullin, Methods employed for control of fouling in MF and UF membranes: A comprehensive review, *Sep. Sci. Technol.* 40 (2005) 1957.

[37] A.G. Fane, C.J.D. Fell, A review of fouling and fouling control in ultrafiltration, *Desalination* 62 (1987) 117.

[38] A.D. Marshall, P.A. Munro, G.Tragardh, The effect of protein fouling in microfiltration and ultrafiltration on permeate flux, protein retention and selectivity - A literature review, *Desalination* 91 (1993) 65.

[39] K. Kim, K. Saito, S. Furusaki, T. Sugo, J. Okamoto, Water flux and protein adsorption of a hollow fibre modified with hydroxyl groups, *J. Membr. Sci.* 56 (1991) 289.

[40] A. Nabe, E. Staude, G. Belfort, Surface modification of polysulfone ultrafiltration membranes and fouling by BSA solutions, *J Membr. Sci.* 133 (1997) 57.

[41] G. Kang, M. Liu, B. Lin, Y. Cao, Q. Yuan, A novel method of surface modification on thin-film composite reverse osmosis membrane by grafting poly(ethylene glycol), *Polymer* 48 (2007) 1165.

[42] J. Gilron, S. Belfer, P. Väisänen, M. Nyström, Effects of surface modification on antifouling and performance properties of reverse osmosis membranes, *Desalination* 140 (2001) 167.

[43] V. Freger, J. Gilron, S. Belfer, TFC polyamide membranes modified by grafting of hydrophilic polymers: an FT-IR/AFM/TEM study, *J. Membr. Sci.* 209 (2002) 283.

[44] J.E. Kilduff, S. Mattaraj, J.P. Pieracci, G. Belfort,Photochemical modification of poly(ether sulfone) and sulfonated poly(sulfone) nanofiltration membranes for control of fouling by natural organic matter, *Desalination* 132 (2000) 133.

[45] Q. Dai, Z. Xu, H. Deng, Z. Liu, J. Wu, P. Seta, Surface modification of microporous polypropylene membranes by graft polymerization of N, N-dimethylaminoethyl-methacrylate, Chin. J. Polym. Sci. 22 (2004) 369.

[46] N. Hilal, L. Al-Khatib, B.P. Atkin, V. Kochkodan, N. Potapchenko, Photochemical modification of membrane surfaces for (bio)fouling reduction: a nano-scale study using AFM, *Desalination* 158 (2003) 65.

[47] J. Lai, Y.C. Chao, Plasma-modified nylon 4 membranes for reverse osmosis desalination, *J. Appl. Polym. Sci.* 39 (1990) 2293.

[48] N. Hilal, O.O. Ogunbiyi, N.J. Miles, R. Nigmatullin, Methods employed for control of fouling in MF and UF membranes: a comprehensive review, Sep. Sci. Technol. 40 (2005) 1957.

[49] S.P. Nunes, M.L. Sforca, K.V. Peinemann, Dense hydrophilic composite membranes for ultrafiltration, *J. Membr. Sci.* 106 (1995) 49.

[50] F.F. Stengaard, Preparation of asymmetric microfiltration membranes and modification of their properties by chemical treatment, *J. Membr. Sci.* 36 (1988) 257.

[51] N. Li, Z. Liu, S. Xu, Dynamically formed poly (vinyl alcohol) ultrafiltration membranes with good anti-fouling characteristics, J. Membr. Sci. 169 (2000) 17.

[52] I. Pinnau, J.H. Ly, R.W. Baker, Reverse osmosis membrane and process, US patent 7,490,725 B2 (2009).

[53] J.R. Du, S. Peldszus, P.M. Huck X. Feng, Modification of poly(vinylidene fluoride) ultrafiltration membranes with poly(vinyl alcohol) for fouling control in drinking water treatment, *Water Research* 43 (2009) 4559.

[54] B. Bolto, T. Tran, M. Hoang, Z. Xie, Crosslinked poly(vinyl alcohol) membranes, *Progress in Polymer Science* 34 (2009) 969.

[55] H.M. Colquhoun, P.J. Williams, A.L. Lewis, Polymer porous structure and process, US patent 5,698,105 (1997).

[56] H. Hachisuka, K. Ikeda, Reverse osmosis composite membrane and reverse osmosis treatment method for water using the same, US patent 6,413,425 B1 (2002).

[57] W. Shan, P. Bacchin, P. Aimar, M.L. Bruening, V.V. Tarabara, Polyelectrolyte multilayer films as backflushable nanofiltration membranes with tunable hydrophilicity and surface charge, *J. Membr. Sci.* (2009), doi:10.1016/j.memsci.2009.11.059.

[58] J. Wang, Y. Yao, Z. Yue, J. Economy, Preparation of polyelectrolyte multilayer films consisting of sulfonated poly(ether ether ketone) alternating with selected anionic layers, J. Membr. Sci. 337 (2009) 200.

[59] C. Ba, D.A. Ladner, J. Economy, Using polyelectrolyte coatings to improve fouling resistance of a positively charged nanofiltration membrane, J. Membr. Sci. 347 (2010) 250.

[60] T. Takekoshi, Polyimides—Fundamentals and Applications, M.K. Ghosh and K.L. Mittal (eds), Marcel Dekker, New York, 1996.

[61] H. Ohya, V.V. Kudryavtsev, S.I. Semenova, Polyimide Membranes: Applications, Fabrications, and Properties, Tokyo, Gordon and Breach, 1996.

[62] W. Albrecht, B. Seifert, Th. Weigel, M. Schossig, A. Hollander, Th. Groth, R. Hilke, Amination of poly(ether imide) membranes using di- and multivalent amines, *Macromol. Chem. Phys.* 204 (2003) 510.

[63] C. Trimpert, G. Boese, W. Albrecht, K. Richau, Th. Weigel, A. Lendlein, Th. Groth, Poly(ether imide) membranes modified with poly(ethylene imine) as potential carriers for epidermal substitutes, *Macromol. Biosci.* 6 (2006) 274.

CHAPTER 2

CHEMICAL MODIFICATION OF P84 COPOLYIMIDE MEMBRANES BY POLYETHYLENIMINE FOR NANOFILTRATION

2.1 Introduction

In the past few decades, nanofiltration (NF) has emerged as an attractive membrane process for removal of colloidal, organic, and ionic contaminants from water [1, 2]. Commercial NF membranes are generally prepared as composites consisting of an ultrathin (< 200 nm) polymeric film deposited onto the surface of a thick, asymmetric porous supporting membrane (usually polysulfone). To date, thin film materials have primarily been limited to polyamides prepared by interfacial polymerization, while some additional polymeric materials such as sulfonated polyethersulfone (SPES), polyvinyl alcohol (PVA) derivatives, and sulfonated polyphenylene oxide (SPPO) have also been developed [3]. Although these membranes provide a variety of separation capabilities, they are generally negatively charged [4] and multivalent anions, like sulfate and phosphate, are rejected more effectively than monovalent anions like chloride [1]. Considering the strong influence of membrane charge on ion permeation due to the Donnan effect [5], it is of interest to develop positively charged NF membranes with enhanced rejection of multivalent cations, such as heavy metal ions (e.g. Ni^{2+}, Cu^{2+}, Zn^{2+}, Pb^{2+}) from industrial wastewater before discharging [6, 7, 8, 9].

In order to prepare positively charged membranes, a common method is to functionalize the membrane surface with amine and/or ammonium groups. Childs et al. developed pore-filled NF membranes by in situ chemical cross-linking of

poly(vinylbenzyl chloride) or poly(4-vinylpyridine) in the pores of microporous polypropylene membranes [10]. Polyelectrolyte gels containing either tertiary amine and quaternary ammonium groups or pyridine and pyridinium groups were formed within the pores. Xu and Yang developed a composite membrane whose top layer was prepared by reaction of brominated polyphenylene oxide with a mixture of trimethylamine and ethylenediamine [11]. The membrane surface in this system contained a combination of primary, secondary, and tertiary amines and quaternary ammonium groups. Du and Zhao reported another composite membrane wherein the top layer was prepared by interfacial crosslinking of poly(N,N-dimethyl-aminoethyl methacrylate) using p-xylylene dichloride [12]. In this case only tertiary amines and quaternary ammonium chloride groups were present at the membrane surface. Recently Wang et al. prepared polyacrylonitrile (PAN) NF membranes by treatment of PAN ultrafiltration membranes with 3-(dimethylamino)propyl amine [13]. Upon reaction, tertiary amine groups were introduced at the membrane surface, which made the membrane positively charged.

Due to their high mechanical strength, good thermal and chemical stability, polyimides (PIs) have been widely used in various membrane processes for separation of liquid and gaseous mixtures [14]. A unique feature of PIs is their chemical reaction with amines, which results in the opening of some of the imide groups to form ortho-diamide functionalities. This reaction may be used to introduce functional groups onto the PI membrane surface by choosing suitable amines. In particular, by reacting with di- or multi-functional amines, PIs can be cross-linked such that the membranes show

improved separation efficiency and solvent resistance. For example, Albrecht et al. studied the surface functionalization of poly(ether imide) membranes by di- and multivalent amines [15]. It was shown when using high molecular weight polyethylenimine (PEI) as a modifying agent, poly(ether imide) membranes became insoluble even in polar aprotic solvents such as N,N-dimethylacetamide (DMAc). High contents of amine groups were detected, making the membranes more hydrophilic and positively charged as shown by contact angle and streaming potential studies, respectively [15, 16].

P84, a co-polyimide of 3,3′,4,4′-benzophenone tetracarboxylic dianhydride with 80% toluenediisocynate and 20% methylphenylenediisocyanate (BTDA-TDI/MDI), has a high glass transition temperature (T_g) of 315˚C, good resistance to many organic solvents including toluene, hydrocarbons, alcohols and ketones, as well as good resistance to a broad range of pH conditions. Chemical modification of P84 membranes via treatment with diamines yields membranes useful for pervaporation dehydration of isopropanol [17] or for nanofiltration in polar aprotic solvents such as N,N-dimethylformamide (DMF) and N-methypyrrolidone (NMP) [18]. However, the diamines may only serve to act as crosslinkers to improve the chemical stability of the P84 membranes. In this study, we used PEI as the modification agent. In addition to enhancing membrane stability, this modification provided positively charged NF membranes due to the free amine groups at the membranes surface. These PEI-modified P84 membranes showed good performance for removal of salts, especially multivalent metal ions, from water.

2.2 Experimental

2.2.1 Chemicals

27% P84 solution in dimethylformamide (DMF) was purchased from Inspec Fibers GmbH, Lenzing, Austria and used without further treatment. PEI (Mw: 25,000, Mn: 10,000) was purchased from Aldrich. All of the organic and inorganic reagents were of analytical grade and used as received.

2.2.2 Preparation of asymmetric porous membranes

Asymmetric porous P84 membranes were cast using the phase inversion method [1]. Casting solutions were prepared by diluting the original 27% polymer solution with DMF to give polymer concentrations of 25%, 23% and 21%. Then, the polymer solution was cast onto polyester support followed by immediate immersion into a room temperature water bath. After precipitation, the membranes were kept in the water bath overnight in order to remove the DMF. The membranes were then rinsed with and stored in deionized (DI) water prior to further chemical treatment.

2.2.3 Chemical modification of the P84 membranes

Chemical modification was conducted by immersing a membrane into a given PEI solution at 70˚C for varied amounts of time ranging from 0 to 120 min. The membrane was then rinsed several times using DI water to remove any loosely bound PEI, and finally stored in DI water until use. In order to determine the optimal modification conditions, several PEI solutions were prepared by dissolving PEI in either DI water, isopropanol, or a mixture of isopropanol and water (volume 1:1) at concentrations of 0.2%, 1% or 5% (wt/vol).

2.2.4 Nanofiltration tests

Desalination performance of the modified P84 membranes was examined using a dead-end filtration cell (Sterlitech HP4750) and 300 mL of a 2.0 g/L NaCl aqueous feed solution under 13.8 bar and room temperature. The feed solution was stirred at a rate of 18.33Hz (1100 rpm) in the cell using a standard magnetic stirrer (Corning Stirrer/Hot Plate, Model PC-420) to minimize concentration polarization. Each membrane was compacted at a pressure of 13.8 bar for at least 1 h prior to measurements to ascertain that a steady state was obtained. The permeated solution was then refilled into the feed and permeate samples were collected as appropriate. The permeation flux F was determined by measuring the permeation volume V (5-10 mL, 1.7-3.3% recovery) flowing across the membrane of area A (14.6 cm^2) in the time period Δt, F ($m^3m^{-2}day^{-1}$) = $V/(A \times \Delta t)$. The NaCl concentration was measured using a Cl^- ion selective electrode (Cole-Parmer) with an OAKTON Benchtop Ion 510 Meter. The salt rejection was calculated as $R = (1 - C_p/C_f) \times 100\%$, where C_p and C_f were the concentrations of the permeate and feed solution, respectively. For each data point, 3-5 membrane samples were tested to give an average value.

Similarly, rejection to $CaCl_2$, NaCl and Na_2SO_4 at four different initial concentrations (0.2, 0.5, 1.0 and 2.0 g/L) in aqueous solution was measured in order to qualitatively determine membrane charge. Concentrations of NaCl and $CaCl_2$ were measured by a Cl^- ion selective electrode and the concentration of Na_2SO_4 was measured by a Na^+ ion selective electrode (Cole-Parmer).

2.2.5 Physical characterization methods

Physical characterization was conducted by attenuated total reflectance Fourier transform infrared spectroscopy (ATR-FTIR), scanning electron microscopy (SEM), thermal gravimetric analysis (TGA) and differential scanning calorimetry (DSC). All membrane samples were dried using the solvent exchange method to prevent the porous structure from collapsing upon drying. Membranes were immersed in isopropanol for 24 hours during which time the solvent was refreshed 3 times in order to displace any water contained in the membranes. Subsequently, isopropanol was replaced by hexane by the same procedure. Finally, the residual solvent was removed from the membranes using vacuum prior to further experiments.

ATR-FTIR spectra were collected at room temperature over a scanning range of 600-4000 cm^{-1} with a resolution of 4.0 cm^{-1}, using a Nexus 670 FT-IR (Thermo Electron Corporation, Madison, WI) with a Golden Gate™ MKII Single Reflectance ATR (Specac Inc., Woodstock, GA). The spectrometer was installed with a deuterated triglycine sulfate-potassium bromide (DTGS-KBr) detector and KBr beamsplitter. Spectra collection was performed using FT-IR software (OMNIC, Thermo Electron Corporation, Madison, WI).

SEM images were obtained using a Hitachi S-4700 with 15.0 kV accelerating voltage. For cross-sectional observations the polyimide layer was peeled off of the polyester support and fractured after immersion in liquid nitrogen. All samples were coated by sputtering with gold and palladium before testing.

DSC was performed on a Mettler-Toledo DSC 821e. For each analysis, approximately 20 mg of sample were accurately weighed (± 0.02 mg) into an

aluminum pan, which was then hermetically sealed. DSC traces recorded heat flow during heating at a rate of 10 ˚C /min over the temperature range 25˚C to 300˚C.

TGA was performed on a Cahn TherMax 500 TGA system. Roughly 100-200 mg of each of the polymer samples were heated from room temperature to 700˚C at a heating rate of 10 ˚C/min under flowing nitrogen.

2.2.6 Membrane stability

Thermal stability of the membranes was performed by annealing membranes (previously dried by solvent exchange) at 100 ˚C, 200 ˚C, or 300 ˚C for 2 hours and comparing the desalination performance of the membranes before and after annealing.

Resistance to organic solvents was evaluated by immersing membranes for 16 hours into one of several representative solvents including tetrahydrofurane (THF), methanol (MeOH), acetone, DMF, NMP and DMAc. Desalination performance of the membranes before and after solvent treatment was compared. Resistance to aqueous solutions of varying pH was evaluated by the same procedure. The pH of these solutions was adjusted using HCl or NaOH.

2.2.7 Membrane performance for removal of multivalent metal ions

Performance for removal of multivalent metal ions from water was determined using a feed solution containing either a single salt of $ZnCl_2$, $CuCl_2$, $FeCl_3$ or $AlCl_3$, or a mixture of $ZnCl_2$/NaCl or $FeCl_3$/NaCl. In order to prevent precipitation, all of the experiments were carried out at a pH of 2 adjusted by HCl. In the single-salt experiments, the salt concentration was 10 mM. For the mixtures, several molar ratios were tested, including 1 mM/10 mM, 10 mM/10 mM and 10 mM/1 mM. The

concentration of each metal ion in the permeate solutions was determined by ICP-MS (PerkinElmer-SCIEX ELAN DRCe ICP-MS).

2.3 Results and discussion

2.3.1 P84 membrane preparation

In order to determine the appropriate polymer concentration for membrane development, four casting solutions containing 27%, 25%, 23% or 21% polymer were used to develop the P84 membranes by the phase inversion method. Their cross-sectional and surface morphologies are shown in Figure 2.1. In all cases, a number of large parallel finger-like voids can be observed, indicating an instantaneous phase separation occurred during the precipitation step due to the strong mutual affinity between water and DMF [19]. As the polymer concentration is decreased, larger numbers of fingers are observed and the size of the pores at the surface becomes larger. This may be due to reduced polymer aggregation at lower polymer concentration [20]. These structural differences have a strong influence on mass transport through the membrane. As shown in Figure 2.2 (modification time = 0), a decrease in polymer concentration corresponds to an increase in water permeability. Negligible salt rejection was observed for the unmodified P84 membranes.

2.3.2 Effect of chemical modification on membrane performance

Chemical modification of the four as-mentioned P84 membranes was carried out by immersion into a PEI solution prepared by dissolving PEI at 1% concentration in a mixture of water and isopropanol (volume 1:1) at 70˚C. Figure 2.2 shows the effect of modification time on the desalination performance of the four P84

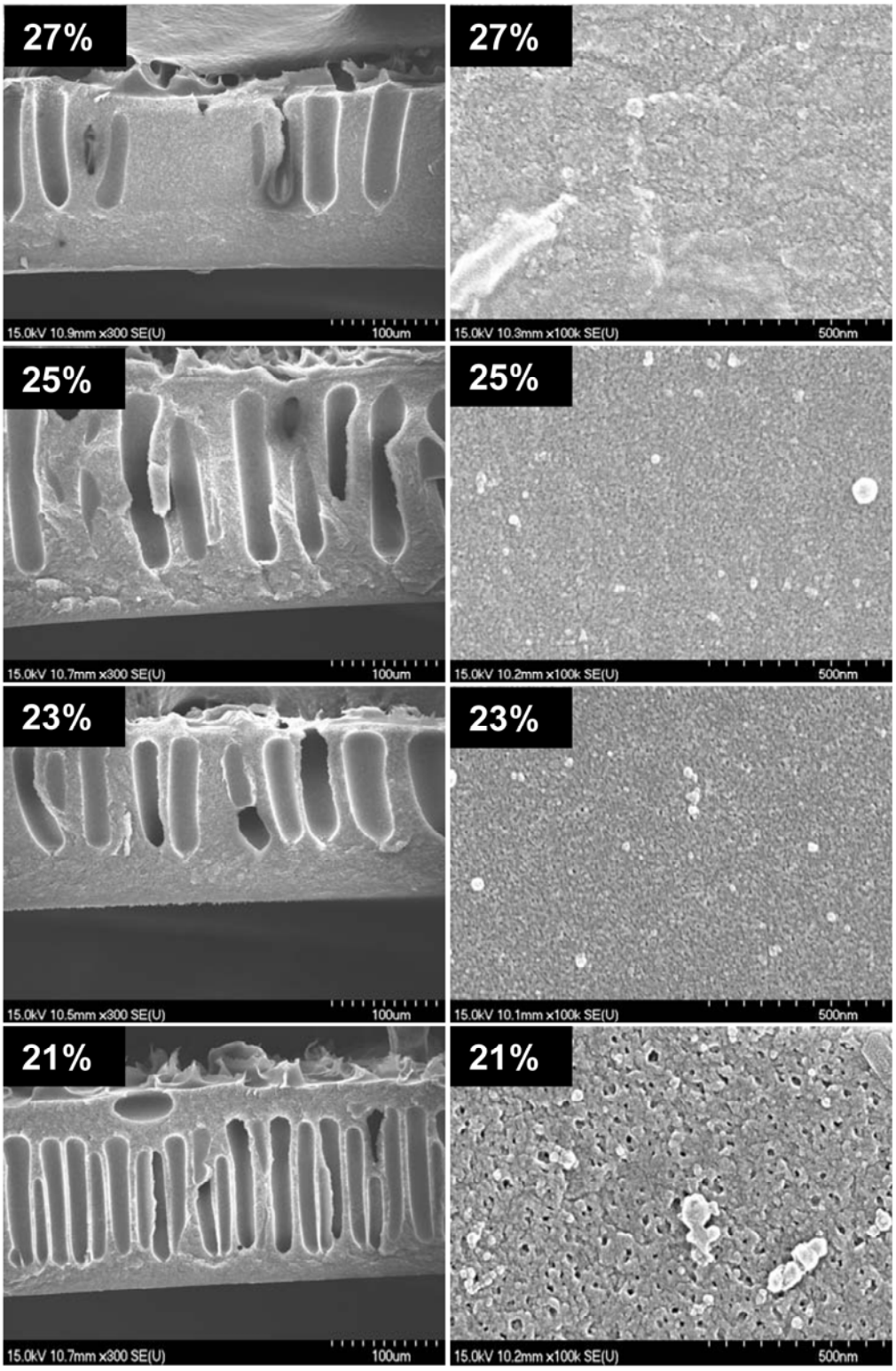

Figure 2.1 Cross-sectional (left) and surface (right) morphologies of the P84 membranes developed from four polymer concentrations.

membranes. With increasing modification time, salt rejection increased gradually and finally reached a stable value while permeation flux decreased throughout the range.

For each membrane, the optimum desalination performance was observed as the point where salt rejection just reached the maximum. Using this definition, the 27% membrane showed its best performance after 20 min modification while the other three membranes required 90 min to reach their optimal level. Comparing the optimum desalination performance of the four membranes, a trade-off between salt rejection and permeation flux can be seen. For example, the membranes developed from 27% to 21% concentrations showed decreasing rejections in the order of 70.4 ± 2.6% > 48.8 ± 2.0% ≈ 50.9 ± 5.1% > 32.9 ± 4.2% whereas the fluxes increased in the order of 0.40 ± 0.073 < 0.95 ± 0.28 < 1.2 ± 0.1 < 1.8 ± 0.1 $m^3m^{-2}day^{-1}$, respectively. We selected the 23% membrane for further studies because both the salt rejection and permeate flux were reasonably high.

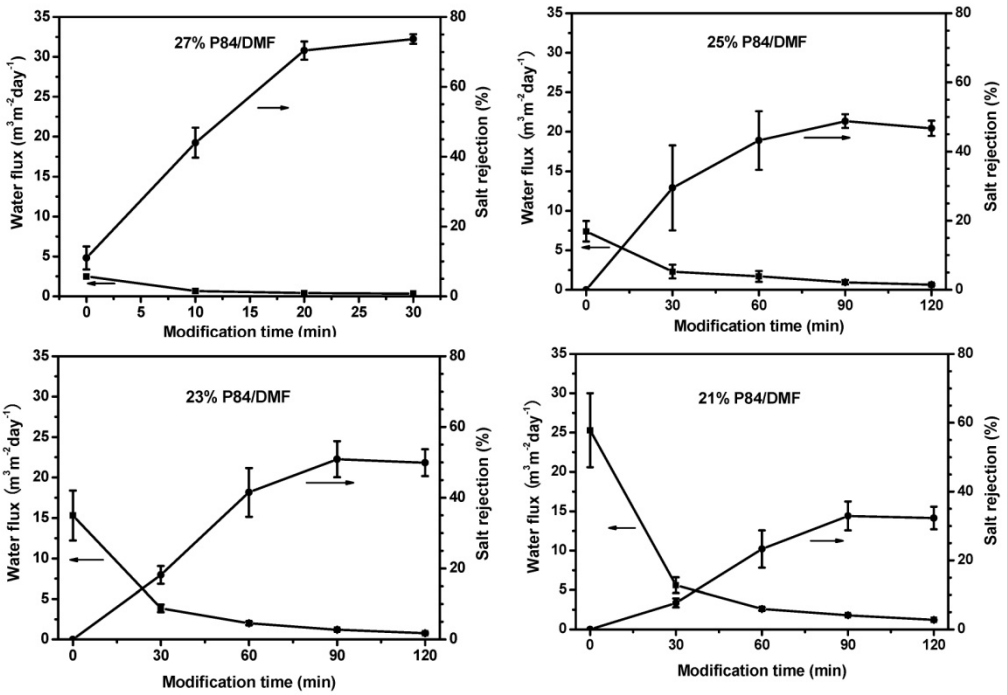

Figure 2.2 Effect of modification time on the desalination performance of the four P84 membranes.

The 23% membrane with 90 min modification was measured with regard to its rejections to $CaCl_2$, NaCl, and Na_2SO_4 at various concentrations. The results are shown in Figure 2.3. A rejection sequence of $CaCl_2$ > NaCl > Na_2SO_4 indicates a positive charge for the membrane [5]. Additionally, the decrease in salt rejection with increasing salt concentration is consistent with the Donnan exclusion model. As ionic strength increases the membrane charge is shielded, resulting in a lower effective charge and consequently lower salt rejection [13].

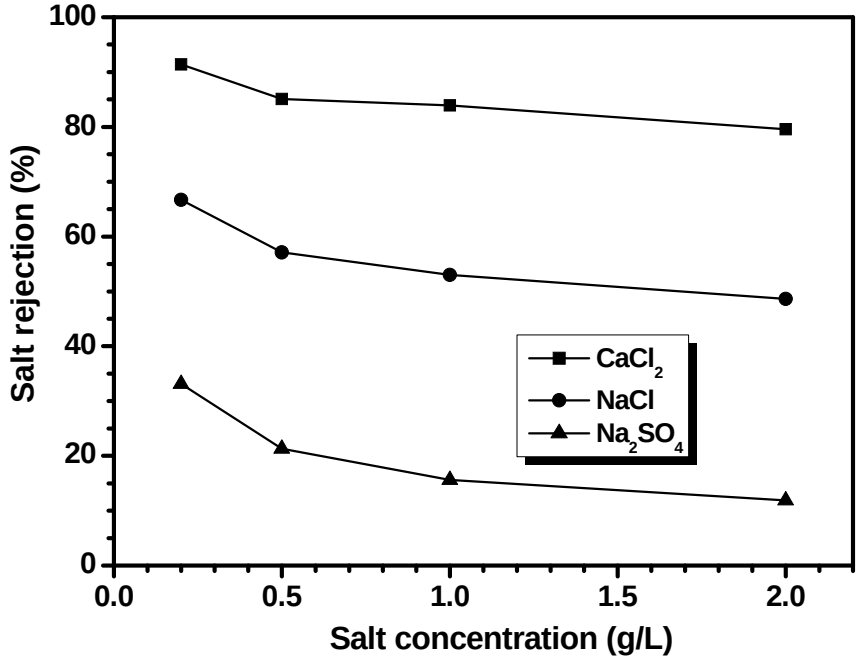

Figure 2.3 Salt rejection sequence of the PEI-modified P84 membrane indicating the positive charge of the membrane.

No obvious improvements in membrane performance were found when different solvents and different concentrations of PEI were used during modification. For example, when water was used as the PEI solvent (see Table 2.1A) the modified membranes showed very low permeation flux although the salt rejection was slightly improved. On the other hand, when isopropanol was used high permeation flux and low salt rejection were obtained. This may be due to increased reactivity of PEI in

water versus isopropanol. In addition, with an increase of the PEI concentration from 0.2% to 5% (see Table 2.1B), only slight increase of salt rejection was obtained. However, the permeation flux decreased 20-fold from 1.6 ± 0.4 $m^3m^{-2}day^{-1}$ to 0.08 ± 0.012 $m^3m^{-2}day^{-1}$. This can be explained by faster reaction in higher PEI concentration solutions. Thus, it appears different reaction conditions only affected the overall speed of modification. It is also interesting to note permeation flux could become very low while there was a limited value of salt rejection. This independent variation may be explained by the changes of morphology and chemical composition of the membranes during modification.

Table 2.1 Effect of various modification conditions on membrane performance[a]

(A) Variation of PEI solvent[b]

Solvent of PEI	Flux ($m^3m^{-2}day^{-1}$)	Salt rejection (%)
Water	0.15 ± 0.02	65.5 ± 2.9
Isopropanol	4.1 ± 1.2	27.6 ± 4.5

(B) Variation of PEI concentration[c]

PEI concentration	Flux ($m^3m^{-2}day^{-1}$)	Salt rejection (%)
0.2%	1.6 ± 0.4	44.4 ± 7.1
5%	0.08 ± 0.012	55.0 ± 3.2

Notes: [a]Membranes prepared from 23% concentration; Test condition: 2.0 g/L NaCl aqueous solution, 13.8 bar and room temperature. [b]Reaction condition: 1% PEI, 70˚C, 90min. [c]Reaction condition: PEI in mixture of water and isopropanol (vol 1:1), 70°C, 90min.

2.3.3 Effect of modification on membrane morphology

For SEM analysis, five membrane samples were prepared by immersing the P84 membranes in 1% PEI solution in water and isopropanol mixture (volume 1:1) at 70˚C for 0, 30, 60, 90 and 120 min, respectively. Morphological observations of the membrane cross-sections and surfaces are displayed in Figure 2.4. The unmodified membrane (0 min) had a pore size of approximately 10 nm. During the reaction with PEI, pore size became smaller (30 min) until eventually no pores were observed. It is

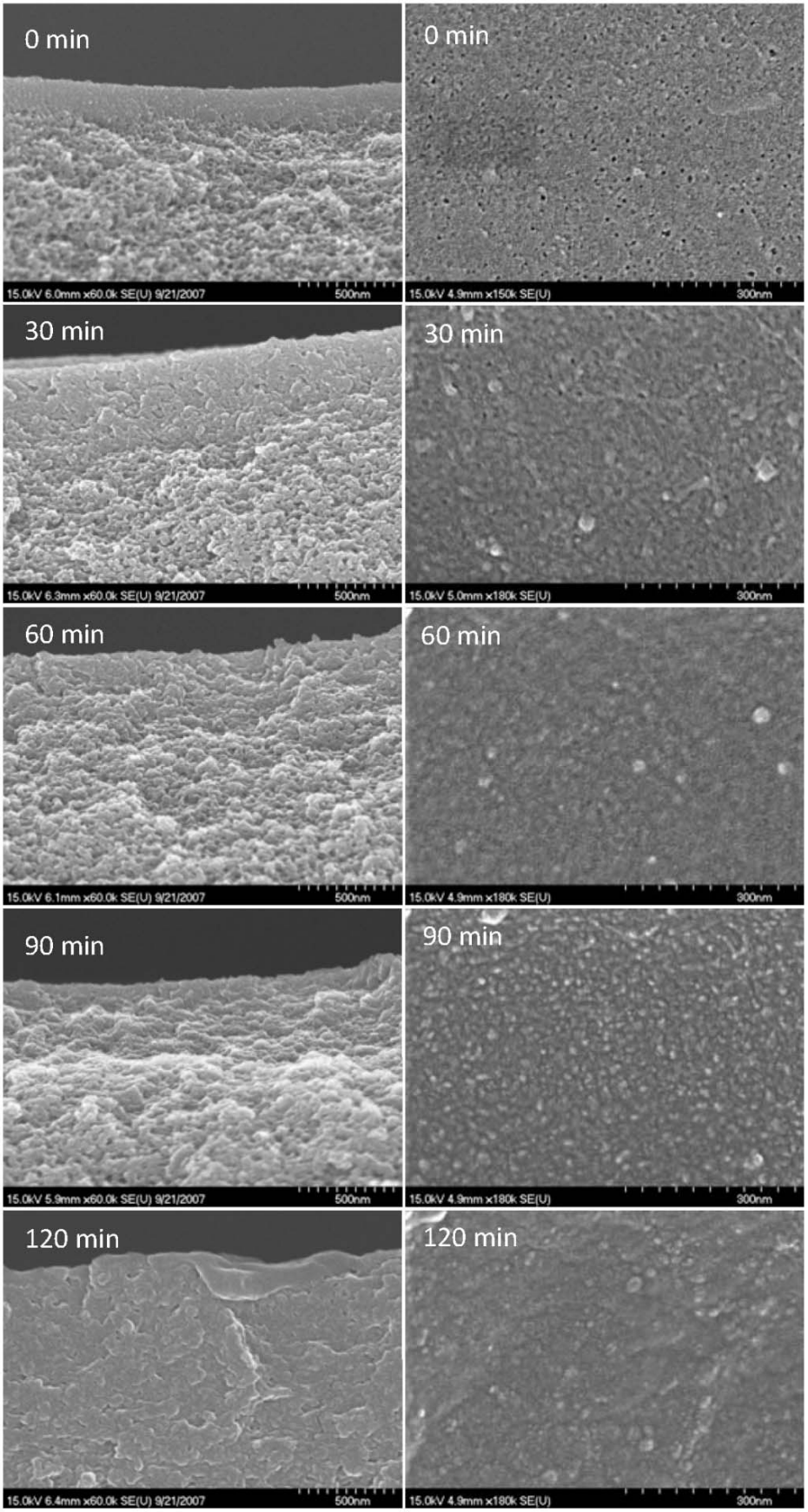

Figure 2.4 Morphological changes of the P84 membrane cross-sections (left) and surfaces (right) when modified by PEI with various modification times.

possible that the membrane surface becomes covered by a thin layer of PEI. Meanwhile, the pores may be filled by PEI molecules on account of their diffusion into the pores and anchoring onto the pore walls. The cross-sectional images show a relatively dense layer on top of the membranes. For the unmodified membrane, the thickness of the dense layer was about 100 nm. After 30 min modification, the thickness of the dense layer increased to approximately 400 nm. With longer modification time, the top layer of the membrane became less porous and the dense layer became thicker (120 min). Both the decrease in pore size near the membrane surface and the increase in thickness of the top dense layer may be responsible for the decrease in permeation flux observed in the PEI-modified P84 membranes [21]. Initially, PEI molecules may diffuse from both the active layer side and the support layer side of the membrane. With the surface pore size decreasing, diffusion from the active layer side would slow gradually. However, diffusion from the support layer side may continue until the membrane is taken out from the PEI solution. Consequently, with high concentration of PEI or long modification time the membrane becomes dense and exhibits low permeation flux [15].

2.3.4 Effect of modification on membrane chemistry

Changes in chemical structure during the modification process were measured by ATR-FTIR and the results are illustrated in Figure 2.5. For the original P84 membrane, a few characteristic absorption bands were observed at 1778 cm^{-1} (symmetric C=O stretching, imide I), 1719 cm^{-1} (asymmetric C=O stretching, imide I) and 1360 cm^{-1} (C-N-C stretching, imide II). As the chemical reaction progressed, the

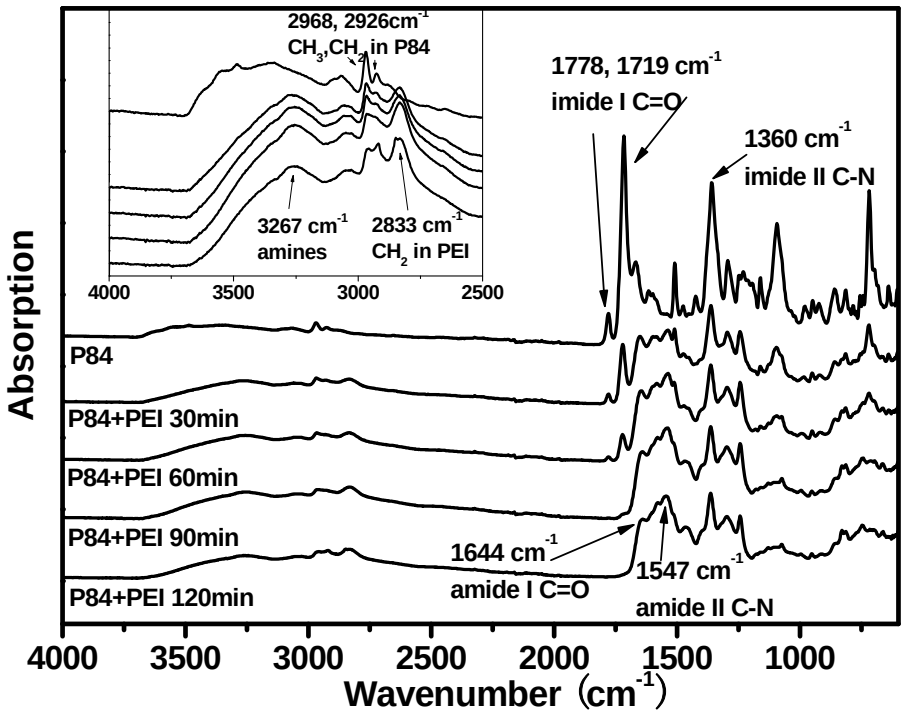

Figure 2.5 ATR-FTIR spectra of P84 membranes modified by PEI with various modification times.

absorption peaks of the imide I bands gradually diminished and disappeared altogether after 90 min. Over this same progression, the characteristic peaks of amide groups at 1644 cm^{-1} (C=O stretching, amide I) and 1547 cm^{-1} (C-N stretching, amide II) appeared and increased progressively [17]. The bands in higher wavenumber regimes (4000-2500 cm^{-1}) are shown in the inset of Figure 2.5. The absorption peaks at 2968 $cm^{-1}$and 2926 cm^{-1} represent CH_3 and CH_2 groups of P84 polyimide, respectively. After reaction with PEI, the absorption band of CH_2 group of PEI appeared at 2833 cm^{-1} and became stronger with increasing reaction time. The band at 3267 cm^{-1} (N-H vibrations) indicates the existence of free amine groups. Judging from the FTIR data, one can conclude that within 90 min of reaction, the imide bonds were completely transformed into amide bonds, resulting in the amine modifier covalently bound to the P84 membrane with free amine functionalities. Interestingly,

there is a good correlation between the extent of modification and the salt rejection performance of the membrane. It seems that upon completion of the modification membrane surface properties such as chemical composition and pore structure remained constant, which made the membrane show a constant value of salt rejection.

2.3.5 Thermal properties of the PEI-modified P84 membranes

Thermal properties of the P84 membranes before and after modification were investigated by TGA and DSC, and the results are displayed in Figure 2.6 (dTGA) and Figure 2.7, respectively. The dTGA trace of the original P84 membrane exhibits two decomposition peaks. The first one at < 100 ˚C is attributed to the release of absorbed water [17]. The P84 membrane is thermally stable up to 400 ˚C and

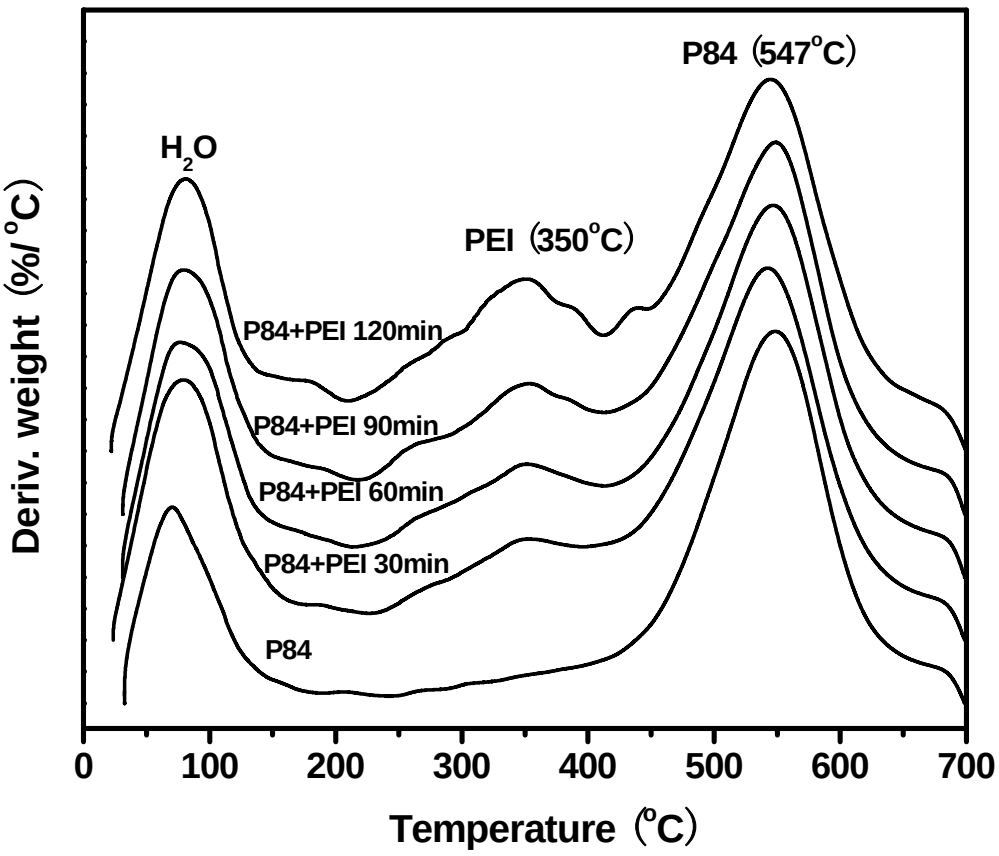

Figure 2.6 Derivative TGA (dTGA) traces of the P84 membranes modified by PEI with various modification times.

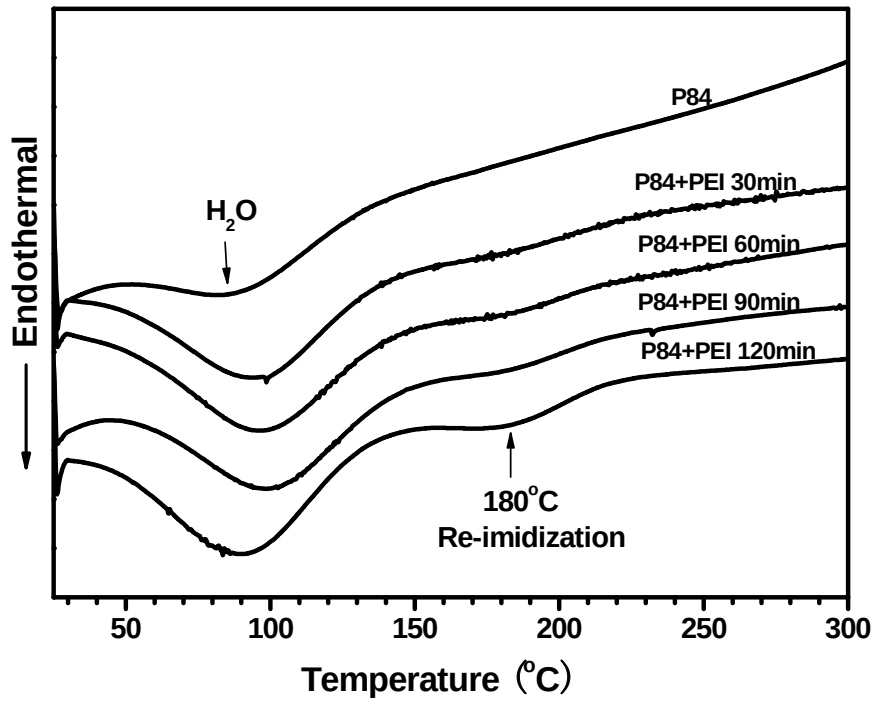

Figure 2.7 DSC traces of the P84 membranes modified by PEI with various modification times.

degradation of the polymer main chain occurs at 547 ˚C. After modification by PEI, however, a new peak at 350 ˚C appears and the peak intensity increases with increasing modification time. This result is in good agreement with the ATR-FTIR results. That is, with additional reaction time, the membrane takes on more PEI. With regard to the DSC curves, the original P84 membrane shows only one transition at roughly 100 ˚C, attributed to the evaporation of absorbed water. After modification, however, a peak at roughly 180 ˚C gradually appears, corresponding to the reaction of re-imidization [22]. The DSC curves suggest the chemical structure of the PEI-modified P84 membrane is stable up to 150 ˚C.

Thermal stability of the membranes was confirmed by ATR-FTIR analysis. The membranes with 90 min modification were annealed under vacuum for 2 hours at 100 ˚C, 200 ˚C and 300 ˚C, respectively. Figure 2.8 gives the ATR-FTIR spectra of these

membranes. No absorption due to imide groups can be detected after 100 ˚C treatment, indicating the chemical structure remained intact at 100 ˚C. After treatment at 200 ˚C, however, strong imide absorption can be seen and the amide absorption has almost disappeared, indicating re-imidization, which is in agreement with the DSC result. The spectrum of the 300 ˚C annealed sample still shows the absorption band of the CH_2 group of PEI at 2822 cm^{-1}, which means the PEI did not burn off completely at this temperature. On the other hand, with heat treatment at temperature higher than 200 ˚C, sample color was observed to change from light yellow to dark brown and the membranes became brittle. One possible explanation for this behavior is that the polymer undergoes backbone scission with incorporation of an amine as an end group [22].

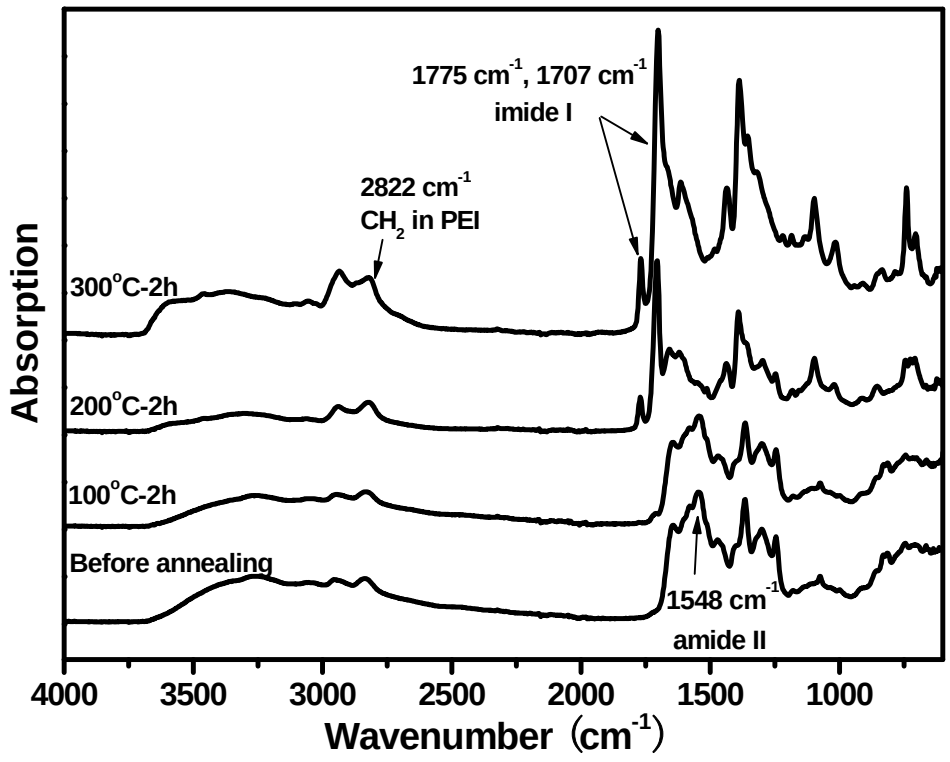

Figure 2.8 ATR-FTIR spectra of the PEI-modified P84 membranes before and after heat treatment at various temperatures.

2.3.6 Effect of annealing on membrane performance

Desalination performance of the membranes after annealing is shown in Table 2.2. Although annealing has been commonly used for improving membrane selectivity due to the densification of the selective skins [23], this treatment afforded no apparent improvement for this system. Instead, the membranes showed good stability at temperature below 100 ˚C. For example, after 100 ˚C treatment, the salt rejection and permeation flux were almost unchanged. It is suggested that the PEI-modified membranes have a rigid cross-linked structure and thus the molecular movement is limited at this temperature. It should be noted that the decrease in flux upon drying was likely induced by the shrinking of the nanopores due to the strong capillary forces [24]. After annealing at 200 ˚C and above, however, pore collapse may happen due to re-imidization. Thus, the permeation flux became impractically low for nanofiltration although the salt rejection did increase somewhat.

Table 2.2 Effect of annealing on membrane performance[a]

Annealing temperature (^{o}C)	Flux ($m^3m^{-2}day^{-1}$)[b]	Salt rejection (%)[b]
R.T.	0.48 ± 0.20	57.0 ± 0.7
100	0.33 ± 0.07	58.3 ± 4.2
200	0.034	90.5
300	Very low	-----

Notes: [a]Membranes were dried by solvent exchange method and annealing was carried out under vacuum for 2h at various temperature. [b]Test condition: 2.0 g/L NaCl aqueous solution, 13.8 bar and room temperature.

2.3.7 Effect of treatment with organic solvents on membrane performance

The membrane samples with 90 min modification were treated for 16 hours by immersion into one of several organic solvents to examine their solvent resistance. Desalination performance of the membranes before and after treatment is shown in Table 2.3. It is interesting that both the salt rejection and permeation flux values were almost unchanged after treatment by THF, methanol, or acetone. Even after treatment

with DMF, NMP or DMAc, salt rejection still did not change much. The slightly decreased permeation flux may be caused by swelling and/or capillary forces induced by solvent exchange with water. These results suggest both the chemical structure and the pore dimension of the membrane should have excellent resistance to most organic solvents, since both of these factors are critical for membrane desalination performance. This solvent resistance is attributed to the cross-linked structure resulting from the reaction between the polyimide and the PEI. Thus this type of membrane shows promise for use in solvent-resistant nanofiltration (SRNF).

Table 2.3 Effect of treatment by organic solvents on membrane performance[a]

Solvents	Before treatment		After treatment	
	Flux ($m^3m^{-2}day^{-1}$)[b]	Salt rejection (%)[b]	Flux ($m^3m^{-2}day^{-1}$)[b]	Salt rejection (%)[b]
THF	1.22	49.2	1.25	48.5
MeOH	1.22	50.0	1.28	51.0
Acetone	1.28	47.0	1.30	46.1
DMF	1.06	52.1	0.80	51.4
NMP	1.10	50.9	0.80	51.0
DMAc	1.25	48.5	0.70	49.9

Notes: [a]The membranes were immersed into various organic solvents for 16h and then immersed into DI water for 2h. [b]Test condition: 2.0 g/L NaCl aqueous solution, 13.8 bar and room temperature.

2.3.8 Effect of treatment with acids and bases on membrane performance

In order to examine their pH resistance, the membranes were immersed into aqueous solutions with pH between 0 and 12 for 16 hours. Desalination performance of the membranes before and after treatment is shown in Table 2.4. It was observed that at a pH of 0 the membrane became brittle while at a pH of 12 the membrane gelled, probably due to the degradation of the polymer main chain at both of the pH extremes. However, under moderate acid and base conditions ($2 \leq pH \leq 10$) the membranes showed good stability. It should be noted that after acid treatment the

membranes had increased salt rejection, while after base treatment the membranes had reduced salt rejection. This rejection variation may be caused by the change of the membrane charge strength. Considering the amine groups on the membranes, residual acid may make the membranes more positively charged whereas residual base may make them less charged.

Table 2.4 Effect of treatment by acids and bases on membrane performance[a]

pH[b]	Before treatment		After treatment	
	Flux ($m^3m^{-2}day^{-1}$)[c]	Salt rejection (%)[c]	Flux ($m^3m^{-2}day^{-1}$)[c]	Salt rejection (%)[c]
0	1.35	45.9	-----[d]	-----[d]
2	1.15	52.7	1.18	58.0
5	1.25	48.1	1.30	50.3
8	1.28	49.4	1.28	38.7
10	1.38	43.0	1.38	35.7
12	1.25	48.5	-----[e]	-----[e]

Notes: [a]The membranes were immersed into various acids and bases for 16h and then immersed into DI water for 2h. [b]The pH was adjusted by HCl and NaOH. [c]Test condition: 2.0 g/L NaCl aqueous solution, 13.8 bar and room temperature. [d]Membranes became brittle. [e]The top layer exhibited poor mechanical integrity.

2.3.9 Membrane performance for removal of multivalent metal ions

Table 2.5 shows the membrane performance for removal of various metal ions from water. It can be seen that the membrane shows better rejection to NaCl in acid condition (72.7%) than in neutral condition (50.9 ± 5.1%). This is because the membrane became more positively charged in acid. In addition, it can be observed that with the same anion Cl^-, the rejection increases in the order of $Na^+ < Zn^{2+}$ or $Cu^{2+} < Fe^{3+}$ or Al^{3+}. Thus, the metal ions with higher valence can be removed more efficiently, in agreement with the Donnan effect. The flux variation for each salt may be related to ionic concentrations.

Table 2.5 Membrane performance for removal of metal ions[a]

Salts	Flux ($m^3m^{-2}day^{-1}$)[b]	Rejection (%)[b]
NaCl	1.16	72.7
$CuCl_2$	1.03	92.9
$ZnCl_2$	0.86	94.5
$FeCl_3$	0.80	98.2
$AlCl_3$	0.92	99.2

Notes: [a]Feed concentration: 10 mM; pH = 2 adjusted by HCl. [b]Test pressure: 13.8 bar; permeate concentrations were measured by ICP-MS analysis.

It is also of interest to consider the separation efficiency in a mixture of ions of different valence. As shown in Table 2.6, the rejection to divalent or trivalent ions was not significantly affected by the variation of salt concentrations. However, the rejection to monovalent Na^+ ion was reduced in the presence of large amount of Zn^{2+} or Fe^{3+}. Similar results have been reported in the literature [8]. This ion selectivity may be determined by several factors, such as the size and charge of each ion, the concentration of anions and cations, and the shielding of membrane charge by ions in solution [1]. With large amount of $ZnCl_2$ or $FeCl_3$, the high concentration of counter-ion Cl^- may result in efficient shielding of membrane charge. Although the less charged membrane may have decreased rejection to all the cations, it has stronger influence on the monovalent cation (Na^+) than on the di- or trivalent ions (Zn^{2+} or Fe^{3+}) because of the Donnan effect. On the other hand, the metal ion with higher valence has a larger hydrated radius and can hold the water molecules more strongly during filtration [25, 26]. For these reasons, the rejection to Na^+ ion was decreased when mixed with Zn^{2+} or Fe^{3+}, while the rejection to Zn^{2+} or Fe^{3+} was almost unchanged.

Table 2.6 Rejection of ionic species in a solution containing mixtures of salts[a]

(a) $ZnCl_2$ and NaCl

Feed Zn^{2+} (mM)	Feed Na^+ (mM)	Flux ($m^3m^{-2}day^{-1}$)[b]	Rejection of Zn^{2+} (%)[b]	Rejection of Na^+ (%)[b]
1	10	0.96	96.0	72.7
10	10	0.91	96.1	57.4
10	1	0.93	97.1	4.8

(b) $FeCl_3$ and NaCl

Feed Fe^{3+} (mM)	Feed Na^+ (mM)	Flux ($m^3m^{-2}day^{-1}$)[b]	Rejection of Fe^{3+} (%)[b]	Rejection of Na^+ (%)[b]
1	10	0.99	78.5 [c]	69.9
10	10	0.83	97.0	56.7
10	1	0.81	97.1	21.3

Notes: [a]pH = 2 adjusted by HCl. [b]Test pressure: 13.8 bar; permeate concentrations were measured by ICP-MS analysis. [c]Result may not be accurate because permeate concentration was close to the test limit.

2.4 Conclusions

This work provided novel positively charged NF membranes via chemical modification of P84 asymmetric membranes using PEI as modifier. It was observed that the modification conditions affected both the pore size of the membranes and their NF properties. For a given P84 membrane, a maximum rejection rate was observed at a certain modification time after which point no additional benefit was attained with additional reaction time. On the other hand, the flux continued decreasing with additional reaction time. It is suggested that the membrane properties are governed by both the chemistry and morphology of the membrane.

Due to their cross-linked structure, the modified membranes showed good stability in various conditions, especially in organic solvents and mild acid or base. This stability is important for application in treatment of industrial wastewater, for example during cleaning after fouling. These positively charged membranes showed good performance for multivalent heavy metal removal. Studies are now ongoing to

evaluate membrane resistance to fouling, including further modifications to improve resistance to common foulants, such as natural organic matter (NOM).

2.5 References

[1] A.I. Schäfer, A.G. Fane, T.D. Waite (Eds.), Nanofiltration - Principles and Applications, Elsevier Ltd., 2005.

[2] R.W. Baker (Ed.), Membrane Technology and Applications, John Wiley & Sons, Ltd., Chichester, 2004.

[3] R.J. Petersen, Composite reverse osmosis and nanofiltration membranes, *J. Membr. Sci.*, 83 (1993) 81.

[4] A. Bhattacharya, P. Ghosh, Nanofiltration and reverse osmosis membranes: theory and application in separation of electrolytes, *Rev. Chem. Eng.* 20 (2004) 111.

[5] J.M.M. Peeters, J.P. Boom, M.H.V. Mulder, H. Strathmann, Retention measurements of nanofiltration membranes with electrolyte solutions, *J. Membr. Sci.*, 145 (1998) 199.

[6] A.W. Mohammad, R. Othaman, N. Hilal, Potential use of nanofiltration membranes in treatment of industrial wastewater from Ni-P electroless plating, *Desalination*, 168 (2004) 241.

[7] A. Bougen, M. Rabiller-Baudry, B. Chaufer, F. Michel, Retention of heavy metal ions with nanofiltration inorganic membranes by grafting chelating groups, *Sep. Purif. Technol.*, 25 (2001) 219.

[8] S. Alami-Younssi, A. Larbot, M. Persin, J. Sarrazin, L. Cot, Rejection of mineral salts on a gamma alumina nanofiltration membrane application to environmental process, *J. Membr. Sci.,* 102 (1995) 123.

[9] L.M. Ortega, R. Lebrun, J.-F. Blais, R. Hausler, Treatment of an acidic leachate containing metal ions by nanofiltration membranes, *Sep. Purif. Technol.,* 54 (2007) 306.

[10] R.F. Childs, A.M. Mika, A.K. Pandey, C. McCrory, S. Mouton, J.M. Dickson, Nanofiltration using pore-filled membranes: effect of polyelectrolyte composition on performance, *Sep. Purif. Technol.,* 22-23 (2001) 507.

[11] T. Xu, W. Yang, A novel positively charged composite membranes for nanofiltration prepared from poly(2,6-dimethyl-1,4-phenylene oxide) by in situ amines crosslinking, *J. Membr. Sci.,* 215 (2003) 25.

[12] R. Du, J. Zhao, Properties of poly(N,N-dimethylaminoethyl methacrylate)/ polysulfone positively charged composite nanofiltration membrane, *J. Membr. Sci.,* 239 (2004) 183.

[13] J. Wang, Z. Yue, J. Economy, Novel method to make a continuous micro-mesopore membrane with tailored surface chemistry for use in nanofiltration, *J. Membr. Sci.*, 308 (2008) 191.

[14] H. Ohya, V.V. Kudryavtsev, S.I. Semenova, Polyimide Membranes: Applications, Fabrications, and Properties, Gordon and Breach, Tokyo, 1996.

[15] W. Albrecht, B. Seifert, Th. Weigel, M. Schossig, A. Hollander, Th. Groth, R. Hilke, Amination of poly(ether imide) membranes using di- and multivalent amines, *Macromol. Chem. Phys.*, 204 (2003) 510.

[16] C. Trimpert, G. Boese, W. Albrecht, K. Richau, Th. Weigel, A. Lendlein, Th. Groth. Poly(ether imide) membranes modified with poly(ethylene imine) as potential carriers for epidermal substitutes, *Macromol. Biosci.*, 6 (2006) 274.

[17] X. Qiao, T.-S. Chung, Diamine modification of P84 polyimide membranes for pervaporation dehydration of isopropanol, *AIChE*, 52 (2006) 3462.

[18] Y.H. See Toh, F.W. Lim, A.G. Livingston, Polymeric membranes for nanofiltration in polar aprotic solvents. *J. Membr. Sci.*, 301 (2007) 3.

[19] M. Mulder, Basic Principles of Membrane Technology, Kluwer, London, 1996.

[20] K. Boussu, C. Vandecasteele, B. Van der Bruggen, Study of the characteristics and the performance of self-made nanoporous polyethersulfone membranes, *Polymer*, 47 (2006) 3464.

[21] Y.H. See-Toh, F.C. Ferreira, A.G. Livingston, The influence of membrane formation parameters on the functional performance of organic solvent nanofiltration membranes, *J. Membr. Sci.*, 299 (2007) 236.

[22] C.E. Powell, X.J. Duthie, S.E. Kentish, G.G. Qiao, G.W. Stevens, Reversible diamine cross-linking of polyimide membranes, *J. Membr. Sci.*, 291 (2007) 199.

[23] X. Qiao, T.-S. Chung, K.P. Pramoda, Fabrication and characterization of BTDA-TDA/MDI (P84) co-polyimide membranes for the pervaporation dehydration of isopropanol, *J. Membr. Sci.*, 264 (2005) 176.

[24] W. MacDonald, C.Y. Pan, Method for drying water-wet membranes, US patent 3,842,515 (1974).

[25] J. Kielland, Individual activity coefficients of ions in aqueous solutions, *J. Am. Chem. Soc.*, 59 (1937) 1675.

[26] B. Tansel, J. Sager, T. Rector, J. Garland, R.F. Strayer, L. Levine, M. Roberts, M. Hummerick, J. Bauer, Significance of hydrated radius and hydration shells on ionic permeability during nanofiltration in dead end and cross flow modes, *Sep. Purif. Technol.*, 51 (2006) 40.

CHAPTER 3

USING POLYELECTROLYTE COATINGS TO IMPROVE FOULING RESISTANCE OF A POSITIVELY CHARGED NANOFILTRATION MEMBRANE

3.1 Introduction

Membrane processes are often hindered by fouling due to a buildup of the material being rejected [1]. As fouling progresses, membrane productivity declines; higher pressures and thus more energy must be expended to achieve the desired throughput. Cleaning strategies must be implemented to remove foulant material and restore productivity. In many cases, however, the fouling is irreversible and the membrane elements must be replaced [2]. Organic impurities in the water such as proteins, humic substances, and polysaccharides have been implicated as strong, irreversible foulants [3]. Such foulants can adsorb to the membrane surface due to hydrophobic interactions, hydrogen bonding, van der Waals attractions, and electrostatic interactions [4]. Therefore, an effective method to reduce fouling is to modify the membrane surface to minimize these adsorptive interactions between foulant and membrane [3, 4, 5].

Several surface characteristics of membranes are known to be strongly related to fouling such as hydrophilicity, roughness and charge [6, 7]. It has been generally acknowledged that membranes with hydrophilic surfaces are less susceptible to fouling [4, 8, 9]. Membranes with rougher surfaces are observed to be more favorable for foulant attachment resulting in more extensive fouling and faster fouling rates [7, 10, 11, 12, 13]. For charged organic compounds, electrostatic attraction or repulsion forces between the component and the membrane, which depend on pH, influence the

degree of fouling; when the surface and foulant have similar charge, foulant adsorption is reduced [14, 15]. Therefore, development of membranes with a smooth hydrophilic surface that has a surface charge similar to the foulant seems to be desirable for antifouling purposes [16].

Over the last few years researchers have devised various strategies to modify membrane surfaces, which can be generally divided into two categories: grafting and coating [4]. In grafting, hydrophilic species such as polyethylene glycol and polyacrylic acid can be covalently bonded to the membrane surface by chemical, low-temperature plasma, or photochemical techniques [17, 18, 19, 20, 21]. Although surface grafting has shown high fouling resistance, the technique leads to a permanent change of membrane chemistry and properties. For example, membrane permeability may be reduced because the grafting layer adds an extra hydraulic resistance [6, 17]. Grafting may also increase manufacturing costs due to process complications, time consumption, and extensive use of organic solvents and monomers [4]. Compared to grafting, coating a thin layer of water-soluble polymers or surfactants from solution by physical adsorption provides certain distinct advantages for surface modification [22, 23, 24, 25]. Adsorbed coatings are relatively simple to apply, the process can be performed in existing membrane installations, and the structure of the membrane is not likely to be affected by the adsorbed molecules. In addition, the type of coating can be tailored to the specific application of interest [25]. Until now, most studies of adsorbed coatings have focused on ultrafiltration membranes. Preparation of

antifouling nanofiltration membranes using the coating technique has not been reported.

Depending on adsorption affinity with the membrane surface, the adsorbed coating layer can be stable or erasable. Thin films formed through layer-by-layer (LbL) deposition of positively and negatively charged polyelectrolytes show good stability due to electrostatic attraction among the membrane surface and the deposited layers [26]. These multilayer polyelectrolyte films have previously been deposited on ultrafiltration substrate membranes to prepare composite membranes for nanofiltration [26, 27]. Although anti-fouling properties of the LbL membranes are still rarely reported [28], this type of membrane may potentially have high fouling resistance due to the hydrophilicity of the applied polyelectrolytes and controllable surface charge [29]. On the other hand, hydrogen-bonded layer-by-layer films have attracted considerable attention in recent years because the hydrogen bonding can be altered by changes in solution pH and thus the films can be erased and replaced [30, 31, 32, 33, 34]. When applying this erasable film to the membrane surface, any foulant material that deposits on top of the film could be effectively removed by detaching the film from the membrane surface, which leaves behind a clean membrane. It may be much easier and more cost-effective to remove and replace the film instead of replacing the membrane. To the authors' knowledge, such an application has not been previously proposed.

In a previous study, positively charged nanofiltration membranes were developed by chemical modification of P84 copolyimide membranes using branched

polyethylenimine (PEI) [35]. The PEI-modified polyimide membranes (P84-PEI membranes) have a highly cross-linked structure which makes these membranes stable in various operating environments including high temperature (100˚C), organic solvents, and mild acid and base ($2 \leq pH \leq 10$). Meanwhile, due to the Donnan repulsion effect, these membranes showed efficient removal of multivalent heavy metal ions (> 95%) and may potentially be used for treatment of industrial wastewater.

In the present study, the P84-PEI membranes were further modified by adsorption of a layer of polymers from a dilute solution in a dynamic manner [36]. Polyvinyl alcohol (PVA), polyacrylic acid (PAA) and polyvinyl sulfate-potassium salt (PVS), were tested as modifying agents. The effect of these coatings on membrane surface roughness and hydrophilicity was characterized by atomic force microscopy (AFM) and contact angle measurements. The charge and pore size of the unmodified and modified membranes were qualitatively analyzed using ions and uncharged sugars as probes. Stability of the coating layers during acid or base cleaning was studied by attenuated total reflectance Fourier transform infrared spectroscopy (ATR-FTIR). Fouling experiments were carried out in a cross-flow setup using three model foulants, bovine serum albumin (BSA), sodium alginate (SA) and humic acid sodium salt (HA) representative of proteins, polysaccharides and natural organic matter (NOM). The effect of the polymer coatings for fouling prevention was tested with respect to both the reduction of flux decline and the cleanability by acid after fouling.

3.2 Experimental

3.2.1 Chemicals

P84 powder was purchased from HP Polymer Inc. and dried in vacuum at 160˚C for 12 hours before use. PEI (MW: 25,000), PVA (MW: 89,000 - 98,000), PAA (MW: 250,000) and PVS (MW: 170,000) were purchased from Aldrich. Three dilute coating solutions with concentrations of 50 mg/L were prepared by dissolving PVA, PAA or PVS in deionized (DI) water at 80˚C overnight. The PVS solution was filtered before use to remove the insoluble impurities. The pH of the PVA, PAA and PVS solutions were 5.7, 4.7, and 5.8, respectively. No pH adjustment was made. The model foulants, BSA (MW: 66,000, ≥98%, Sigma), HA (sodium salt, Aldrich) and SA (Fluka) were used without further treatment. A concentration of 100 mg/L was applied for all the fouling experiments and the pH of these foulant solutions were 6 - 7 without any adjustment. Three sugars, D-(+)-galactose (Sigma-Aldrich, ≥99%), D-(+)-maltose monohydrate (Sigma-Aldrich, ≥99%) and D-(+)-raffinose pentahydrate (Sigma, ≥99%), were used as received. All of the other inorganic reagents including HCl, NaOH, NaCl, Na_2SO_4, $CaCl_2$ were of analytical grade and used as received.

3.2.2 Cross-flow apparatus

A cross-flow system was used for the dynamic coating of polyelectrolyte on membrane surfaces and the following fouling experiments. The system was continuous, able to achieve steady state, and allowed for long-term operation. The cross-flow unit was designed as described in a concurrent study [37]. Running the experiment involved placing a rectangular (19.1 cm × 14.0 cm) flat sheet membrane of 140 cm^2 active area into a permeation cell (SEPA II, GE Osmonics) and securing it

with an O-ring and a hydraulic press. A pump was used to circulate the feed solution with a flow rate of around 800 mL/min regulated by the variable-frequency motor. The trans-membrane pressure was controlled by a metering valve installed in the concentrate line immediately after the membrane cell. The operating temperature was controlled between 20 and 21˚C by a heat exchanger. For measurement of permeate flux, the permeate was fed into a collection vessel mounted on a balance. Balance measurements were logged automatically by the data acquisition/control system. For continuous balance measurements, a self-emptying collection vessel was used. Data analysis was performed with programs written in Matlab. Salt rejection was calculated as $R = (1 - \sigma_p/\sigma_f) \times 100\%$, where σ_p and σ_f were the conductivity of the permeate and the feed, respectively. Conductivity was measured with a bench-top conductivity meter (Oakton CON 510).

3.2.3 Preparation of the positively charged NF membranes (P84-PEI membranes)

The P84-PEI membranes were prepared with a procedure slightly modified from that described previously in Chapter 2 [35]. The casting solution was prepared by dissolving P84 powder in N, N-dimethylformamide (DMF) to give a polymer concentration of 23%. The polymer solution was then cast onto a polyester support (Calendered PET from Crane Nonwovens) followed by immediate immersion into a room temperature water bath. After overnight immersion in the water bath the membrane was rinsed with and stored in DI water.

Chemical modification was conducted by immersing a membrane into a 5% PEI solution (wt/vol) in a mixture of isopropanol and water (volume 1:1) at 80˚C for 40 -

60 min until the desired permeability was obtained. The membrane was then rinsed several times using dilute HCl solution at pH 3 to remove any loosely bound PEI, and finally stored in DI water until use.

3.2.4 Preparation of surface coatings onto the P84-PEI membranes

Surface coating experiments were carried out with the cross-flow apparatus. First, the P84-PEI NF membrane was compacted at a pressure of 13.8 bar (200 psi) for 10 – 12 hours until a steady state was obtained. In order to accelerate the compaction process, a higher pressure of 20.7 bar (300 psi) was applied for several hours previously. Six liters of a 2.0 g/L NaCl aqueous solution were used as feed. Permeation flux and salt rejection performance of the membrane were recorded. After compaction, the membrane was rinsed with copious amounts of DI water to remove salt. Then the feed was changed to 6L of a 50 mg/L polyelectrolyte (PVA, PAA or PVS) aqueous solution. This feed was circulated for 8 - 12 hours until the flux reached a steady state. At this time, the maximum amount of polyelectrolyte was assumed to be adsorbed on the membrane surface forming a protective layer. After rinsing with DI water to remove any non-sorbed polyelectrolyte, the coated membrane was tested for its desalination performance (permeation flux and salt rejection) at 13.8 bar using 6L of a 2.0 g/L NaCl aqueous solution as feed. This test was conducted to examine the stability of the surface coating in the salt solution and the effect of the coating on membrane desalination performance.

3.2.5 Removability of the surface coatings by acid or base cleaning

In order to determine if the coating was removable, the coated membrane was washed for 10 - 12 hours at a low pressure of 4.8 bar (70 psi) with an HCl solution at pH 2. After cleaning, the coated membrane was examined for its desalination performance at 13.8 bar using 6L of a 2.0 g/L NaCl aqueous solution as feed. The removability of the coating was characterized by comparison of the flux change before and after acid cleaning.

ATR-FTIR measurements were made on three membrane samples coated with PVA, PAA and PVS, respectively. Then the samples were cleaned by HCl at pH 2 or base at pH 9.1 under stirring for 15 - 20 hours. The base solution was prepared using 0.1 mol/L NH_4Cl solution and 0.1 mol/L $NH_3 \cdot H_2O$ solution with a volume ratio of 2:1 to give a buffer solution of pH 9.1. The cleaned samples were re-measured by ATR-FTIR to determine if the coating materials were removed.

3.2.6 Membrane fouling and cleaning experiments

For the fouling studies, the uncoated or coated membranes were first compacted until a stable flux was reached (refer to section 2.4). Then the feed was changed to 6L of an aqueous solution containing 100 mg/L model foulant and 2 g/L NaCl. The fouling experiments were performed for 12 - 20 hours, and the flux decline was recorded.

Following the fouling experiments, membrane cleaning was conducted to determine if the flux could be restored. The uncoated or coated membranes after fouling were washed for 10 - 12 hours at a low pressure of 4.8 bar (70 psi) with an HCl solution at pH 2. After cleaning, the membrane was rinsed with copious amounts

of DI water. Its desalination performance was examined at 13.8 bar using 6L of a 2.0 g/L NaCl aqueous solution as feed. The cleanability of the uncoated and coated membranes was characterized by comparison of the flux change before and after acid cleaning. Conductivity was also measured to determine changes in salt rejection with modification.

3.2.7 Characterization of surface charge and surface pore size

Surface charge and surface pore size of the uncoated and coated membranes were characterized qualitatively using ions and uncharged sugars as probes, respectively. The order of rejection to three salts of $CaCl_2$, NaCl and Na_2SO_4 may indicate the membrane surface charge to be negative or positive [1, [38]]. Experiments were performed using a dead-end filtration cell (Sterlitech HP4750) with a procedure as described in a previous study [35]. A 2.0 g/L aqueous solution of each salt was used as feed. Salt rejection was calculated from the conductivity of the permeate and the feed (see section 2.2).

The rejection to uncharged solutes may be determined primarily by the surface pore size of the membrane [1, 39]. Therefore, rejection to three sugars galactose (180 Da), maltose (342 Da) and raffinose (504 Da) was used to characterize relative pore size of the uncoated and coated NF membranes. A 10 mmol/L aqueous solution of each sugar was used as feed. Sugar concentrations in the permeate and feed solutions were determined by a colorimetric method based on treatment with phenol and sulfuric acid [40].

3.2.8 Physical characterization methods

ATR-FTIR spectra were collected at room temperature over a scanning range of 600 - 4000 cm^{-1} with a resolution of 4.0 cm^{-1}, using a Nexus 670 FT-IR (Thermo Electron Corporation, Madison, WI) with a Golden Gate™ MKII Single Reflectance ATR (Specac Inc., Woodstock, GA). The spectrometer was installed with a deuterated triglycine sulfate-potassium bromide (DTGS-KBr) detector and KBr beamsplitter. Spectral analysis was performed using FT-IR software (OMNIC, Thermo Electron Corporation, Madison, WI).

Atomic force microscopy (AFM) was performed in air using a Veeco / Digital Instruments Dimension 3100 AFM. Surface roughness of the membranes was obtained by surface image analysis. Membrane hydrophobicity was estimated by water drop contact angle measurement using a goniometer (KSV Instruments Model: CAM 200). The dry membranes were fixed flat on a glass slide using double-sided tape. Five measurements were taken for the static contact angle immediately after the droplet was placed on the membrane.

3.3 Results and discussion

3.3.1 Preparation and characterization of membranes with surface coatings

3.3.1.1 Surface chemistry of the P84-PEI NF membrane

Figure 3.1 shows the chemical reaction between P84 copolyimide and PEI. It can be seen that the resultant P84-PEI NF membrane contains carbonyl, amide, amine, ammonium and phenyl groups on the surface. Among them, the amine and ammonium groups provide positive charge on the membrane surface [35]. Therefore, this membrane could adsorb negatively charged foulants via electrostatic attraction.

Common foulants like BSA, HA and SA contain carboxylic groups and thus are negatively charged at neutral pH [41, 42, 43].

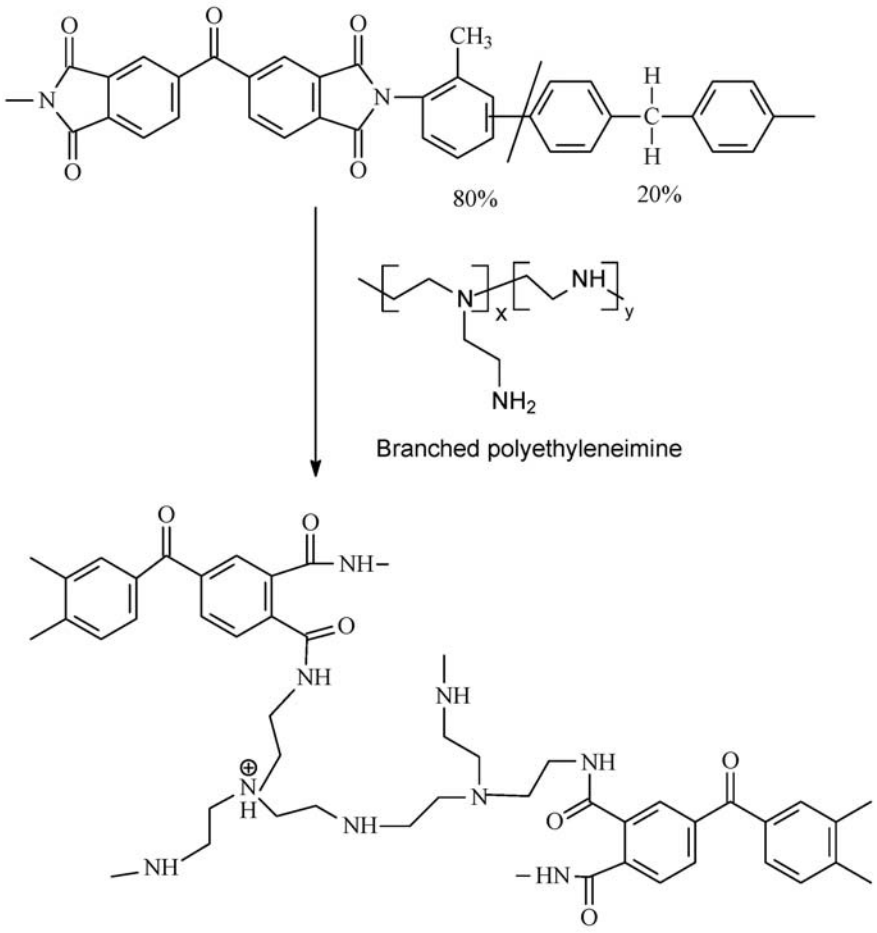

Figure 3.1 Chemical reaction between P84 copolyimide and branched polyethylenimine.

To address this problem, a polymeric coating was applied as a protective layer. By selecting different coating materials the membrane surface properties like hydrophilicity, roughness and charge could be modified and optimized for different feed compositions. In this research, we used three high molecular weight polymers PVA, PAA and PVS as the coating materials representing neutral, partially charged and highly charged polyelectrolytes, respectively.

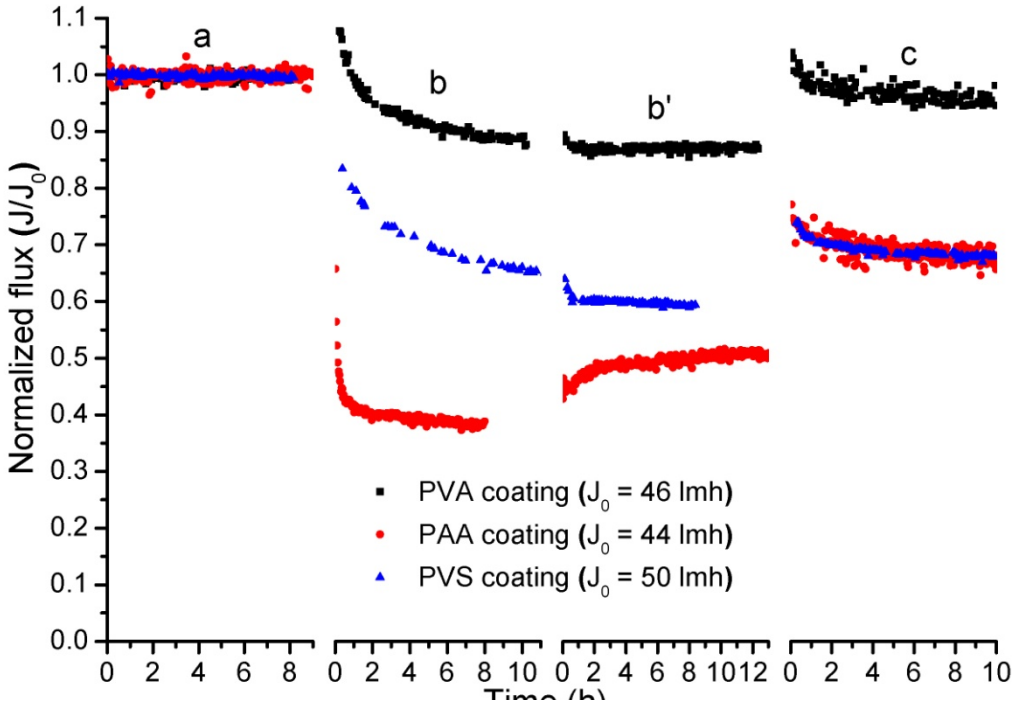

Figure 3.2 Normalized flux at different stages of the coating/cleaning experiments. (a) Membrane compaction with 2 g/L NaCl solution; (b) flux during coating with 50 mg/L polymer solution; (b′) flux with 2 g/L NaCl solution after coating; (c) flux with 2 g/L NaCl solution after cleaning with HCl solution at pH 2. A pressure of 13.8 bar was applied for all the stages.

3.3.1.2 Effect of surface coating on membrane desalination performance

Figure 3.2 shows the membrane permeate flux at different stages of the coating and cleaning experiments. Figure 3.2a gives the stabilized water fluxes of the P84-PEI NF membranes after compaction for several hours. For comparison, the water flux at any given time was normalized to the initial flux which was defined as the stable water flux at the end of the compaction period. The initial fluxes for each membrane are shown in the legend and were averaged to be 46.7 ± 3.1 $L/m^2 \cdot h$ (lmh). Figure 3.2b shows that when PVA was applied as the coating agent, the water flux gradually declined and leveled off after 10 hours, resulting in an 11% flux loss in total. It should be noted that at the start of PVA coating the water flux became higher than the initial flux. This was due to relaxation of the membrane structure during the lower pressure

membrane rinse step. The membrane with PVA coating was then tested using 2 g/L NaCl solution as the feed. The result is shown in Figure 3.2b′. An almost constant water flux was observed indicating that the PVA coating was stable during desalination. In order to study the removability of the PVA layer from the membrane surface, a cleaning step was performed using pH 2 HCl. The result is shown in Figure 3.2c; after acid cleaning the water flux was almost completely restored to the initial flux.

These findings suggest that PVA could be adsorbed onto the surface of the P84-PEI NF membranes forming a protective layer and subsequently removed. Considering that PVA is a non-ionic polymer, the PVA molecules were most likely attached to the membrane surface by hydrogen bonding between the hydroxyl group of PVA and the carbonyl and amine groups of the membrane surface [44]. This hydrogen bonding was unique in that it remained stable at neutral pH during desalination and could be erased by the acid afterward. Any foulants that accumulate on the PVA layer could be removed altogether by acid cleaning to give a fresh membrane surface.

When PVS was applied as the coating agent, flux was reduced by 35% (Figure 3.2b). This coating was also stable during desalination (Figure 3.2b′). Acid cleaning could only slightly improve the water flux (Figure 3.2c). It was likely that the adsorption of PVS was induced by the ionic attraction between the opposite charges of the PVS and the membrane surface. A molecularly thin layer may be formed because of the repulsion forces among already adsorbed molecules and those in

solution of like charge. Similar PVS layers are known to be very homogeneous and stable [45, 46, 47]. Because the charge of PVS is nearly independent from the solution pH, this layer is not easily erased by changing the pH.

Interestingly, PAA behaved differently than PVS as a coating. A rapid flux decline of 62% was induced by PAA within 1 h and then flux leveled off (Figure 3.2b). This coating layer was unstable in the salt solution; a gradual increase of water flux was observed during desalination (Figure 3.2b′). Similar to PVS, the PAA layer could not be completely removed by acid cleaning. However, much better flux restoration was observed than that of PVS (Figure 3.2c). It has been reported that weak polyelectrolytes like PAA can form a film with the thickness depending on solution pH [48]. In this study, the pH of the PAA solution was 4.7 so PAA was partially charged. The adsorbed polymer chains tended to produce a thick layer, which may result in higher flux loss than the PVS monomolecular layer. However, when the pH increased to near 7 during desalination this thick PAA layer likely became thermodynamically unstable. At pH 7, the degree of ionization of the PAA molecules would approach 100%. The repulsion force among PAA chains may induce desorption of some of the material. This would then cause thinning of the PAA layer and an increase in flux [48, 49]. After cleaning, flux increased much further. It is possible that cleaning removed some PAA material even though the coating should be stable at low pH. Alternatively, when the feed changed to HCl solution at pH 2 for membrane cleaning, the molecular chains of PAA may have become protonated and

less charged which may have led to contraction of the PAA chains. Such contraction would increase the pore size leading to a relatively high flux restoration [49].

Table 3.1 Membrane rejection data at different stages of the coating/cleaning experiments[a].

Sample	Rejection before coating[b] (%)	Rejection after coating[c] (%)	Rejection after cleaning[d] (%)
P84-PEI/PVA	55.0	59.6	62.3
P84-PEI/PAA	58.7	74.5	68.8
P84-PEI/PVS	46.5	48.5	52.5

Notes: [a]Test condition: 2.0 g/L NaCl aqueous solution, 13.8 bar and room temperature. [b]After compaction at 13.8 bar. [c]Coating with 50 mg/L polymer solution. [d]After cleaning with HCl solution at pH 2.

Table 3.1 shows rejection data of the NF membranes at different stages of the coating and cleaning experiments. Salt rejection improved in the presence of the coating layers, indicating these layers performed as secondary filters to reject more ions [50]. As will be mentioned later in Section 3.3.1.4, the coating materials could reduce membrane surface pore size, which may be the main reason for increased rejection. After acid cleaning, the PVA coating should have been removed; however, salt rejection did not decrease to the original value of the membrane before coating. It is possible that some PVA material remained on the membrane even after acid cleaning. It is also possible that the membrane became more positively charged by forming more quaternary ammonium groups during acid cleaning [35]. The PAA-coated membrane showed lower salt rejection after acid cleaning. As discussed earlier, acid treatment could remove some PAA material, or it could induce contraction of the PAA chains leading to wider pores, which may allow more ions to pass through [49]. Salt rejection of the PVS-coated membrane did not change as much

as the PAA-coated membrane probably because of the good stability of the PVS coating at the tested pH values.

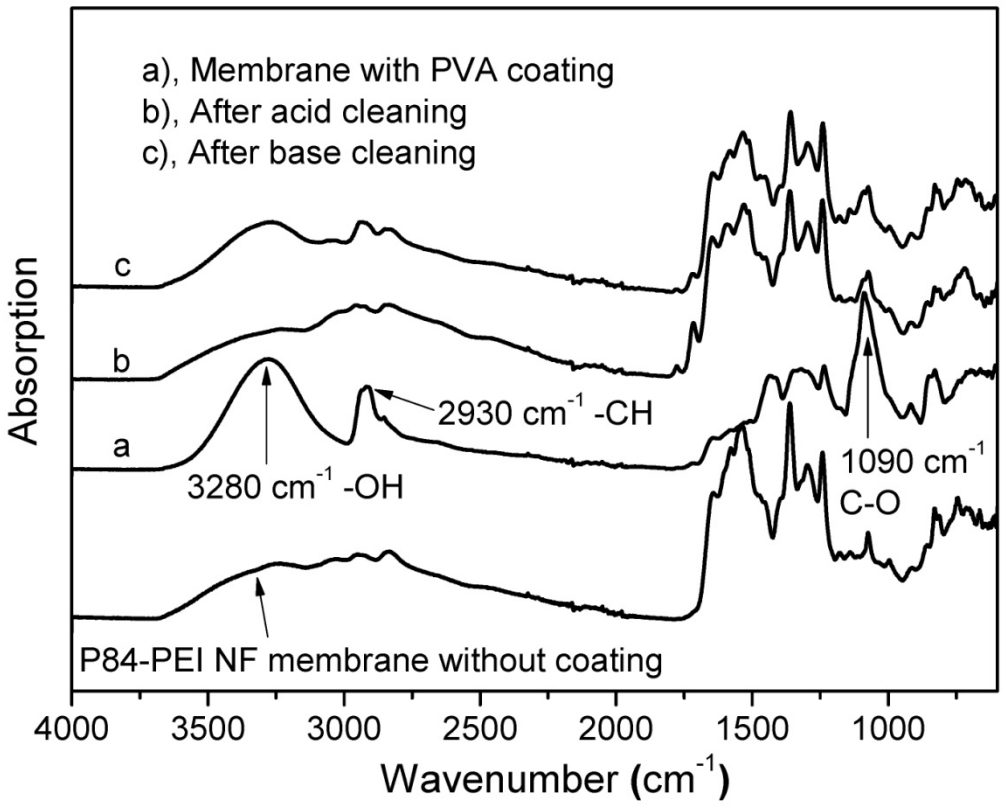

Figure 3.3 ATR-FTIR spectra of the PVA-coated membranes before and after acid (pH 2) or base (pH 9.1) cleaning.

3.3.1.3 ATR-FTIR characterization of the stability of the coating layers

Figure 3.3 shows the ATR-FTIR spectra of the P84-PEI/PVA membranes before and after cleaning. After coating a layer of PVA, a few characteristic absorption bands were observed at 3280 cm^{-1} (O-H stretching), 2930 cm^{-1} (CH_2 stretching) and 1090 cm^{-1} (C-O stretching), indicating PVA had been effectively attached to the membrane surface. PVA was completely removed by acid cleaning, as indicated by the disappearance of the characteristic peaks. This result is in good agreement with previous analyses in section 3.3.1.2. After base cleaning these peaks

still existed, though their intensity was diminished. From this it appears that under weak basic conditions the interaction between PVA and the membrane remained strong enough that not all the PVA molecules were removed.

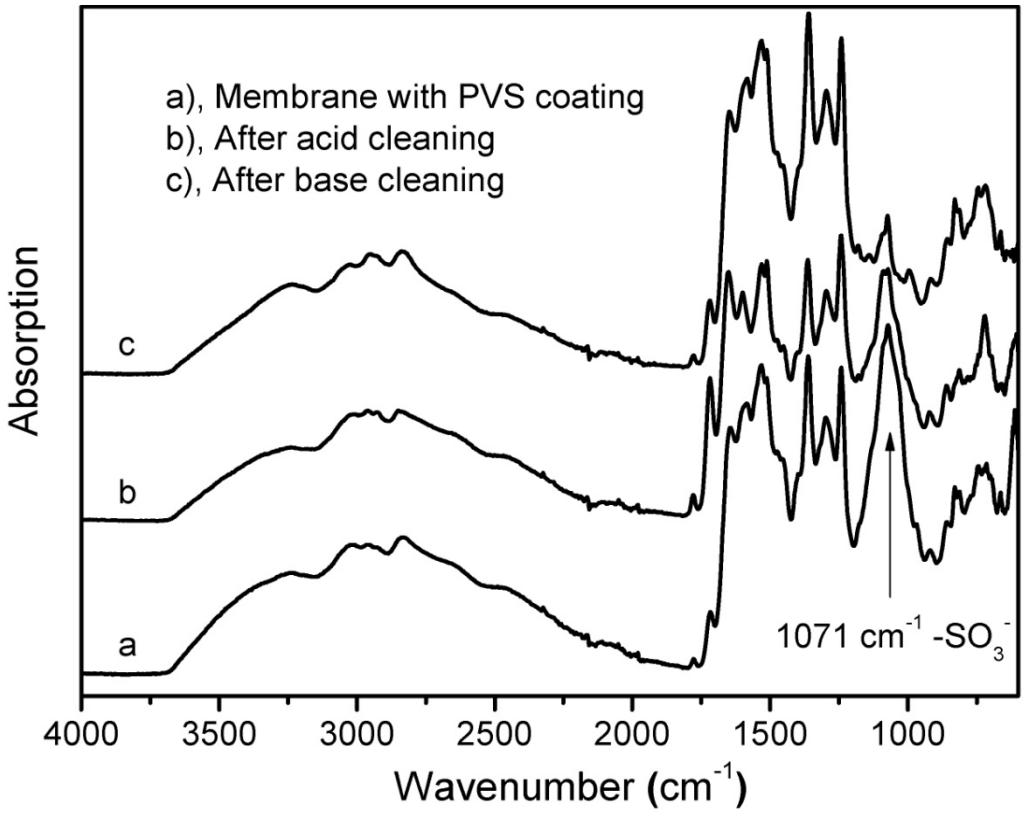

Figure 3.4 ATR-FTIR spectra of the PVS-coated membranes before and after acid (pH 2) or base (pH 9.1) cleaning.

Figure 3.4 shows the ATR-FTIR spectra of the P84-PEI/PVS membranes before and after cleaning. The strong absorption band at 1071 cm^{-1} was attributed to the sulfur-oxygen vibrations of $-SO_3^-$ groups [51]. The intensity of this band remained strong after acid cleaning and became much weaker after base cleaning. These results suggest that the PVS layer is stable in acidic conditions but unstable in basic conditions. It is likely that under acidic conditions the surface of the P84-PEI membrane was more positively charged so that the PVS could be held firmly to the

membrane surface by electrostatic attraction. Under basic conditions, however, the surface charge of the P84-PEI membrane may be effectively neutralized so that the electrostatic force was weakened.

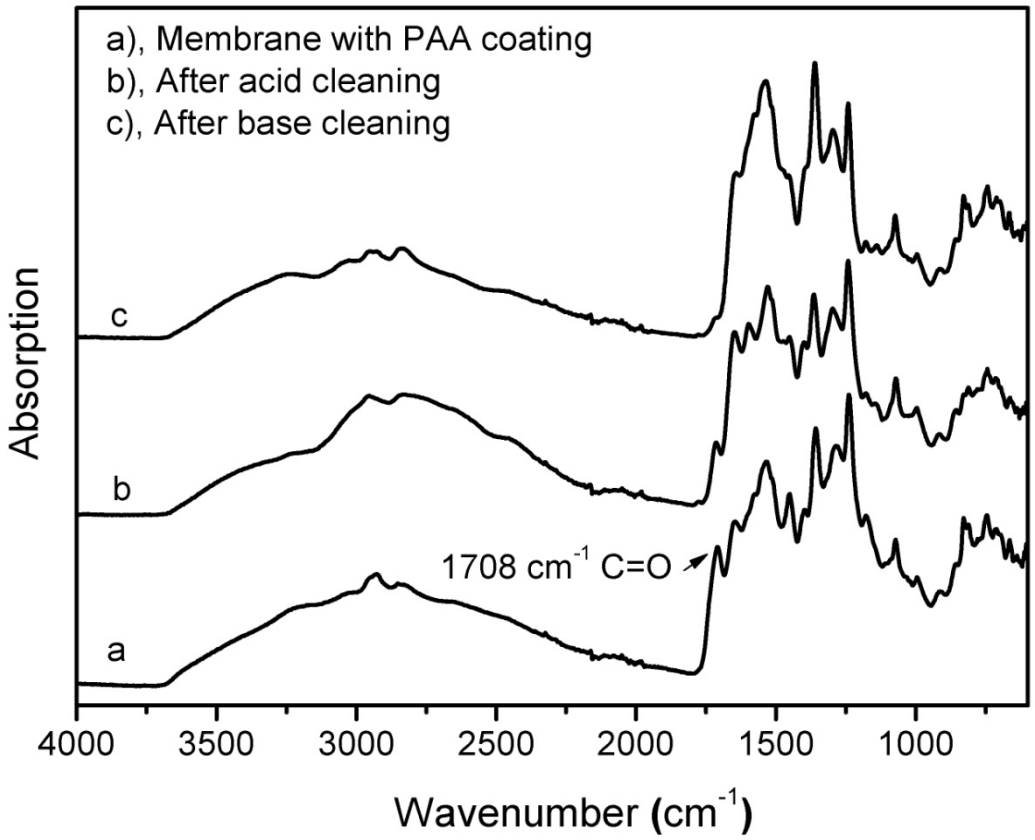

Figure 3.5 ATR-FTIR spectra of the PAA-coated membranes before and after acid (pH 2) or base (pH 9.1) cleaning.

The P84-PEI/PAA membranes show similar stability with the P84-PEI/PVS membranes during acid or base cleaning. In Figure 3.5, the absorption peak at 1708 cm^{-1} represents the carbonyl group of PAA. This peak was only slightly diminished after acid cleaning. After base cleaning the peak almost completely disappeared. At pH 2, the strong positive charge of the P84-PEI membrane may prevent PAA desorption. At pH 9.1, the P84-PEI membrane may become less charged and unable

to hold the PAA layer effectively. PAA is deprotonated at high pH and repulsion between PAA molecules may accelerate desorption.

Table 3.2 Surface properties of the uncoated and coated membranes.

Membrane	P84-PEI	P84-PEI/PVA	P84-PEI/PAA	P84-PEI/PVS
Contact angle (°)[a]	86.6 ± 3.3	76.6 ± 5.2	81.0 ± 4.5	75.7 ± 2.4
Surface roughness (nm)[b]	8.4	3.0	7.3	12.7
Surface charge[c]	+	+	Close to neutral	Close to neutral

Notes: [a]Five measurements were taken for the static contact angle immediately after the droplet was placed on the membrane. [b]Based on a scan area of 10μm × 10μm. [c]Based on a qualitative analysis using three salts of NaCl, Na_2SO_4 and $CaCl_2$ as probes.

3.3.1.4 Effect of surface coating on membrane hydrophilicity and roughness

Surface properties of the membranes before and after coating are summarized in Table 3.2. Contact angle decreased after applying the coatings because of the hydrophilic character of the water-soluble polymers. This improved surface hydrophilicity is favorable for antifouling purposes [4, 9]. AFM images shown in Figure 3.6 illustrate the surface morphologies of these membranes. The uncoated membrane has a very smooth surface with a roughness of only 8.4 nm (Table 3.2). For comparison, the surface roughness of commercial polyamide membranes prepared by interfacial polymerization has been reported to be around one order of magnitude higher than that of this membrane [7]. After coating a layer of PVA or PAA, the membrane surface became even smoother. This was likely caused by the pressure during the dynamic coating process. The PVS coating induced slightly increased surface roughness, which might be caused by insoluble impurities in the PVS solution. Still, the resultant membrane remained quite smooth and visibly shiny.

Therefore, the overall effect of these coatings on membrane hydrophilicity and roughness would be positive for fouling resistance although the charge effect seems the most notable parameter as will be shown in section 3.3.2.

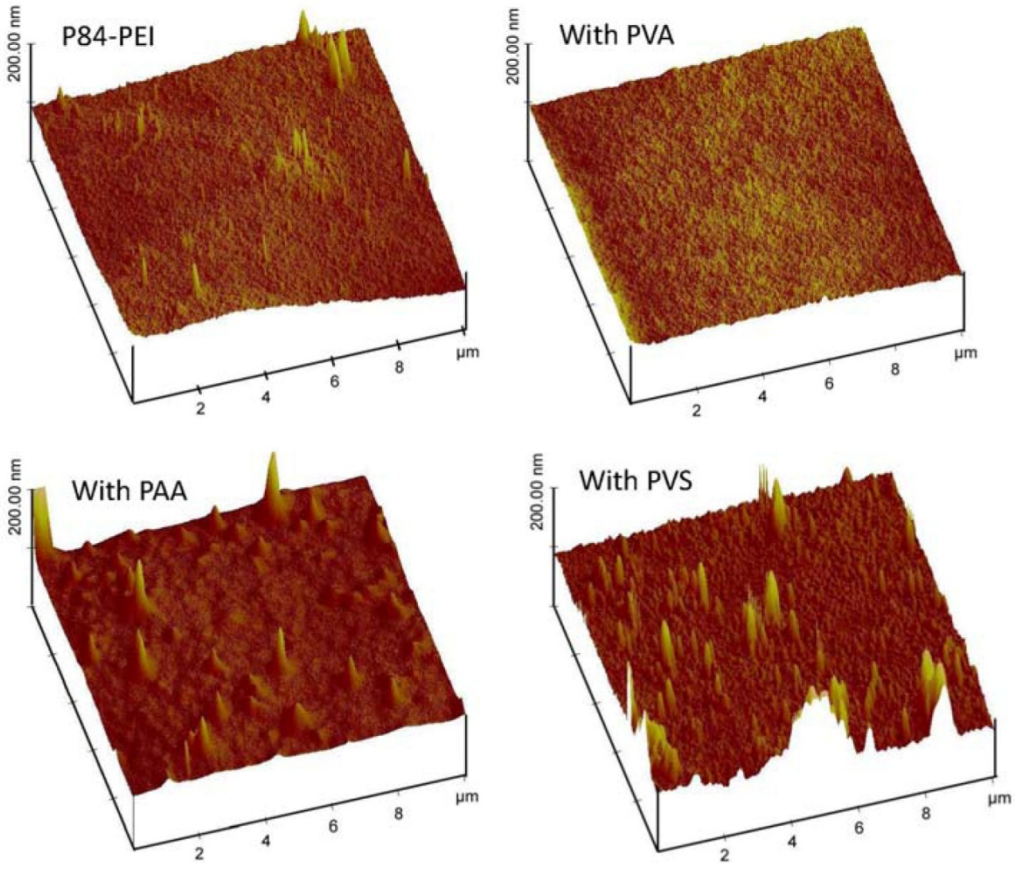

Figure 3.6 AFM images of the uncoated and coated membranes.

3.3.1.5 Effect of surface coating on membrane charge and pore size

The four uncoated and coated membranes were measured with regard to their rejections to three charged solutes $CaCl_2$, NaCl, and Na_2SO_4. The results are shown in Figure 3.7. The uncoated P84-PEI membrane had a rejection sequence of $CaCl_2$ > NaCl > Na_2SO_4 indicating a positive charge for the membrane [38]. For the PVA-coated membrane, the same rejection sequence was observed. While rejections of NaCl and $CaCl_2$ were only slightly improved, Na_2SO_4 rejection became much greater than that of the uncoated membrane. This suggests that the positive charge of the P84-

PEI membrane was weakened by the non-ionic PVA coating. However, the PVA-coated membrane was still positively charged and the Donnan exclusion effect was likely dominant during ion filtration. When PVS and PAA were applied, the rejection to Na_2SO_4 was significantly improved resulting in a rejection sequence of $CaCl_2$ > Na_2SO_4 > NaCl. This cannot be explained by Donnan exclusion. It is probable that the negative charge of PVS and PAA balanced the positive charge of the P84-PEI membrane resulting in a slightly negative surface layer. The overall membrane charge then became almost neutral and the Donnan exclusion effect did not govern the ion separation behavior. Instead, the hydrated diameter of each ion and the diffusion coefficient of each salt determined the different retentions [1, 38].

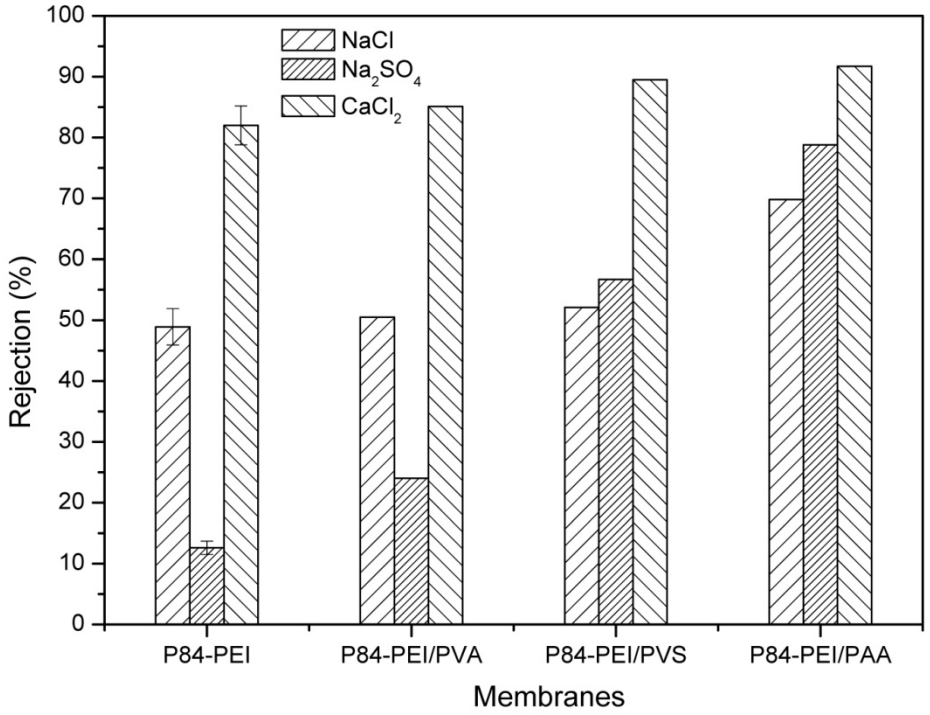

Figure 3.7 Rejections to three charged solutes of the four uncoated and coated membranes indicating membrane charge.

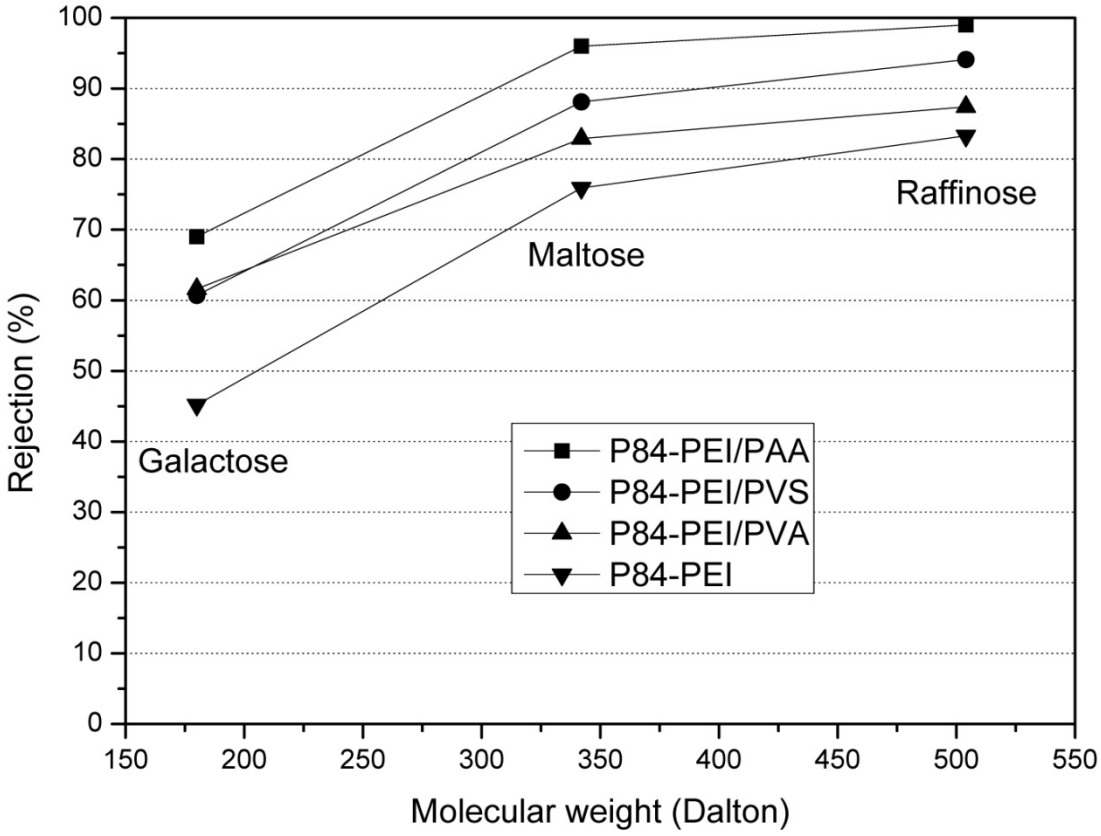

Figure 3.8 Rejections to three uncharged solutes of the four uncoated and coated membranes indicating relative pore size of these membranes.

Figure 3.8 shows rejection data for three uncharged solutes: galactose, maltose and raffinose. Rejection occurs by a sieving mechanism for these uncharged molecules so pore size effects can be investigated [1]. For each membrane, rejection increased with increasing molecular weight. The molecular weight cut-off (MWCO) was around several hundred Dalton. This result confirms that the separation performance of the four membranes is in the nanofiltration range. Sugar rejection decreased going from P84-PEI/PAA, P84-PEI/PVS, P84-PEI/PVA to P84-PEI suggesting that the PAA-coated membrane had the smallest pores and the uncoated membrane (P84-PEI) had the largest. As discussed earlier, PAA may form a thicker layer than PVS, resulting in smaller pores. PVA most likely was not able to form a

layer as tight as PVS and PAA because hydrogen bonding is weaker than electrostatic interaction.

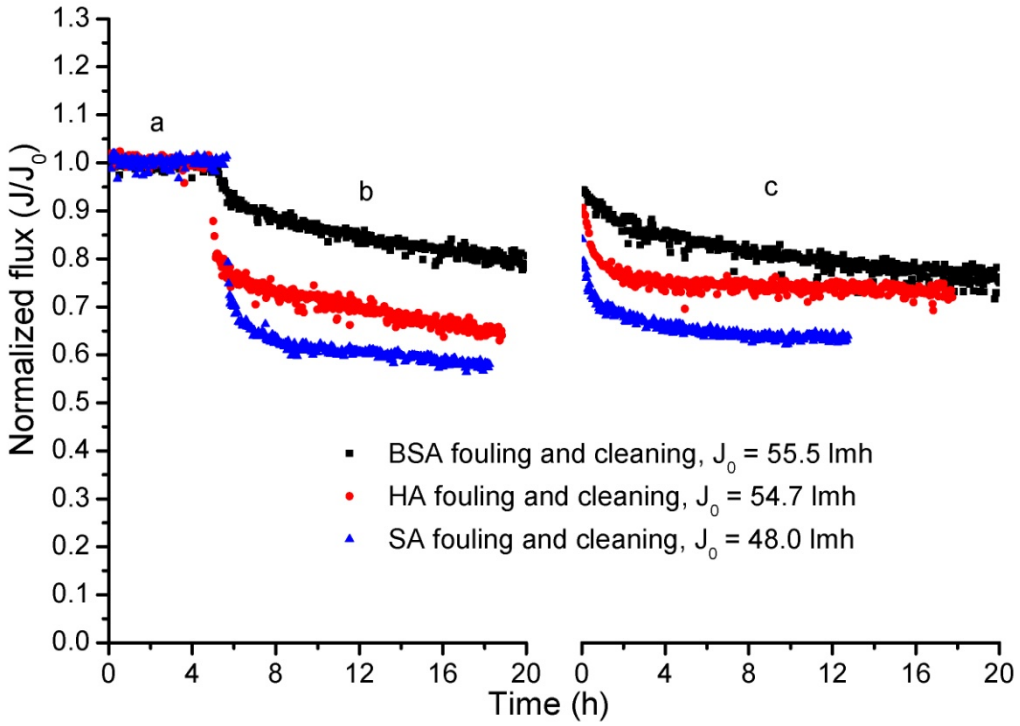

Figure 3.9 Normalized flux of the P84-PEI NF membrane during fouling and after cleaning. (a) Membrane compaction with 2 g/L NaCl solution; (b) flux with a solution containing 2 g/L NaCl and 100 mg/L BSA, HA or SA; (c) flux with 2 g/L NaCl solution after cleaning with HCl solution at pH 2. A pressure of 13.8 bar was applied for all the stages.

3.3.2 Effect of surface coatings on membrane fouling and cleaning

3.3.2.1 Fouling behavior of the uncoated P84-PEI membrane

Figure 3.9 shows flux decline during cross-flow filtration of feed solutions containing 2 g/L NaCl and 100 mg/L BSA, HA or SA and the flux restoration by cleaning using HCl at pH 2. Figure 3.9a shows the normalized stable fluxes after compaction. The initial fluxes for each membrane are given in the legend; the average initial flux was 52.7 ± 4.1 lmh. As seen in Figure 3.9b, all three model foulants induced rapid flux decline within the first 1 - 2 hours. Flux decline became much

slower after 2 h, but no stable state was observed over a period of 12 - 15 h. This fouling behavior may be explained by the attractive force between the positively charged membrane and the negatively charged foulants, which results in quick adsorption of the foulants onto the membrane surface in the initial stage forming a monomolecular layer. Once the membrane surface is covered with foulants, these foulant layers may neutralize the membrane surface and shield it from direct interactions with additional foulants. Further slow flux loss may be caused by the interactions between adsorbed foulants and foulants in solution forming a multilayer cake. Also, in later stages the flux is reduced so convection of foulants toward the surface is minimized and cake-layer buildup is slowed.

Different foulants induced varying degrees of fouling. The total flux loss caused by BSA, HA and SA was 20, 35 and 42%, respectively. This difference may be correlated to the chemical characteristics of the three foulants. Their carboxylic acidities were reported to be 1.0, 3.4 and 3.5 mequiv./g for BSA, HA and SA, respectively [41, 42, 43]. The higher the concentration of carboxylic functional groups, the higher the adhesion force between foulant and membrane resulting in faster adsorption. In addition, the resultant fouling layer may be tighter causing a more dramatic flux loss.

Figure 3.9c shows that cleaning by acid only partially restored the water flux, suggesting that foulant adsorption was sufficiently strong that some material remained after cleaning. The relatively high flux immediately after cleaning was likely due to

relaxation of the membrane structure because the cleaning process was performed at a lower pressure (4.8 bar) than the operating pressure (13.8 bar) during desalination.

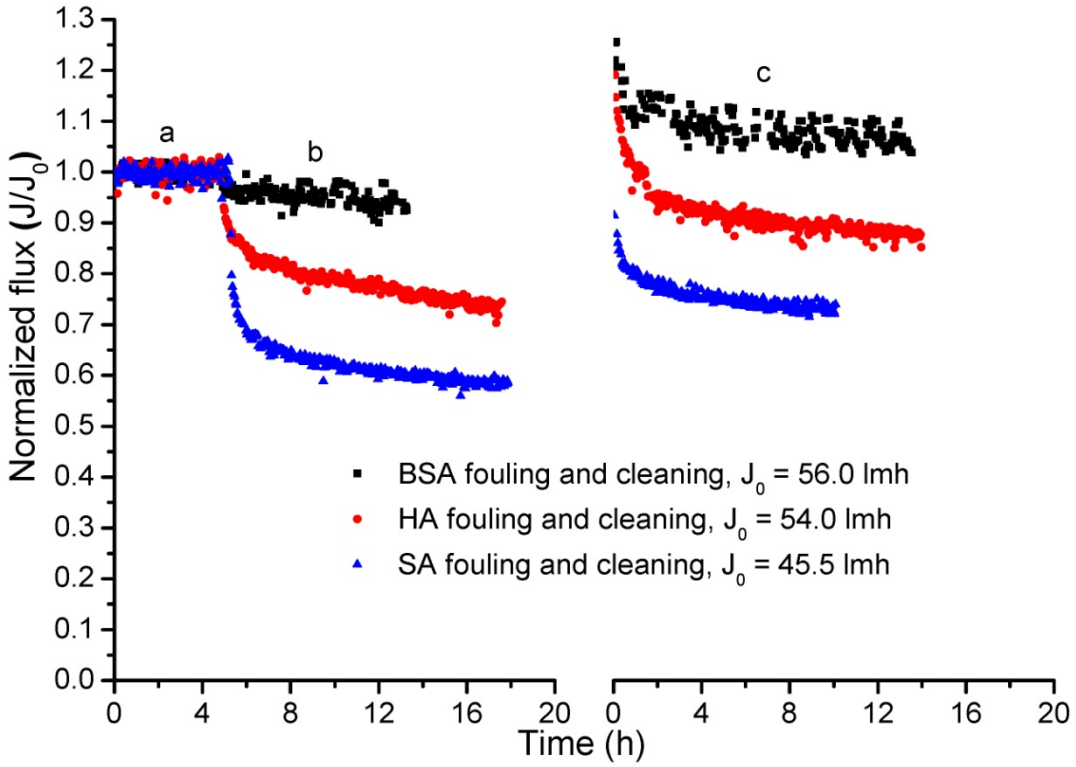

Figure 3.10 Normalized flux of the P84-PEI/PVA membranes during fouling and after cleaning. (a) Membrane compaction with 2 g/L NaCl solution; (b) flux with a solution containing 2 g/L NaCl and 100 mg/L BSA, HA or SA; (c) flux with 2 g/L NaCl solution after cleaning with HCl solution at pH 2. A pressure of 13.8 bar was applied for all the stages.

3.3.2.2 Effect of PVA coating on membrane fouling

Figure 3.10 shows the flux versus time profiles for the membranes with a layer of PVA coating during fouling and after cleaning. Generally, membrane antifouling properties were improved. Figure 3.10b shows that the total flux loss caused by BSA, HA and SA was 5, 27 and 41%, respectively, lower than that of the uncoated membranes. However, similar to the uncoated membranes, the PVA-coated membrane still showed a two-stage fouling process. The flux decline was very quick in the first hour and then became much slower. This result suggests that the

interaction force between the foulants and the membrane surface was still dominated by electrostatic attraction because the PVA-coated membrane was still positively charged. The lower charge strength of the PVA-coated membrane than that of the uncoated membrane may result in less buildup of the fouling layer and thus less flux loss. For the foulants with strong negative charge such as HA and SA, severe membrane fouling was still observed. However, for the weakly charged foulant BSA, charge interaction with the membrane was minimized leading to low fouling. Therefore, the PVA layer could effectively protect the membrane to prevent adsorption of proteins.

Cleanability results are given in Figure 3.10c. The PVA-coated membrane with BSA fouling exhibited over 100% flux restoration after acid cleaning. This result proves the previous hypothesis that the PVA layer can be removed together with the BSA layer during the cleaning process. Although the PVA-coated membranes with HA and SA fouling were not able to be cleaned completely due to the electrostatic force, better flux restoration than the uncoated membranes was still observed. Therefore, it can be concluded that a PVA coating can be used effectively to prevent protein fouling. PVA was not as effective for the negatively charged foulants like HA and SA, presumably because of the positive charge of the PVA-coated membrane.

3.3.2.3 Effect of PVS coating on membrane fouling

Figure 3.11 shows the flux versus time profiles for the membranes with a layer of PVS coating during fouling and after cleaning. Figure 3.11b shows that the total flux loss caused by BSA, HA and SA was 4, 17 and 14%, respectively. The rapid flux

decline step seen with the virgin and PVA-coated membranes was diminished greatly here. This indicates that the PVS-coated membrane had less charge resulting in lower fouling potential.

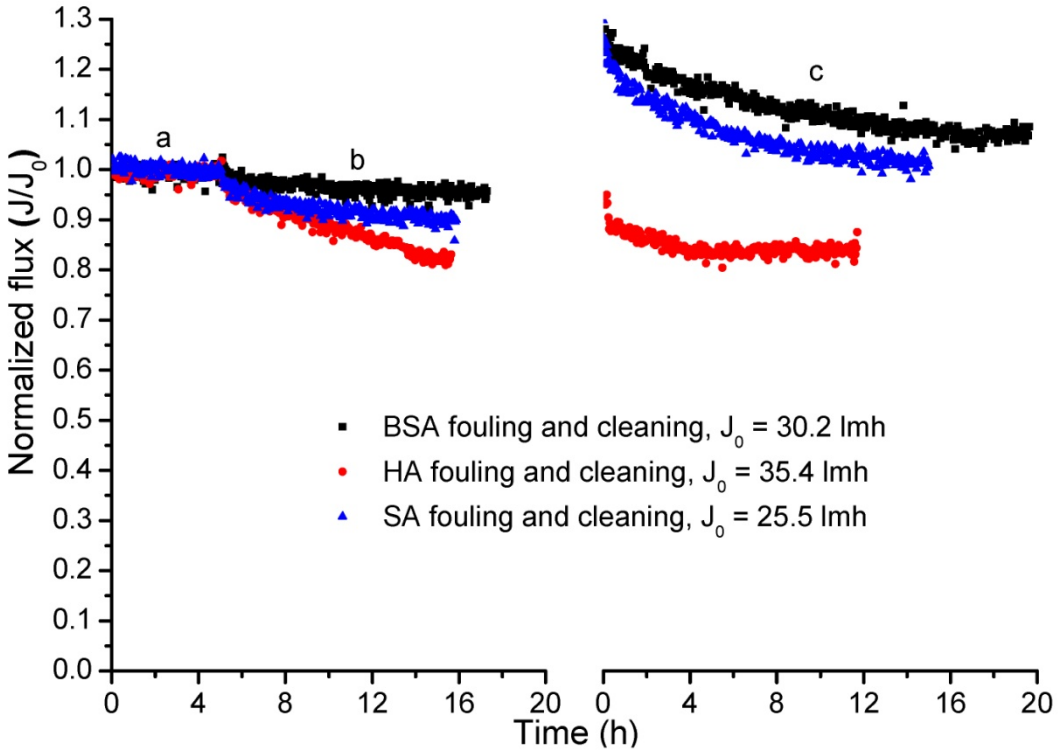

Figure 3.11 Normalized flux of the P84-PEI/PVS membranes during fouling and after cleaning. (a) Membrane compaction with 2 g/L NaCl solution; (b) flux with a solution containing 2 g/L NaCl and 100 mg/L BSA, HA or SA; (c) flux with 2 g/L NaCl solution after cleaning with HCl solution at pH 2. A pressure of 13.8 bar was applied for all the stages.

In addition to the prevention of foulant adsorption, this PVS layer also improved cleanability after fouling. As shown in Figure 3.11c, BSA and SA were effectively removed and flux restoration was about 100%. It is likely that the PVS-coated membrane would remain almost neutral under acidic conditions so the charge interaction between the membrane and BSA or SA was small and the foulants could be gradually desorbed. However, HA was not as effectively cleaned, probably

because HA is more hydrophobic resulting in additional attractive interactions with the membrane.

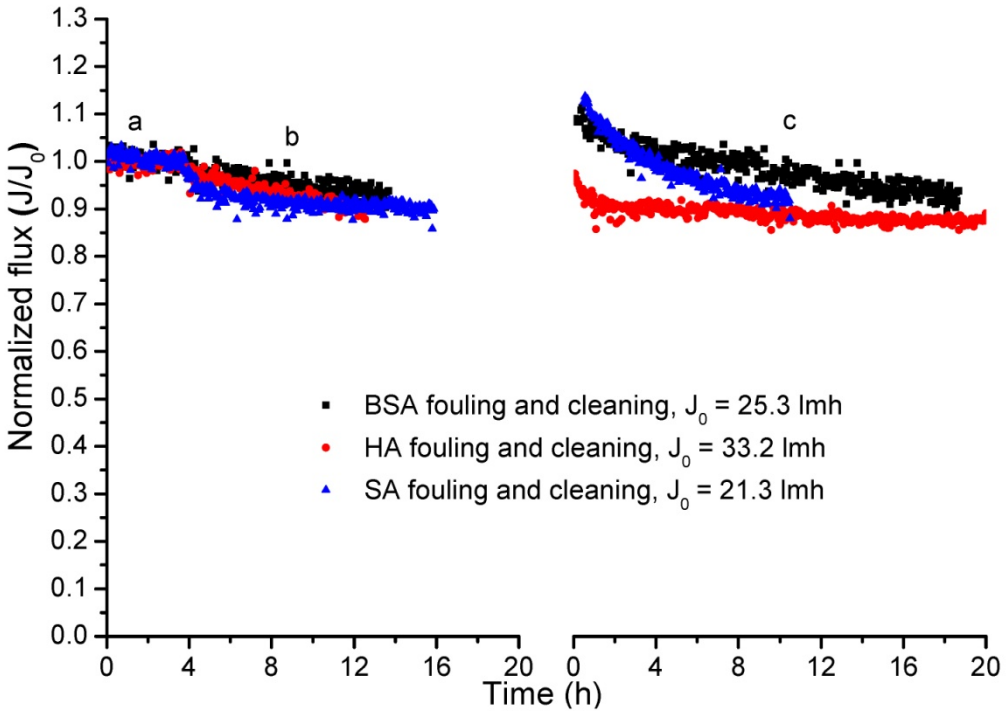

Figure 3.12 Normalized flux of the P84-PEI/PAA membranes during fouling and after cleaning. (a) Membrane compaction with 2 g/L NaCl solution; (b) flux with a solution containing 2 g/L NaCl and 100 mg/L BSA, HA or SA; (c) flux with 2 g/L NaCl solution after cleaning with HCl solution at pH 2. A pressure of 13.8 bar was applied for all the stages.

3.3.2.4 Effect of PAA coating on membrane fouling

Coating the membrane with PAA gave similar results as PVS. As shown in Figure 3.12b, the total flux loss caused by BSA, HA and SA was 5, 10 and 10%, respectively. Again, the rapid flux decline step initiated by electrostatic forces was minimized, indicating an almost neutral surface was obtained due to charge compensation by PAA. However, the cleanability of the PAA-coated membranes was not as good as the PVS-coated membranes since flux was not completely restored (Figure 3.12c). This was likely due to the surface charge of the PAA-coated

membrane. During acid treatment, PAA would be protonated and less negatively charged while the P84-PEI membrane below the PAA layer would be more positively charged due to the formation of additional ammonium groups. The overall effect of acid was to make the PAA-coated membrane more positively charged. For this reason, the negatively charged foulants were not easily desorbed.

3.4 Conclusions

In this study we used three water-soluble polymers PVA, PVS and PAA to form a protective coating layer on the surface of a positively charged NF membrane to improve membrane fouling resistance. After applying these coatings, pore size was reduced, permeation flux decreased, and rejection to uncharged sugars and charged salts increased. Hydrophilicity and smoothness were improved by these coatings, which was favorable for fouling resistance. Surface charge varied with different coating materials. The PVA-coated membrane showed positive charge because the non-ionic PVA did not significantly alter the positive charge of the P84-PEI membrane. However, PVS- and PAA-coated membranes had surface charge close to neutral because the negative charge of PVS and PAA could balance the positive charge of the P84-PEI membrane.

The coating layer of PVA, PVS and PAA showed different stability toward acid cleaning. PVA can be adsorbed onto the membrane surface by hydrogen bonding and the PVA layer was stable at neutral pH (~ 7), which is the normal condition for desalination. However, this layer could be removed by acid cleaning at pH 2 and thus it was possible to regenerate the membrane after fouling. The PVS- and PAA-coated

membranes showed high stability during acid cleaning because of strong electrostatic interactions with the membrane surface. These coatings are not as easily regenerable as PVA.

Membrane surface charge played the most important role in foulant adsorption. The uncoated membrane had strong positive charge so that foulants like BSA, humic acid and sodium alginate were adsorbed quickly and firmly. The PVA-coated membrane also had positive charge and fouling by negatively charged materials like humic acid and sodium alginate was still severe. PVA worked very well to resist weakly charged proteins like BSA. PVS- and PAA-coated membranes had a low surface charge and fouling due to charge interactions was diminished. These results suggest that membrane surface properties can be tailored by different coating materials; the technique is flexible for membrane modification to meet various industrial demands. Currently, we are testing and optimizing such antifouling NF membranes for application in membrane bioreactor (MBR) processes for wastewater treatment.

3.5 References

[1] A.I. Schäfer, A.G. Fane, T.D. Waite (Eds.), Nanofiltration - Principles and Applications, Elsevier Ltd., 2005.

[2] K. Kimura, Y. Hane, Y. Watanabe, G. Amy, N. Ohkuma, Irreversible membrane fouling during ultrafiltration of surface water, *Water Res.* 38 (14-15) (2004) 3431.

[3] M.F.A. Goosen, S.S. Sablani, H. Al-Hinai, S. Al-Obeidani, R. Al-Belushi, D. Jackson, Fouling of reverse osmosis and ultrafiltration membranes: a critical review, *Sep. Sci. Technol.* 39 (10) (2004) 2261.

[4] N. Hilal, O.O. Ogunbiyi, N.J. Miles, R. Nigmatullin, Methods employed for control of fouling in MF and UF membranes: a comprehensive review, *Sep. Sci. Technol.* 40 (2005) 1957.

[5] Y. Uyama, K. Kato, Y. Ikada, Surface modification of polymers by grafting, *Adv. Polym. Sci.* 137 (1998) 1.

[6] I.C. Escobar, E.M. Hoek, C.J. Gabelich, F.A. DiGiano, et al, Committee report: recent advances and research needs in membrane fouling, *J. Am. Water Works Assoc.* 97 (8) (2005) 79.

[7] Q. Li, Z. Xu, I. Pinnau, Fouling of reverse osmosis membranes by biopolymers in wastewater secondary effluent: role of membrane surface properties and initial permeate flux, *J. Membr. Sci.* 290 (2007) 173.

[8] M. Kabsch-Korbutowicz, K. Majewska-Nowak, T. Winnicki, Analysis of membrane fouling in the treatment of water solutions containing humic acids and mineral salts, *Desalination* 126 (1999) 179.

[9] A.G. Fane, C.J.D. Fell, A review of fouling and fouling control in ultrafiltration, *Desalination* 62 (1987) 117.

[10] M. Elimelech, X. Zhu, A.E. Childress, S. Hong, Role of membrane surface morphology in colloidal fouling of cellulose acetate and composite aromatic polyamide reverse osmosis membranes, *J. Membr. Sci.* 127 (1997) 101.

[11] P.J. Evans, M.R. Bird, A. Pihlajamäki, M. Nyström, The influence of hydrophobicity, roughness and charge upon ultrafiltration membranes for black tea liquor clarification, *J. Membr. Sci.* 313 (2008) 250.

[12] A. Weis, M.R. Bird, M. Nyström, C. Wright, The influence of morphology, hydrophobicity and charge upon the long-term performance of ultrafiltration membranes fouled with spent sulphite liquor, *Desalination* 175 (2005) 73.

[13] E.M.V. Hoek, S. Bhattacharjee, M. Elimelech, Effect of membrane surface roughness on colloid-membrane DLVO interactions, *Langmuir* 19 (2003) 4836.

[14] B. Van der Bruggen, M. Mänttäri, M. Nyström, Drawbacks of applying nanofiltration and how to avoid them: a review, *Sep. Purif. Technol.* 63 (2008) 251.

[15] M. Mänttäri, L. Puro, J. Nuortila-Jokinen, M. Nyström, Fouling effects of polysaccharides and humic acid in nanofiltration, *J. Membr. Sci.* 165 (2000) 1.

[16] A. Al-Amoudi, R.W. Lovitt, Fouling strategies and the cleaning system of NF membranes and factors affecting cleaning efficiency, *J. Membr. Sci.* 303 (2007) 4.

[17] P. Wang, K.L. Tan, E.T. Kang K.G. Neoh, Synthesis, characterization and anti-fouling properties of poly(ethylene glycol) grafted poly(vinylidene fluoride) copolymer membranes, *J. Mater. Chem.* 11 (2001) 783.

[18] M.S. Kang, B. Chun, S.S. Kim, Surface modification of polypropylene membrane by low-temperature plasma treatment, *J. Appl. Polym. Sci.* 81 (6) (2001) 1555.

[19] Y. Chang, T.-Y. Cheng, Y.-J. Shih, K.-R. Lee, J.-Y. Lai, Biofouling-resistance expanded poly(tetrafluoroethylene) membrane with a hydrogel-like layer of surface-immobilized poly(ethylene glycol) methacrylate for human plasma protein repulsions, *J. Membr. Sci.* 323 (2008) 77.

[20] L.-P. Zhu, H.-B. Dong, X.-Z. Wei, Z. Yi, B.-K. Zhu, Y.-Y. Xu, Tethering hydrophilic polymer brushes onto PPESK membranes via surface-initiated atom transfer radical polymerization, *J. Membr. Sci.* 320 (2008) 407.

[21] H.-Y. Yu, J.-M. He, L.-Q. Liu, X.-C. He, J.-S. Gu, X.-W. Wei, Photoinduced graft polymerization to improve antifouling characteristics of an SMBR, *J. Membr. Sci.* 302 (2007) 235.

[22] S.P. Nunes, M.L. Sforca, K.-V. Peinemann, Dense hydrophilic composite membranes for ultrafiltration, *J. Membr. Sci.* 106 (1995) 49.

[23] K.J. Kim, A.G. Fane, C.J.D. Fell, The performance of ultrafiltration membranes pretreated by polymers, *Desalination* 70 (1988) 229.

[24] A.-S. Jönsson, B. Jönsson, The influence of nonionic and ionic surfactants on hydrophobic and hydrophilic ultrafiltration membranes, *J. Membr. Sci.* 56 (1991) 49.

[25] L.E.S. Brink, D.J. Romijn, Reducing the protein fouling of polysulfone surfaces and polysulfone ultrafiltration membranes: optimization of the type of presorbed layer, *Desalination*, 78 (1990) 209.

[26] M.L. Bruening, D.M. Dotzauer, P. Jain, L. Ouyang, G.L. Baker, Creation of functional membranes using polyelectrolyte multilayers and polymer brushes, *Langmuir* 24 (2008) 7663.

[27] R. Klitzing, B. Tieke, Polyelectrolyte membranes, *Adv. Polym. Sci.* 165 (2004) 177.

[28] J. Wang, Y. Yao, Z. Yue, J. Economy, Preparation of polyelectrolyte multilayer films consisting of sulfonated poly (ether ether ketone) alternating with selected anionic layers, *J. Membr. Sci.* 337 (2009) 200.

[29] L. Ouyang, R. Malaisamy, M.L. Bruening, Multilayer polyelectrolyte films as nanofiltration membranes for separating monovalent and divalent cations, *J. Membr. Sci.* 310 (2008) 76.

[30] S.A. Sukhishvili, S. Granick, Layered, erasable, ultrathin polymer films, *J. Am. Chem. Soc.* 122 (2000) 9550.

[31] S.A. Sukhishvili, S. Granick, Layered, erasable polymer multilayers formed by hydrogen-bonded sequential self-assembly, *Macromolecules* 35 (2002) 301.

[32] E. Kharlampieva, S.A. Sukhishvili, Hydrogen-bonded layer-by-layer polymer films, *Polym. Rev.* 46 (4) (2006) 377.

[33] J. Cho, F. Caruso, Polymeric multilayer films comprising deconstructible hydrogen-bonded stacks confined between electrostatically assembled layers, *Macromolecules* 36 (8) (2003) 2845.

[34] E. Kharlampieva, S.A. Sukhishvili, Ionization and pH stability of multilayers formed by self-assembly of weak polyelectrolytes, *Langmuir* 19 (4) (2003) 1235.

[35] C. Ba, J. Langer, J. Economy, Chemical modification of P84 copolyimide membranes by polyethylenimine for nanofiltration, *J. Membr. Sci.* 327 (2009) 49.

[36] N. Li, Z. Liu, S. Xu, Dynamically formed poly (vinyl alcohol) ultrafiltration membranes with good anti-fouling characteristics, *J. Membr. Sci.* 169 (2000) 17.

[37] D. A. Ladner, Effects of bloom-forming algae on fouling of integrated membrane systems in seawater desalination, PhD dissertation, University of Illinois at Urbana-Champaign, August 2009.

[38] J.M.M. Peeters, J.P. Boom, M.H.V. Mulder, H. Strathmann, Retention measurements of nanofiltration membranes with electrolyte solutions, *J. Membr. Sci.* 145 (1998) 199.

[39] B.V.d. Bruggen, J. Schaep, D. Wilms, C. Vandecasteele, Influence of molecular size, polarity and charge on the retention of organic molecules by nanofiltration, *J. Membr. Sci.* 156 (1999) 29.

[40] M. Dubois, K.A. Gilles, J.K. Hamilton, P.A. Rebers, F. Smith, Colorimetric method for determination of sugars and related substances, *Anal. Chem.* 28 (1956) 350.

[41] S.K. Hong, M. Elimelech, Chemical and physical aspects of natural organic matter (NOM) fouling of nanofiltration membranes, *J. Membr. Sci.* 132 (1997) 159.

[42] W. Ang, M. Elimelech, Protein (BSA) fouling of reverse osmosis membranes: implications for wastewater reclamation, *J. Membr. Sci.* 296 (2007) 83.

[43] B. Mi, M. Elimelech, Chemical and physical aspects of organic fouling of forward osmosis membranes, *J. Membr. Sci.* 320 (2008) 292.

[44] W.B. Stockton, M.F. Rubner, Molecular-level processing of conjugated polymers. 4. Layer-by-layer manipulation of polyaniline via hydrogen-bonding interactions, *Macromolecules* 30 (1997) 2717.

[45] O.N. Oliveira Jr., J.-A. He, V. Zucolotto, S. Balasubramanian, L. Li, H.S. Nalwa, J. Kumar, S.K. Tripathy, Layer-by-Layer Polyelectrolyte-Based Thin Films for Electronic and Photonic Applications, in Handbook of Polyelectrolytes and their Applications, volume 1: Polyelectrolyte-Based Multilayers, Self-Assemblies and Nanoestructures, American Scientific Publishers, 2002.

[46] G. Decher, J.D. Hong, J. Schmitt, Buildup of ultrathin multilayer films by a self-assembly process. III. Consecutively alternating adsorption of anionic and cationic polyelectrolytes on charged surfaces, *Thin Solid Films* 210/211 (1992) 831.

[47] J.H. Cheung, W.B. Stockton, M.F. Rubner, Molecular-level processing of conjugated polymers. 3. Layer-by-Layer manipulation of polyaniline via electrostatic interactions, *Macromolecules* 30 (1997) 2712.

[48] S.S. Shiratori, M.F. Rubner, pH-dependent thickness behavior of sequentially adsorbed layers of weak polyelectrolytes, *Macromolecules* 33 (2000) 4213.

[49] J. Meier-Haack, S. Derenko, J. Seng, Fouling reduction by graft-modification with hydrophilic polymers, *Sep. Sci. Technol.* 42 (2007) 2881.

[50] A.E. Childress, M. Elimelech, Relating nanofiltration membrane performance to membrane charge (electrokinetic) characteristics, *Environ. Sci. Technol.* 34 (17) (2000) 3710.

[51] M. Lakshmi, R.T.S.V. Choudhary, I.K. Varma, Sulphonated poly(ether ether ketone): synthesis and characterisation, *J. Mater. Sci.* 40 (2005) 629.

CHAPTER 4

DESIGN OF ANTIFOULING NANOFILTRATION MEMBRANES FOR POTENTIAL MEMBRANE BIOREACTOR APPLICATION

4.1 Introduction

Nanofiltration (NF) is an attractive membrane process for removal of colloidal, organic, and ionic contaminants from water [1, 2]. NF membranes have relatively high charge and pores on the order of 1 nm. Consequently, both charge effects and sieving mechanisms influence the rejection behavior of solutes with NF membranes, which are typically characterized by high rejection of divalent ions, lower rejection of monovalent ions, and higher fluxes than reverse osmosis (RO) membranes [3, 4]. NF membranes have a variety of applications, including desalination of brackish and seawater, reclamation of wastewater, in biological processes such as membrane bioreactors (MBR), and other industrial separations [3, 5]. However, the use of membrane filtration in all applications has often limited by fouling caused by inorganic and organic materials, which can adhere to the surface and pores, resulting in deterioration of performance and increase in costs of energy and membrane replacement [6, 7, 8]. Therefore, it is critically important to develop advanced NF membranes that have high chemical and biological stability, high resistance to fouling, and separation abilities that can be tailored to meet various demands.

Composite membranes consisting of a polysulfone membrane as support for a very thin skin layer have been the standard design since invented in 1980s [4]. To date, polyamides prepared by interfacial polymerization are still the dominant thin film material [4]. Although the polyamide membranes have very good separation capabilities, their surfaces are generally rough, negatively charged and hydrophobic [9]. The rough surface of thin-film composite membranes was found to increase fouling rate, which is explained by the fact that particles preferentially accumulate in

the ‘valleys’ of rough membranes, resulting in ‘valley clogging’ and hence in a severe flux decline [10, 11, 12, 13]. The strongly negatively charged polyamide membranes experienced higher fouling rates than less negatively charged membranes during a field study [14]. Also, hydrophilic membranes such as regenerated cellulose membranes have been observed to have a lower fouling tendency than the polyamide membranes [10]. Hence, development of membranes with a smooth, hydrophilic and less charged surface seems desirable for antifouling purposes [15, 16, 17, 18, 19, 20, 21]. Indeed, the polyamide membranes have often been chemically or physically modified to improve fouling resistance [22]. For example, fouling was greatly reduced by coating a layer of polyvinyl alcohol (PVA) onto the polyamide surface, resulting in a smoother, less charged and hydrophilic surface due to the neutral and hydrophilic characteristics of PVA [23]. The low fouling nature of a commercial polyamide membrane, ESNA1-LF, was attributed to the smoothness of the surface and the near neutral surface charge [24].

Nanofiltration membranes have been applied in MBR processes for wastewater treatment in recent years [25, 26, 27, 28, 29]. Although the MBR using ultrafiltration (UF) membranes showed a high removal efficiency of bacterial flocs and suspended solids, the system was not adequate to remove known and unknown dissolved organic matter with several hundred Dalton range, due to the relatively coarse pore size distribution of the UF membranes [25, 26]. Concerning organic contaminants in natural waters, especially drinking water sources, may potentially affect human health through chronic exposure, it is essential to reduce or minimize the contaminants released into the water environment [27]. The NF-based MBR process has potential here. However, the MBR filtration performance inevitably decreases with filtration time due to membrane fouling [30]. The foulants include dissolved inorganic or

organic compounds, colloids, bacteria and suspended solids. In addition, many extracellular polymeric substances (EPS) such as polysaccharides, proteins, and natural organic matter (NOM) have often induced irreversible flux decline. Thus development of antifouling membranes is still highly demanded for widespread application of MBRs [31, 32].

During the past few years, we have developed several advanced NF membranes, including positively charged NF membranes for multivalent heavy metal ion removal and antifouling NF membranes using a coating technique [33, 34, 35]. The positively charged NF membrane was still polyamide prepared by chemical modification of polyimide membrane using polyethylenimine (PEI). The resultant NF membrane was very smooth: the surface roughness is one order of magnitude less than the interfacial polymerized polyamide membranes. By coating a layer of water soluble polyelectrolytes, the membrane surface was modified to reduce fouling by common foulants such as proteins, humic substances, and polysaccharides [35]. This improved fouling resistance is believed to be related to the smooth and low charged surface. Considering the common foulants like NOM are heterogeneous mixtures and may have a variety of functional groups [36], the low charged membranes may have advantages to minimize any charge related adsorption.

In this study, we continued to prepare and characterize antifouling NF membranes with an aim to apply them in MBR process. In the first approach, we tried to improve membrane flux by partial modification of polyimide membranes at room temperature and controlled reaction time. PVA and polyvinyl sulfate-potassium salt (PVS) were tested as surface modifying agents. In the second approach, another coating material sulfonated poly(ether ether ketone) (SPEEK) was used for surface modification. Membrane preparation and optimization, membrane morphology and

chemistry characterization, membrane separation capability and fouling resistance were extensively studied. Finally, the membranes prepared by these two approaches were tested for their fouling resistance to activated sludge.

4.2 Experimental

4.2.1 Chemicals

P84 powder was purchased from HP Polymer Inc. and dried in vacuum at 160˚C for 12 hours before use. Poly(pyromellitic dianhydride-*co*-4,4'-oxydianiline) amic acid solution (PMDA-ODA PAA) was purchased from Aldrich as a 15% solution in N-methyl-2-pyrrolidone (NMP) and stored in a freezer. PEI (MW: 25,000), PVA (MW: 89,000 - 98,000) and PVS (MW: 170,000) were purchased from Aldrich. Poly (ether ether ketone) (PEEK) pellets were purchased from Polysciences Inc. The water soluble sulfonated PEEK (SPEEK) was prepared according to the literature [37]. Three coating solutions with concentrations of 0.3 g/L were prepared by dissolving PVA, PVS or SPEEK in deionized (DI) water at 80˚C overnight. The PVS solution was filtered before use to remove the insoluble impurities. The pH of the PVA, PVS and SPEEK solutions were 5.7, 5.8, and 1.0, respectively. All of the other organic and inorganic reagents including D-(+)-galactose (Sigma-Aldrich, ≥99%), propionic acid, acetic anhydride, triethylamine, NaCl, Na_2SO_4, $CaCl_2$, $MgSO_4$, were of analytical grade and used as received.

4.2.2 Preparation of partially modified P84 copolyimide membranes with PEI (p-P84-PEI)

The p-P84-PEI membranes were prepared with a procedure slightly modified from that described previously [33]. Four casting solutions were prepared by dissolving P84 powder in N, N-dimethylformamide (DMF) to give polymer concentrations of 19%, 21%, 23% and 25%, respectively. The polymer solution was

then cast onto a polyester support (Calendered PET from Crane Nonwovens) followed by immediate immersion into a room temperature water bath. After overnight immersion in the water bath the membranes were rinsed with and stored in deionized (DI) water.

Chemical modification was conducted by immersing a membrane into a 5% PEI aqueous solution (wt/vol) at room temperature for up to 20 min until a stable permeability was obtained. After rinsing by DI water, the membrane was annealed at 90 ˚C for 5 min to complete the chemical reaction and finally stored in DI water until use.

4.2.3 Preparation of PEI modified PMDA-ODA polyimide membranes (PI-PEI)

Five casting solutions were prepared by adding 0%, 10%, 20%, 40% and 60% propionic acid into the 15% PAA/NMP solution. With more than 60% propionic acid, the polymer will precipitate since propionic acid is a nonsolvent for PAA. The percentage of added propionic acid was based on the polymer solution. For example, to make a casting solution with 10% propionic acid, 10 g of propionic acid was added to 100 g of the 15% PAA/NMP solution. The mixture was then stirred by a mechanical stirrer until a clear solution was obtained. After that, the solution was degassed under vacuum to remove all the bubbles. The casting solution was then cast onto a polyester support (Calendered PET from Crane Nonwovens) and immersed immediately into a water coagulation bath at room temperature. The membrane thickness was controlled at roughly 100 micron. After 30 min, the membrane was removed from the water bath and washed thoroughly with DI water. Then the PAA membrane was dried by an isopropanol-hexane displacement sequence [38]: the membrane was immersed in the isopropanol for 90 min during which the isopropanol was refreshed 3 times. Subsequently, the isopropanol was replaced by hexane using

the same procedure. Chemical imidization was performed by immersing the PAA membranes into a mixture of acetic anhydride (Ac_2O) and triethylamine (TEA) (volume 4:1) at 100 ˚C for 36 hours. The resultant PI membranes were then washed using isopropanol several times and stored in isopropanol.

Chemical modification was conducted by immersing a membrane into a 1% PEI solution (wt/vol) in a mixture of isopropanol and water (volume 1:1) at 80˚C for 60 min until the permeability became stable. The membrane was then rinsed several times using dilute HCl solution at pH 3 to remove any loosely bound PEI, and finally stored in DI water until use.

4.2.4 *Preparation of surface coatings onto the p-P84-PEI and the PI-PEI membranes*

Surface coating experiments were carried out with a dead-end filtration cell (Sterlitech HP4750). Either the p-P84-PEI or the PI-PEI membranes were loaded in the cell followed by filling the cell with about 200 mL of a given coating solution so that only the surface of the membranes contacted the coating solution. Then the coating solution was pressed through the membrane under a pressure of 13.8 bar for 10 min. Vigorous stirring at a rate of 18.33Hz (1100 rpm) was applied using a standard magnetic stirrer (Corning Stirrer/Hot Plate, Model PC-420) in order to make an uniform coating. The membrane was then rinsed with copious amount of tap water.

4.2.5 Membrane performance measurement

Desalination performance of the polyelectrolyte-coated membranes was examined in dead-end mode using 300 mL of a 2.0 g/L NaCl aqueous feed solution under 13.8 bar and room temperature. The feed solution was stirred at a rate of 18.33Hz in the cell to minimize concentration polarization. Each membrane was

compacted at a pressure of 13.8 bar for at least 1 h prior to measurements to ascertain that a steady state was obtained. The permeated solution was then refilled into the feed and permeate samples were collected as appropriate. The permeation flux F was determined by measuring the permeation volume V (15-20 mL, 5 – 6.7% recovery) flowing across the membrane of area A (14.6 cm^2) in the time period Δt, F ($m^3m^{-2}day^{-1}$) = $V/(A \times \Delta t)$. Salt rejection was calculated as $R = (1 - \sigma_p/\sigma_f) \times 100\%$, where σ_p and σ_f were the conductivity of the permeate and the feed, respectively. Conductivity was measured with a bench-top conductivity meter (Oakton CON 510).

Similarly, rejection to $CaCl_2$, NaCl, Na_2SO_4 and $MgSO_4$ at four different initial concentrations (10, 50, 100 and 200 mmol/L) in aqueous solution was measured in order to test the separation capability of the membranes to various ions and qualitatively determine membrane charge. The rejection to uncharged solutes may be determined primarily by the surface pore size of the membrane [39]. Therefore, rejection to a sugar molecule galactose (180 Da) was used to estimate surface pore size and characterize pore size change during chemical modification of the polyimide membranes. A 10 mmol/L aqueous solution of galactose was used as feed. Sugar concentrations in the permeate and feed solutions were determined by a colorimetric method based on treatment with phenol and sulfuric acid [40].

4.2.6 Characterization of the antifouling property of membranes

The antifouling measurement was conducted according to the process in the Ref. [58] with some modifications. Three membrane samples, namely positively charged NF membrane PI-PEI, near neutrally charged NF membranes SPEEK-coated PI-PEI and commercial negatively charged NF membrane NTR-7450, were tested and compared under the same experimental conditions. Three kinds of model foulants were used: (1) 1% (w/v) bovine serum albumin (BSA) in phosphate buffered saline

(PBS) (pH 7.4, powder form from Sigma); (2) 1.0 g/L humic acid (HA, from Aldrich) with 1mM $CaCl_2$ in DI water; and (3) 1.0 g/L sodium alginate (SA, from Aldrich) in DI water. Membranes were assembled into a SterlitechTM HP475 stirred dead-end cell with a cell volume of 300 ml. The applied pressure was adjusted according to the flux of each membrane to ascertain the initial flux close to a certain value. DI water was first passed through the membrane for at least 2 h until the flux remained stable. The DI water was then replaced by a given foulant solution and the flux change with time was recorded. When permeate exceeded about 100 ml, the permeated solution was then refilled into the feed and the experiment was resumed until the flux was almost stable.

4.2.7 Fouling resistance of membranes to activated sludge

Similar to the antifouling tests, membrane fouling was measured using activated sludge as the feed. Three membrane samples, namely PVS-coated p-P84-PEI, SPEEK-coated PI-PEI and NTR-7450 were tested and compared under the same experimental condition. Fresh activated sludge was taken from a municipal activated sludge wastewater treatment plant located in Urbana, Illinois. On the day of sampling, mixed liquor suspended solids (MLSS) was measured to be 3000 – 4300 mg/L.

4.2.8 Physical characterization methods

ATR-FTIR spectra were collected at room temperature over a scanning range of 600 - 4000 cm^{-1} with a resolution of 4.0 cm^{-1}, using a Nexus 670 FT-IR (Thermo Electron Corporation, Madison, WI) with a Golden Gate^{TM} MKII Single Reflectance ATR (Specac Inc., Woodstock, GA). The spectrometer was installed with a deuterated triglycine sulfate-potassium bromide (DTGS-KBr) detector and KBr beamsplitter. Spectral analysis was performed using FT-IR software (OMNIC, Thermo Electron Corporation, Madison, WI).

SEM images were obtained using a Hitachi S-4700 with 15.0 kV accelerating voltage. For cross-sectional observations the polyimide layer was peeled off of the polyester support and fractured after immersion in liquid nitrogen. All samples were coated by sputtering with gold and palladium before testing.

Membrane hydrophobicity was estimated by water drop contact angle measurement using a goniometer (KSV Instruments Model: CAM 200). The dry membranes were fixed flat on a glass slide using double-sided tape. Five measurements were taken for the static contact angle immediately after the droplet was placed on the membrane.

4.3 Results and discussion

4.3.1 Preparation and characterization of PVA- or PVS-coated p-P84-PEI NF membranes

4.3.1.1 Preparation and characterization of p-P84-PEI

In previous studies [33], we described the preparation of a chemically modified polyimide membrane by polyethylenimine. It was found that the polyimide could be completely transformed into polyamide with free amine groups remaining, which led to a positive charge on the surface. The resultant NF membranes showed very good desalting capability and could especially be used for multivalent heavy metal ion removal. The highly cross-linked structure of the membranes could resist attack by most organic solvents. However, such rigid chemical structure would induce membrane embrittlement. Membrane permeability was also relatively low for MBR application. Thus, it is advantageous to develop membranes with a more modest degree of cross-linking so that both membrane toughness and permeability would be improved.

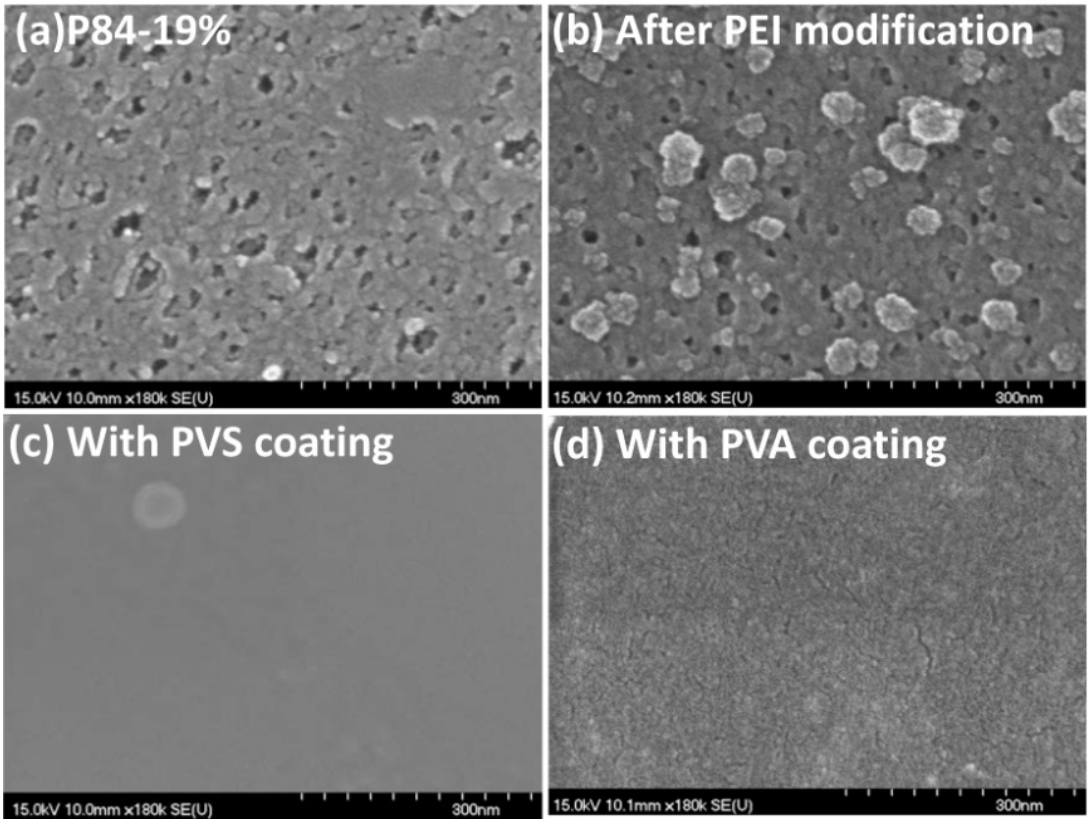

Figure 4.1 Surface morphology of membranes at different preparation stages.

In order to determine the appropriate polymer concentration for membrane development, four casting solutions containing 25%, 23%, 21% or 19% polymer were used to develop the P84 membranes by the phase inversion method. A concentration of lower than 19% would result in large pores and cracks on the membrane surface. The resultant membranes were designated as P84-25%, P84-23%, P84-21% and P84-19%, respectively. Surface structure of the P84-25%, P84-23% and P84-21% membranes can be found in the previous study [33]. It can be seen that the less concentration of the casting solution was used, the larger pore size of the resultant membrane was observed. The pore size of the P84-19% membrane can reach 20 – 30 nm, as shown in Figure 4.1a. This may be due to reduced polymer aggregation at lower polymer concentration [41]. These structural differences have a strong influence on mass transport through the membrane. As shown in Table 4.1 (Original

membrane), a decrease in polymer concentration corresponds to an increase in water permeability. No salt rejection was observed for all the unmodified P84 membranes (Table 4.2, Original membrane).

Table 4.1 Water flux data of membrane at different preparation stages[a].

	19%	21%	23%	25%
Original membrane	76.0 ± 6.3	41.4 ± 3.4	16.0 ± 4.5	5.4 ± 0.6
20 min reaction with 5% PEI/H_2O	19.1 ± 1.8	12.8 ± 1.1	3.0 ± 0.5	2.2 ± 0.2
10 min adsorption with 0.3 g/L PVS	3.8 ± 0.6	2.4 ± 0.7	1.5 ± 0.1	0.9 ± 0.2
60 min adsorption with 0.3 g/L PVA	17.3 ± 2.5	11.0 ± 0.5	2.0 ± 0.6	2.3 ± 0.3

Note: [a]Test condition: 2.0 g/L NaCl aqueous solution, 13.8 bar and room temperature.

Table 4.2 Salt rejection data of membrane at different preparation stages[a].

	19%	21%	23%	25%
Original membrane	0	0	0	0
20 min reaction with 5% PEI/H_2O	0	0	6.6 ± 1.1	6.7 ± 1.5
10 min adsorption with 0.3 g/L PVS	2.3 ± 0.9	14.8 ± 4.4	46.4 ± 2.7	27.7 ± 3.1
60 min adsorption with 0.3 g/L PVA	0	0	37.6 ± 3.5	17.9 ± 1.0

Note: [a]Test condition: 2.0 g/L NaCl aqueous solution, 13.8 bar and room temperature.

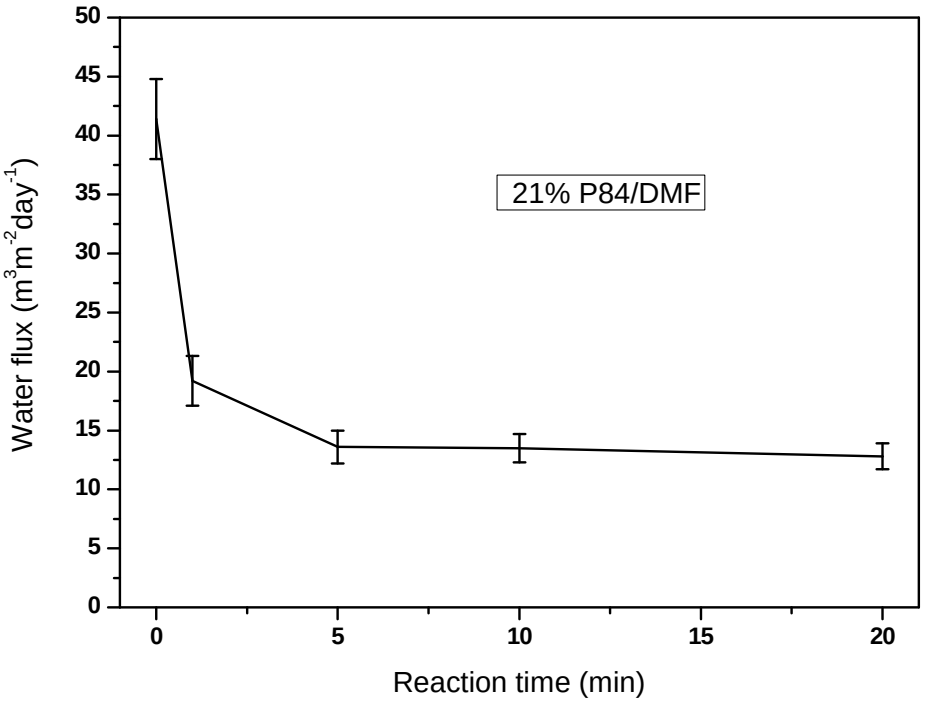

Figure 4.2, Effect of modification time on membrane flux. The P84-21% membrane was modified by a 5% PEI/H_2O solution at room temperature.

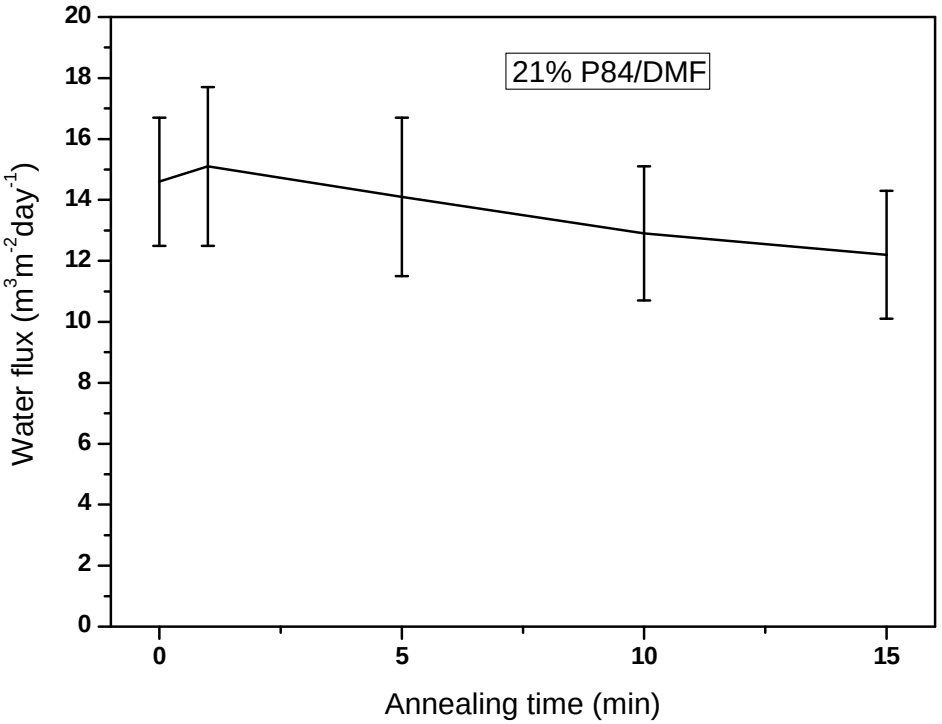

Figure 4.3 Effect of annealing at 90 ˚C on membrane flux. The partially modified P84-21% membrane was annealed to complete reaction.

Chemical modification of the four as-mentioned P84 membranes was carried out by immersion into a 5% PEI/H_2O solution at room temperature. Figure 4.2 shows the effect of modification time on water flux of the P84-21% membrane (tap water was used). With increasing modification time, water flux decreased quickly and finally reached a stable value within 20 min. It was assumed that the maximum amount of PEI was reacted with the polyimide membrane at this modification condition. After that, the membrane was cured at 90 ˚C to complete the reaction. As shown in Figure 4.3, 5 min annealing would be sufficient since longer annealing time resulted in flux decreasing due to the pore shrinking upon drying.

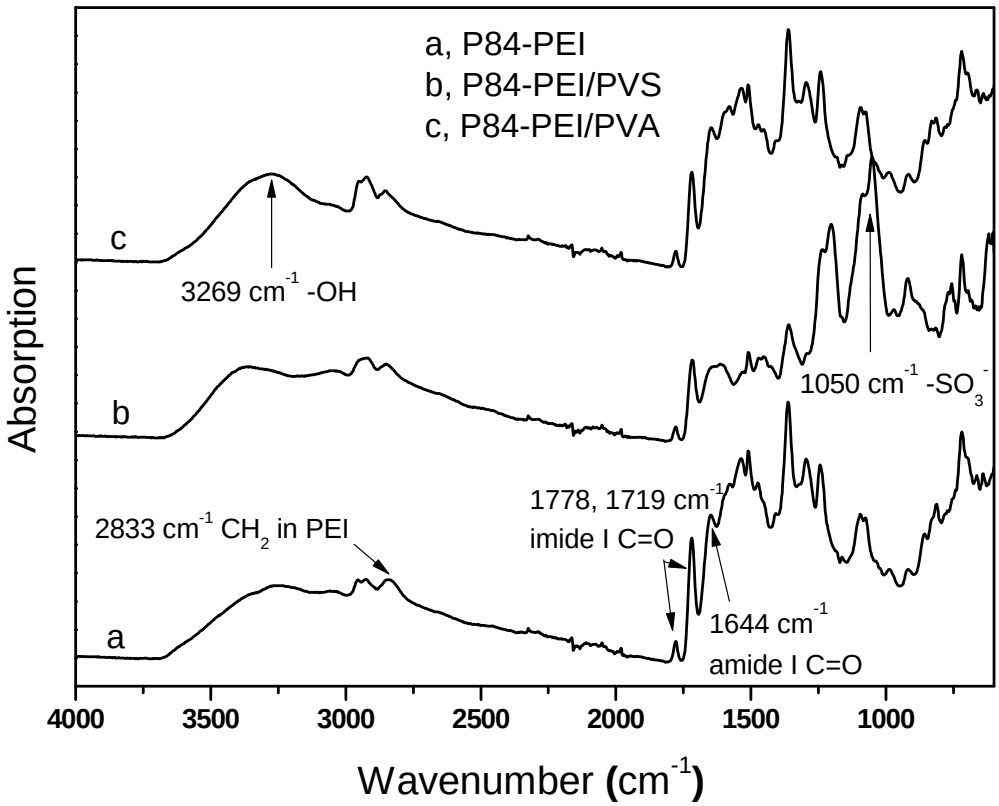

Figure 4.4, ATR-FTIR spectra of membranes at different preparation stages. (a) Partially modified P84 (P84-21%) membrane (p-P84-PEI); (b) With PVS coating; (c) with PVA coating.

The partial modification of the P84 membrane by PEI was confirmed by ATR-FTIR. As shown in Figure 4.4a, the characteristic absorption bands of the imide

groups remained strong at 1778 cm^{-1} (symmetric C=O stretching, imide I), 1719 cm^{-1} (asymmetric C=O stretching, imide I), while the characteristic peaks of amide groups at 1644 cm^{-1} (C=O stretching, amide I) appeared. The absorption peaks at 2833 $cm^{-1}$and 2926 cm^{-1} represent CH_2 groups of PEI. The band at 3267 cm^{-1} (N-H vibrations) indicates the existence of free amine groups.

Membrane desalination properties of the four kinds of partially modified membranes are summarized in Table 4.1 and Table 4.2. Water flux was decreased after PEI modification because PEI molecules may fill the pores by diffusing into the pores. Figure 4.1b shows the surface morphology of the PEI modified P84-19% membrane. It looks that the large pores could not be effectively blocked while some areas containing small pores became much denser. Therefore, this membrane showed ultrafiltration properties with high flux and no salt rejection. However, the PEI modified membranes gradually became less permeable when using the membranes developed from 19% to 25% concentrations as the starting membranes. The latter two membranes showed nanofiltration properties with some desalting capability.

4.3.1.2 Preparation and characterization of PVS- and PVA-coated p-P84-PEI

PVS and PVA were used to modify surface properties of the p-P84-PEI membranes. Figure 4.5 and Figure 4.6 show the effect of coating time on the water flux using the PEI modified P84-21% membrane as an example. It appeared that water flux decreased with increasing adsorption time and finally reached a stable state. The PVS coating was formed much quicker (5 – 10 min) than the PVA coating (30 – 60 min). On the other hand, the PVS coating displayed a more sever flux loss (84.6%) than the PVA coating (14.1%). These results suggest that the electrostatic attraction force between the PVS and the modified membrane makes the adsorption faster and the coating layer denser while the hydrogen bonding between the PVA and

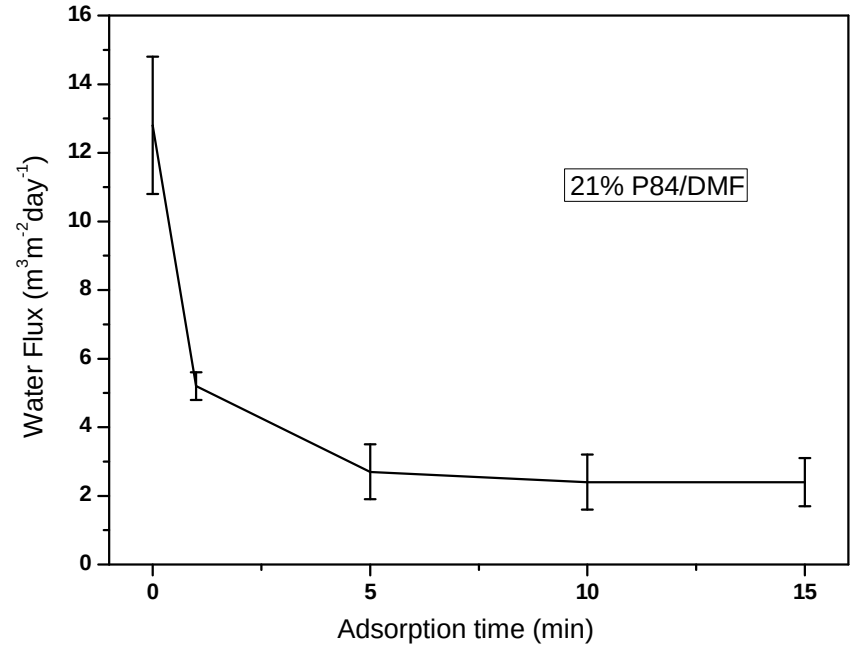

Figure 4.5 Effect of PVS coating on membrane flux.

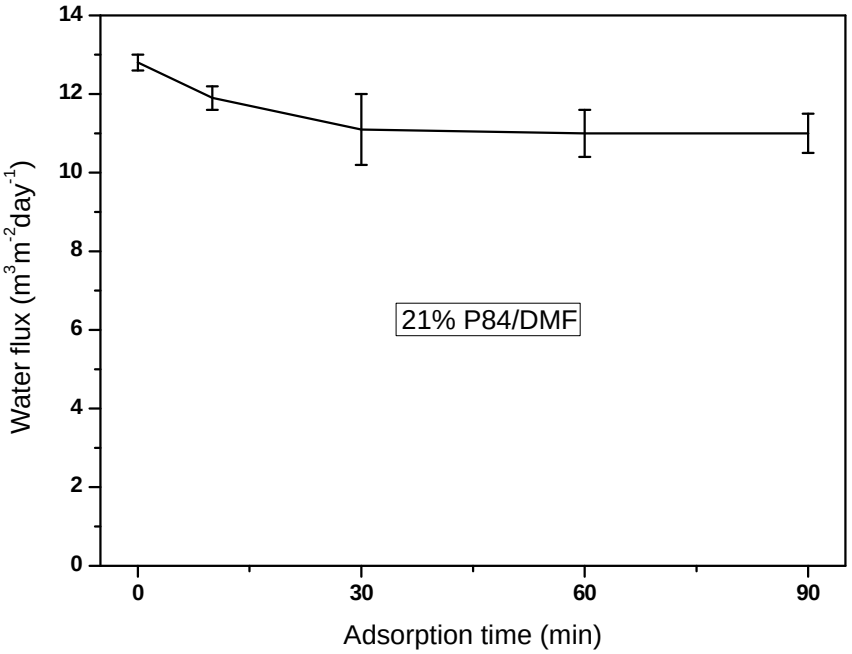

Figure 4.6 Effect of PVA coating on membrane flux.

the modified membrane make the adsorption slower and the coating layer looser. From Figure 4.1c and Figure 4.1d, it can also be observed that the original porous membrane surface could be completely covered by PVS or PVA. The PVA coating appeared looser that the PVS coating. ATR-FTIR characterization of the PVS- and PVA-coated membranes is shown in Figure 4.4b and Figure 4.4c respectively. The

characteristic peaks of PVS at 1050 cm^{-1} ($-SO_3^-$) and PVA at 3269 cm^{-1} (-OH) can be clearly observed.

Desalination properties of the PVS- or PVA-coated membranes are summarized in Table 4.1 and Table 4.2. These membranes showed a variety of desalination properties. For example, for both PVS- and PVA-coated membranes, the membrane originating from P84-19% membrane showed the highest flux and lowest salt rejection while the membrane originating from P84-23% membrane showed the highest salt rejection. Therefore, these two kinds of membrane will be used as the representatives of ultrafiltration membrane and nanofiltration membrane for further antifouling test, which will be described in Section 4.3.3.

4.3.2 Preparation and characterization of SPEEK-coated PI-PEI NF membranes

4.3.2.1 Preparation and characterization of PMDA-ODA polyimide (PI) membranes

Because PMDA/ODA polyimide is an insoluble material, membrane preparation was processed from its precursor polyamic acid (PAA) followed by chemical imidization to transform the PAA into PI. This reaction process is shown in Figure 4.7 (i). In preparing asymmetric membranes by phase inversion, propionic acid was added to the initial PAA/NMP system to modify membrane morphology and permeability. The resultant polyimide membranes prepared with 0%, 10%, 20%, 40% and 60% propionic acid additive will be referred to as PI-0%, PI-10%, PI-20%, PI-40% and PI-60%, respectively.

Figure 4.8 shows the effect of propionic acid additive on membrane permeability. By adding 10% propionic acid, the resultant PI membrane became less permeable than the membrane prepared without additive. However, adding more than 10% propionic acid led to higher permeability of the obtained membranes. With over 60% additive, PAA would precipitate because propionic acid is a nonsolvent.

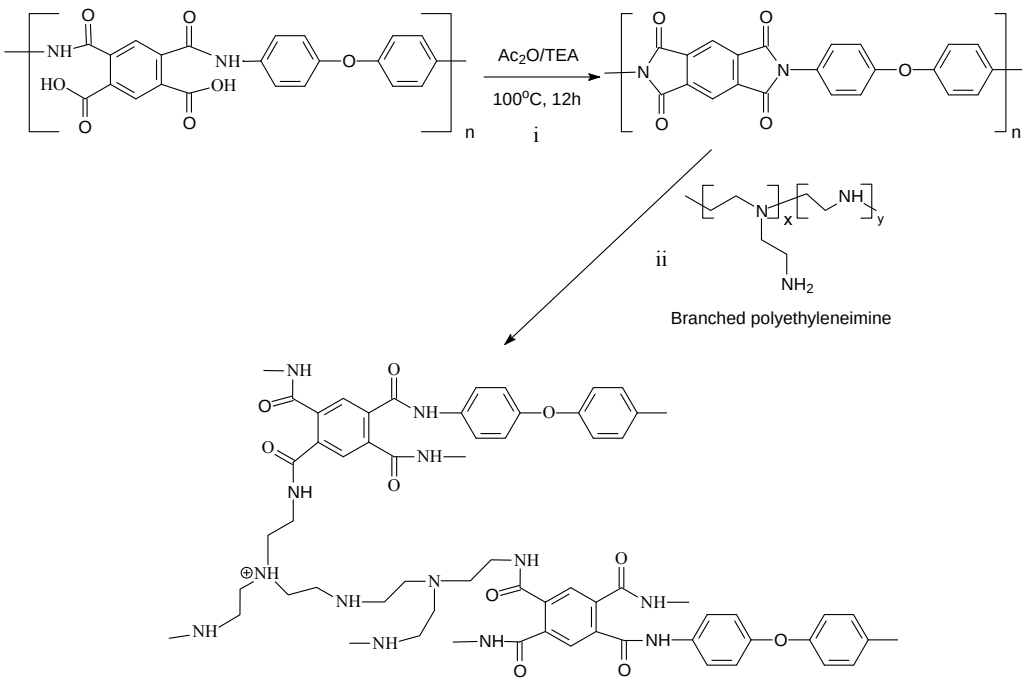

Figure 4.7 (i) Synthesis of polyimide from polyamic acid precursor via chemical treatment; (ii) Chemical modification route of polyimide with PEI.

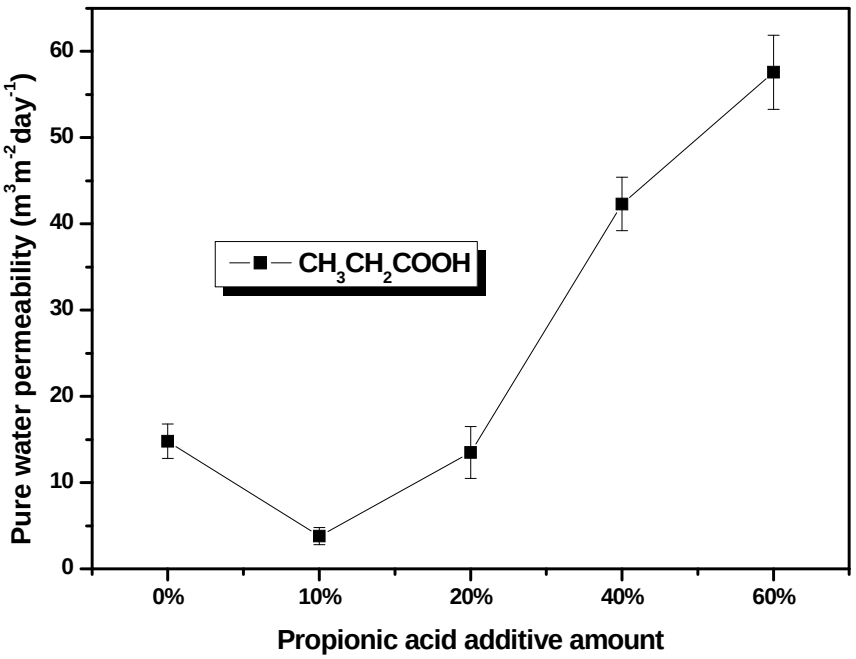

Figure 4.8 Effect of propionic acid additive on membrane permeability

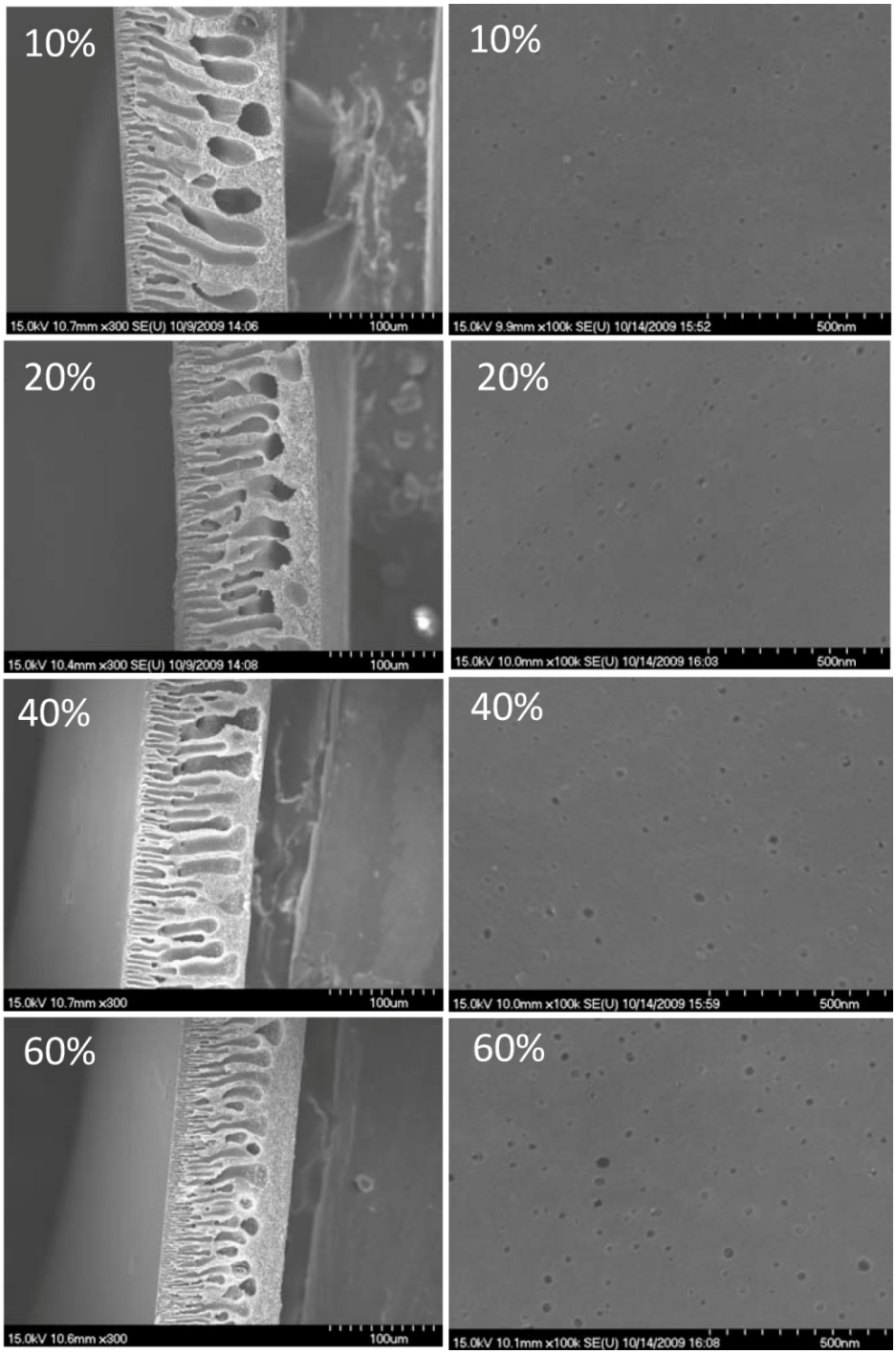

Figure 4.9 Cross-sectional (left) and surface (right) morphologies of the polyimide membranes developed from polyamic acid solutions with different amount of propionic acid additive.

Figure 4.9 presents SEM images of the membrane cross-sections and surfaces. In the previous study [42], it was shown that the PI-0% membrane had a highly porous structure containing a large amount of macrovoids, which led to mechanical weakness. With 10% propionic acid additive, however, the macrovoids show a typical

finger-like structure and surface pores become smaller. With more propionic acid, the macrovoids appear to be thinner and more densely packed. Surface pores also become larger. The structures of these membranes are closely correlated to their water permeability as shown in Figure 4.8.

These results may be explained by the complex formation between propionic acid and the solvent NMP [43]. Hydrogen bonding between them can be represented in Figure 4.10 [44]. Such interaction would greatly decrease the solvent power of NMP resulting in stronger polymer-polymer interaction. Therefore, during coagulation in a water bath rapid polymer gelation will take place to form a skin layer. Such rapid skin formation could help to avoid surface inhomogeneities such as pinholes. Moreover, the complex can be quickly dissociated by water into solvent and nonsolvent species. Thus the polymer solution will contain a higher level of nonsolvent and correspondingly a lower level of solvent than what could be obtained without the complexation effect. The sudden large increase in effective concentration of nonsolvent leads to a dramatically accelerated coagulation process [43]. It has been known that instantaneous phase separation could often induce parallel finger-like structure [45]. Therefore the more propionic acid added, the more significance of the complexation effect may be observed resulting in larger number of fingers. On the other hand, polymer concentration would decrease with the increased amount of propionic acid added, which induced larger pore size of the membrane due to reduced polymer aggregation at lower polymer concentration [46].

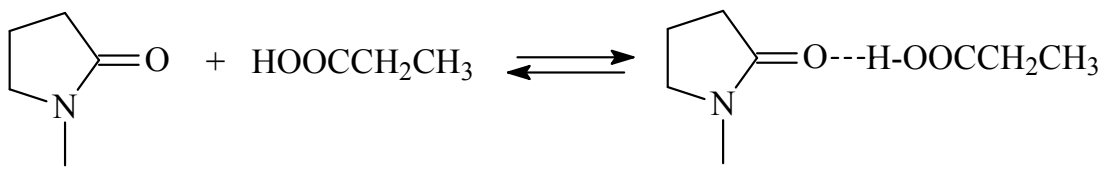

Figure 4.10 Formation of complex between propionic acid and NMP through hydrogen bonding

4.3.2.2 Preparation and characterization of PEI modified polyimide (PI-PEI) NF membranes

Figure 4.7 (ii) shows the chemical reaction between PMDA-ODA polyimide and PEI. It can be seen that the resultant PI-PEI NF membrane has a fully cross-linked structure and contains ether, amide, amine, ammonium and phenyl groups on the surface. Such chemical characteristics make the membrane positively charged and rather hydrophilic. This positive charge permits the adsorption of a layer of negatively charged polyelectrolyte (SPEEK) to prepare a near neutrally charged NF membrane due to charge compensation.

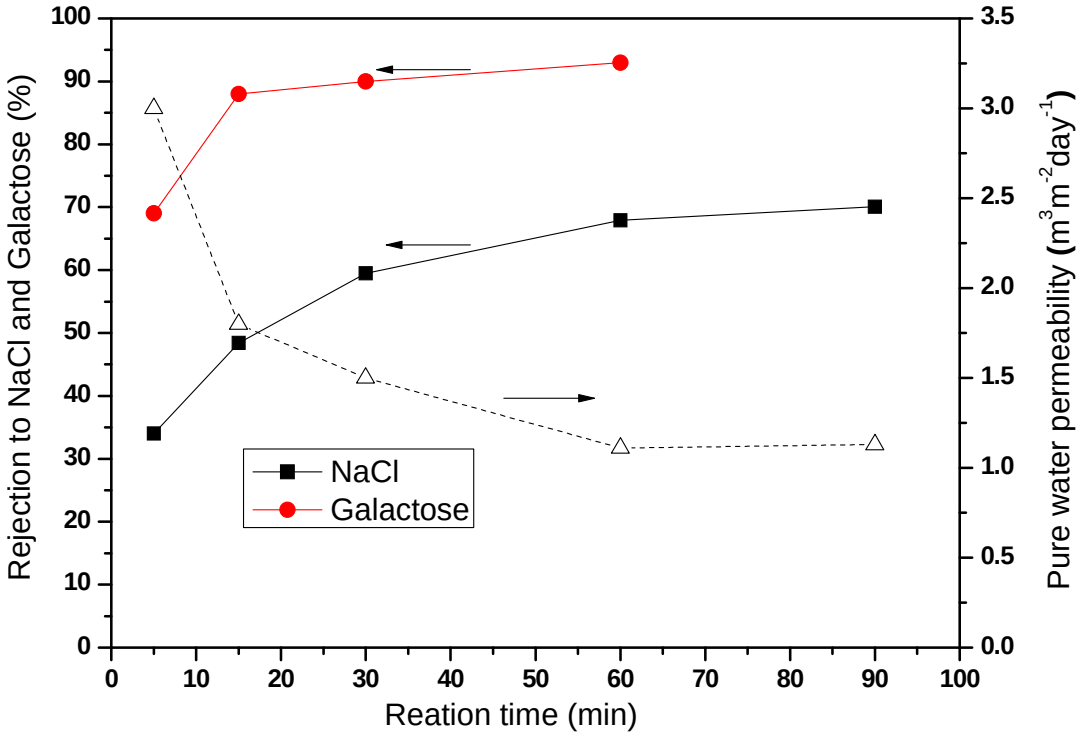

Figure 4.11 Effect of reaction time of polyimide membranes with PEI on the water permeability, NaCl rejection and galactose rejection performance of the PI-20% membrane sample.

Figure 4.11 shows the effect of reaction time on the water permeability, NaCl rejection and galactose rejection performance of the PI-20% membrane. With increasing modification time, water flux decreased gradually and finally reached a stable value after 1 h. Meanwhile, both galactose rejection and salt rejection increased

until a maximum value was reached. The rejection of galactose may be determined primarily by the surface pore size of the membrane while the rejection of salt may be determined by both the surface pore size and surface charge of the membrane [1]. Therefore, these results indicate that both surface pore size and surface chemistry became stable with 1 h modification. The optimum separation performance of the obtained membrane would be 67.9% NaCl rejection and 93% galactose rejection with a 1.1 $m^3m^{-2}day^{-1}$ water flux.

Table 4.3 Desalination performance of the various membranes

Samples	Flux ($m^3m^{-2}day^{-1}$)	Rejection (%)
PI-10%	0.5	78
PI-40%	1.6	48.6
PI-60%	2.9	25.7

Prepared under the same modification and test conditions, the other three PI membranes demonstrated a trade-off trend between salt rejection and permeation flux (Table 4.3). For each membrane, surface chemistry should be the same after modification. However, their surface pore size may maintain the same order as the initial PI membranes assuming that same amount of PEI was anchored onto the pore wall. Larger pores would allow faster mass transport and consequently lower salt retention and vice versa. We selected the PI-20% membrane for further studies because both the salt rejection and permeate flux were reasonably high.

Figure 4.12 shows the change in static contact angles of the PEI modified polyimide membranes in dependence on the modification time. The initial membrane (PI-20%) was relatively hydrophobic with a contact angle of 75 ± 8°. With increasing reaction time contact angle was observed to decrease gradually and finally reach a stable value of 59 ± 4° after 1 h. This considerable decrease of contact angle suggests that membrane hydrophilicity was improved by introducing hydrophilic functional groups like amines and ammonium onto membrane surface. These results are in good

agreement with the desalination data, confirming that highest modification degree was reached within 1 h to give a fully modified PI-PEI membrane. Surprisingly, the 30 min modified membrane showed a contact angle of 48 ± 4°, lower than that of the membrane with longer modification time. It is likely that at 30 min, the large PEI molecules could only partly bond to the membrane surface. The nonbonding parts of PEI may cover the membrane surface so that contact angle became very low due to the hydrophilic amine groups.

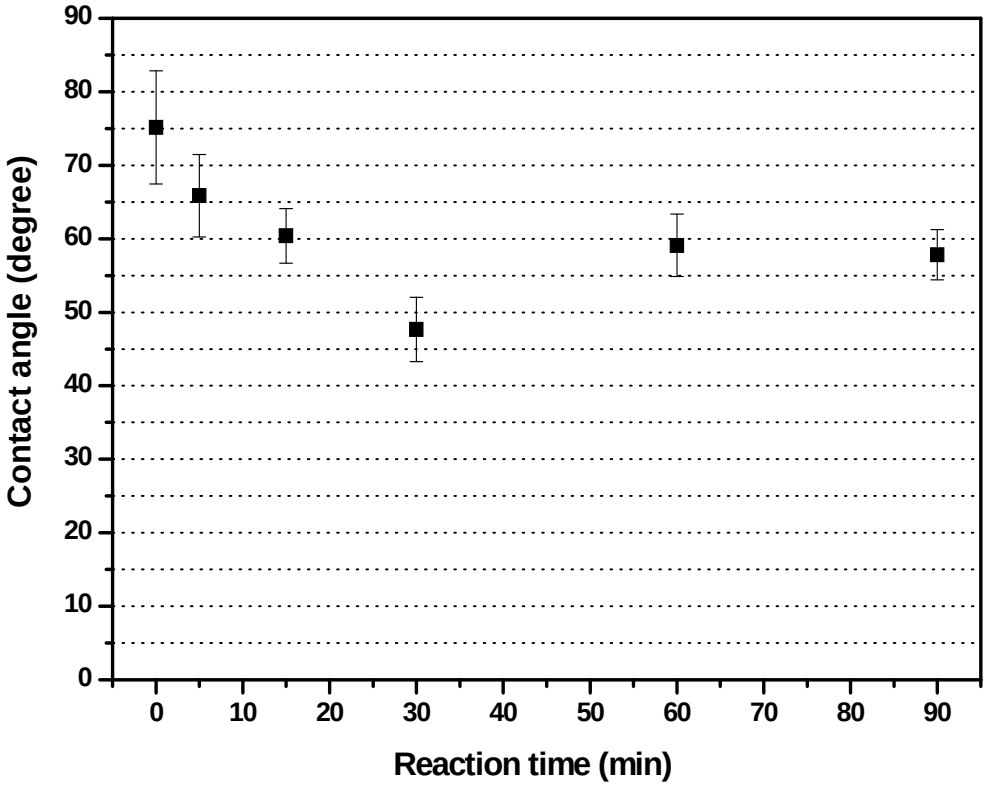

Figure 4.12 Contact angle of the PEI modified polyimide membranes in dependence on the modification time.

Figure 4.13 shows the rejection to various salts as a function of the feed concentration for the PEI modified polyimide membranes. A rejection sequence of $CaCl_2 > MgSO_4 > NaCl > Na_2SO_4$ indicates a positive charge for the membrane [33]. Additionally, the decrease in salt rejection with increasing salt concentration is consistent with the Donnan exclusion model. As ionic strength increases the

membrane charge is shielded, resulting in a lower effective charge and consequently lower salt rejection [1].

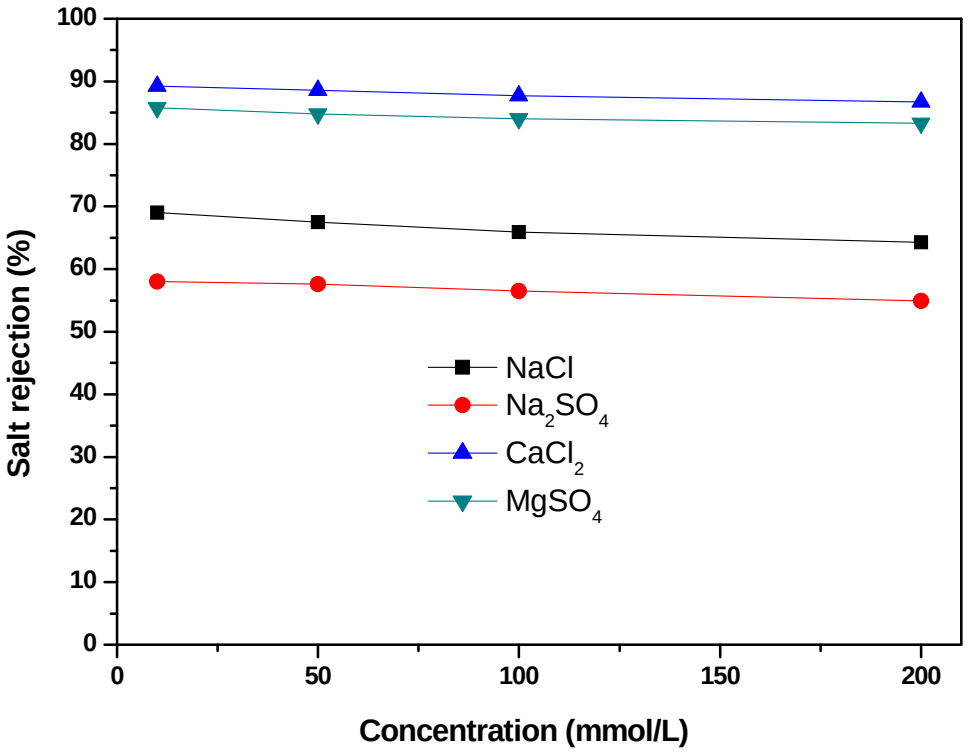

Figure 4.13 Rejection to various salts as a function of the feed concentration for the PEI modified polyimide membranes.

4.3.2.3 Preparation and characterization of SPEEK-coated PI-PEI NF membranes

SPEEK is a negatively charged polyelectrolyte which can be adsorbed firmly onto the positively charged PI-PEI membranes due to electrostatic attractions. During coating process, a pressure of 13.8 bar was applied to pass a vigorously stirred SPEEK solution through the PI-PEI membrane. It has been shown that pressure may compact the coating film and make it uniform and free of defects [58]. A low concentration of 0.3 g/L was used in order to control the film thickness and make the membrane charge nearly neutral [35]. If a high concentration of several grams per liter was used, excessive material may deposit on the membrane resulting in membrane charge overbalanced [47]. In addition, a short adsorption time of 10 min was used as referred to the optimum preparation conditions of PVS coating (see

section 4.3.1.2). The resultant PI-PEI/SPEEK NF membranes showed a pure water flux of about 1 $m^3m^{-2}day^{-1}$ when tested at room temperature and 13.8 bar.

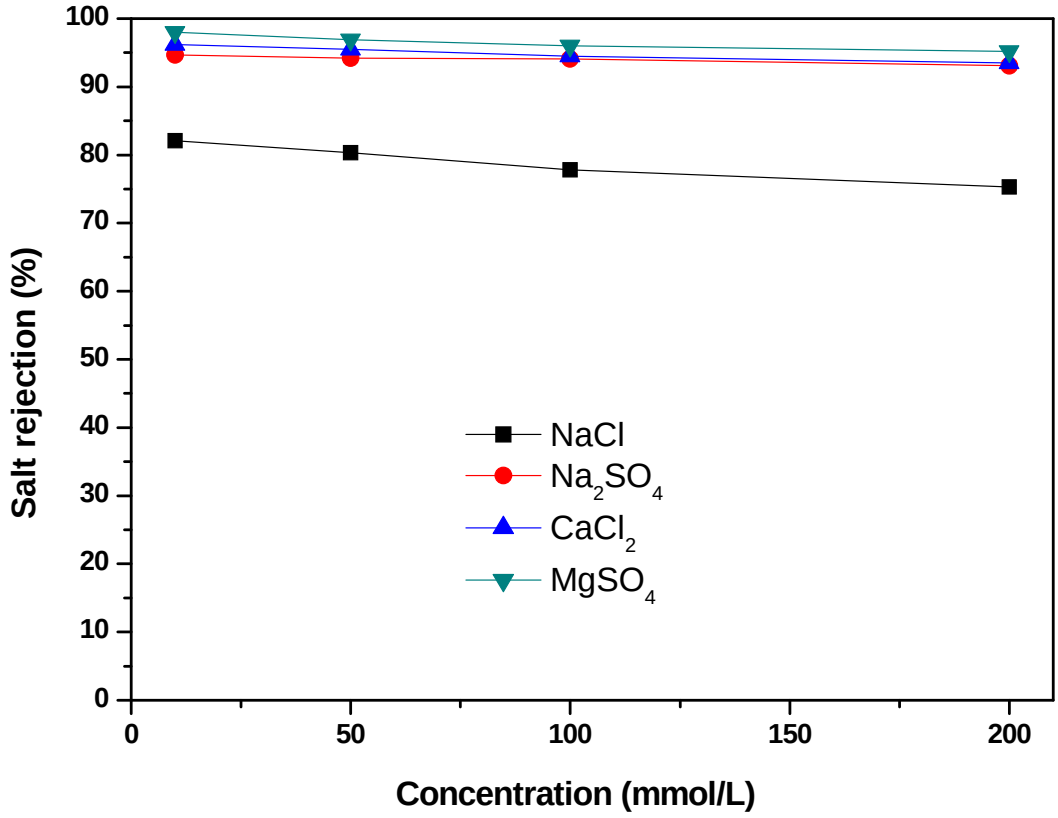

Figure 4.14 Rejection to various salts as a function of the feed concentration for the SPEEK-coated PI-PEI NF membranes.

The PI-PEI/SPEEK NF membrane was measured with regard to its rejection to four charged solutes $CaCl_2$, $MgSO_4$, NaCl, and Na_2SO_4. The results are shown in Figure 4.14. Within the concentration range between 10 and 200 mmol/L, a similar rejection value to $CaCl_2$, $MgSO_4$, and Na_2SO_4 can be observed to be around 95%. The rejection to NaCl was around 80%, lower than the other three salts. Therefore, this membrane could remove multivalent ions, both cations and anions, more efficiently than monovalent ions. This cannot be explained by Donnan exclusion. It is probable that the negative charge of SPEEK balanced the positive charge of the P84-PEI membrane resulting in a slightly negative surface layer. The overall membrane charge then became almost neutral and the Donnan exclusion effect did not govern the ion

separation behavior. Instead, the hydrated diameter of each ion and the diffusion coefficient of each salt determined the different retentions [1, 48].

4.3.2.4 Characterization of membranes at different preparation stages

Figure 4.15 shows the ATR-FTIR spectra of membranes at different preparation stages. The PMDA/ODA polyimide (PI) membrane exhibits several characteristic bands as follows: 1778 cm^{-1} (symmetric C=O stretching, imide I), 1722 cm^{-1} (asymmetric C=O stretching, imide I), and 1378 cm^{-1} (C-N-C stretching, imide II). The peaks at 1500 cm^{-1} and 1245 cm^{-1} are from the C-C stretching of benzene ring and the C-O-C stretching of ODA, respectively [49]. On the other hand, the typical polyamic acid absorption bands at 1660 cm^{-1} (C=O stretching, amide I) and 1550 cm^{-1} (C-N stretching, amide II) [50], and typical isoimide bands at 1800 cm^{-1} [51] are

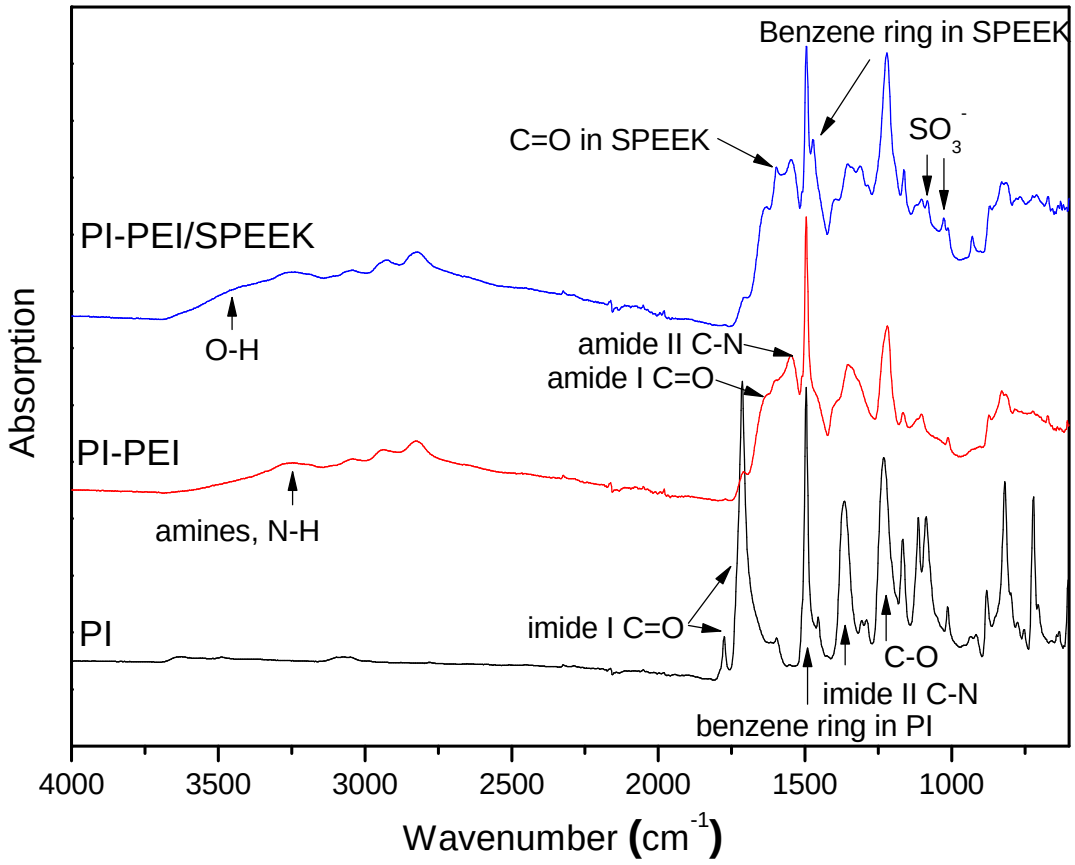

Figure 4.15 ATR-FTIR spectra of membranes at different preparation stages.

totally absent. Therefore, this membrane has an identical infrared spectrum to the polyimide film cured by thermal process [49, 50, 51], indicating the polyamic acid was completely transformed to polyimide under these reaction conditions.

After reaction with PEI, the absorption peaks of the imide I bands almost disappeared. Meanwhile, the characteristic peaks of amide groups at 1644 cm^{-1} (C=O stretching, amide I) and 1547 cm^{-1} (C-N stretching, amide II) appeared [52]. The band at 3267 cm^{-1} (N-H vibrations) indicates the existence of free amine groups. From the FTIR data, one can conclude that within 1 h of reaction, the imide bonds were completely transformed into amide bonds, resulting in the amine modifier covalently bound to the PI membrane with free amine functionalities.

When SPEEK was coated, a few new absorption peaks of SPEEK clearly appeared at 1600 cm^{-1} (C=O stretching), 1472 cm^{-1} (phenyl ring), 1084 cm^{-1} (symmetric O=S=O), 1027 cm^{-1} (S=O stretching) and 3450 cm^{-1} (O-H), indicating SPEEK was successfully deposited on the membrane surface.

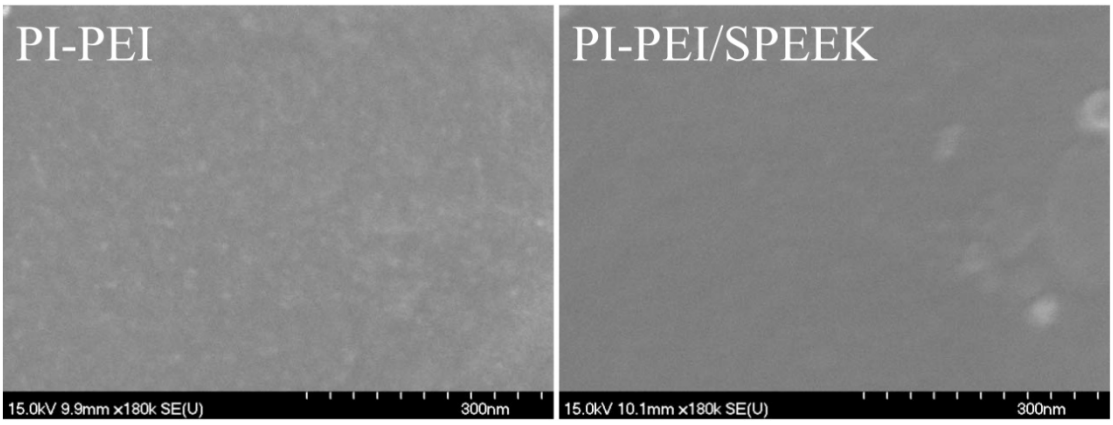

Figure 4.16 SEM spectra of the PI-PEI and the PI-PEI/SPEEK NF membranes.

Figure 4.16 shows SEM morphology of the PI-PEI and the PI-PEI/SPEEK NF membranes. No pore could be observed on the surface of these two membranes. The PI-PEI membrane looks a little rough while the PI-PEI/SPEEK membrane is very

smooth which could be attributed to the preparation method. This smooth surface is beneficial for fouling resistance.

4.3.2.5 Antifouling property of the PI-PEI/SPEEK membrane in comparison with the PI-PEI and NTR-7450 membranes

Three NF membranes PI-PEI, PI-PEI/SPEEK and commercial NTR-7450 were used as representative of positively charged, near neutrally charged and negatively charged membranes respectively. The NTR-7450 membrane was selected because it has similar sulfonated surface with the PI-PEI/SPEEK membrane. However, The NTR-7450 membrane has higher permeability than the PI-PEI/SPEEK membrane. Therefore, a lower pressure of 10.3 bar (150 psi) was used for NTR-7450 while a pressure of 13.8 bar was used for both the PI-PEI and the PI-PEI/SPEEK membranes which resulted in similar water fluxes for three of them. It has been shown that the initial flux, rather than applied pressure, seems to directly affect the extent of flux reduction [53]. With similar initial fluxes and the same other experimental conditions, the difference in degree of flux decline during fouling tests may reflect different fouling resistance of these membrane with different surface charging. Their fouling resistance was measured in dead-end mode using three model foulants of BSA, HA and SA as representative of proteins, NOM and polysaccharides, respectively.

Figure 4.17 shows flux decline during dead-end filtration of a feed solution containing 1% (w/v) BSA in 0.01 M PBS. For each membrane, the water flux at any given time was normalized to the initial stabilized flux after compaction. The initial fluxes for each membrane are shown in the legend. For all the membranes, fluxes decreased with the increase of filtration time. The flux decline may be caused by both membrane fouling and concentration of the feed solution due to the high retention of the solutes. In order to remove the concentration effect, at certain filtration time (90

min or 120 min), the permeate was refilled into the feed to restore the initial feed concentration. Then the flux would be restored to a higher value which may be caused primarily by the fouling effect. By this definition, the PI-PEI/SPEEK membrane had very little fouling since the flux was almost fully recovered after feed refill. Both the PI-PEI and the NTR-7450 membranes showed similar flux profile. The foulant-caused flux decline of these was much more than that of the PI-PEI/SPEEK membrane. These results suggest that the neutrally charged membrane has much better fouling resistance than both the positively charged and the negatively charged membranes. Although the overall charge of BSA is close to neutral, it has a variety of functional groups including amines and carboxylic acid, which provide both positive sites and negative sites respectively. It is likely that these charged sites could be adsorbed on an oppositely charged surface via electrostatic interactions. However, for a membrane with a low surface charge, such electrostatic interaction could be minimized resulting in very little BSA adsorption.

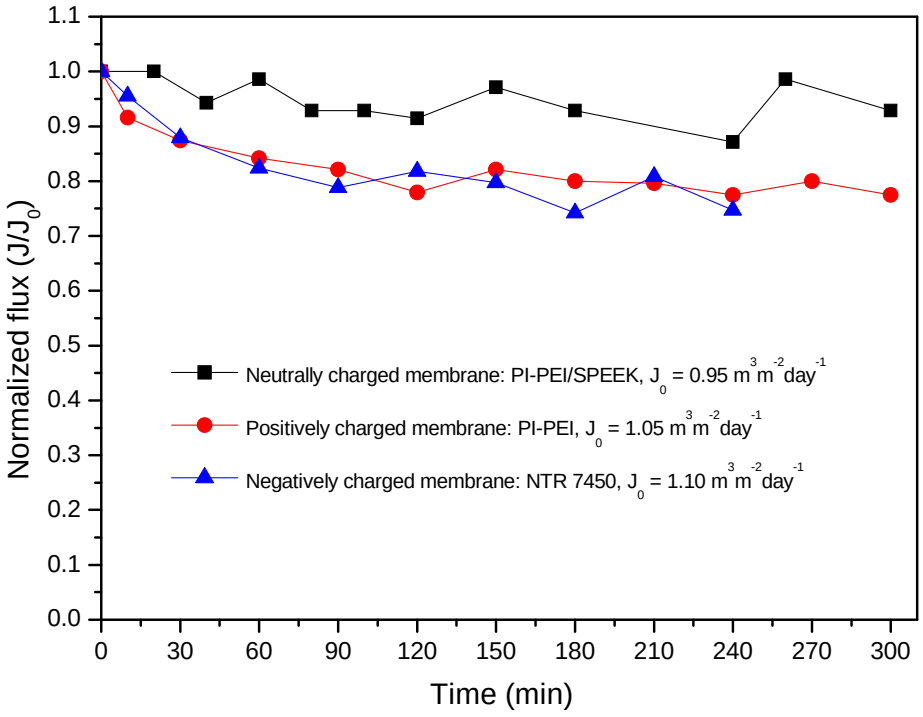

Figure 4.17 Dead-end filtration of model protein solution (bovine serum albumin, 1.0 g/L, 13.8 bar) with PI-PEI, PI-PEI/SPEEK and NTR-7450

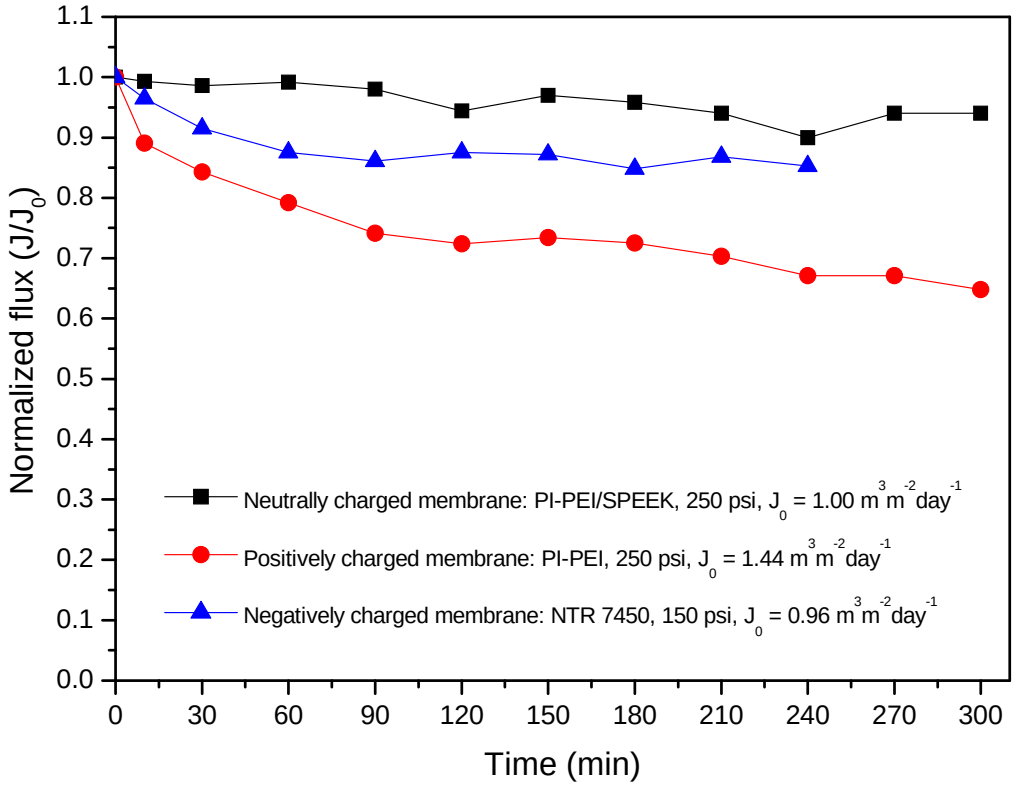

Figure 4.18 Dead-end filtration of model NOM solution (humic acid, 1.0 g/L, 1 mM $CaCl_2$, 13.8 bar) with PI-PEI, PI-PEI/SPEEK and NTR-7450

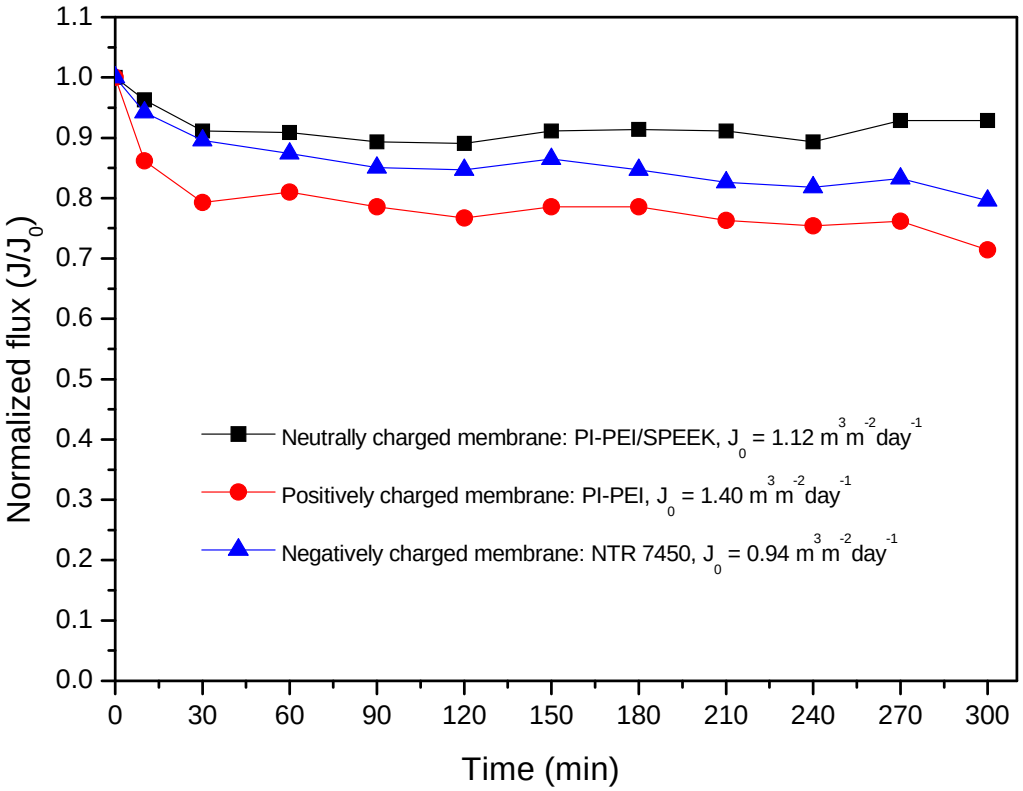

Figure 4.19 Dead-end filtration of model polysaccharide solution (sodium alginate, 1.0 g/L, 13.8 bar) with PI-PEI, PI-PEI/SPEEK and NTR-7450

Flux decline caused by 1.0 g/L HA or 1.0 g/L SA is shown in Figure 4.18 and Figure 4.19 respectively. The HA solution also contains 1mM $CaCl_2$ to enhance fouling tendency of humic acid because Ca^{2+} ions can bridge the carboxyl groups of humic acid. Both figures show the same sequence of flux decline: PI-PEI/SPEEK < NTR-7450 < PI-PEI indicating the fouling resistance of the three membranes has a reversed order. Both the HA and SA contain a lot of carboxylic groups and thus are negatively charged. As expected, the positively charged membrane could adsorb the oppositely charged foulants due to charge attractions giving the highest flux decline. Although a negatively charged membrane could repulse negatively charged small molecules like surfactants, it may not be true for large complicated polymers like HA and SA. Similar to BSA, HA and SA may also have some positive sites. The charge interaction with a negative surface could be stronger than that with a neutral surface. Therefore, the neutral membrane would show the lowest foulant adsorption by eliminating any charge related interactions.

4.3.3 Resistance to activated sludge of the PI-PEI/SPEEK and the P84-PEI/PVS membranes in comparison with the NTR-7450 membrane

The results from above studies suggest that the newly designed NF membranes by coating a layer of negatively charged polyelectrolytes onto the surface of positively charged NF membranes should exhibit lower fouling and produce higher quality effluents in MBR operations compared with UF membranes conventionally employed. For potential MBR application, fouling tendency of three membranes, PI-PEI/SPEEK, P84-PEI/PVS and commercial NTR-7450 was preliminarily investigated in dead-end mode using activated sludge taken from an aerobic bioreactor. Figure 4.20 compares the normalized flux data for the three NF membranes. The PI-PEI/SPEEK membrane showed less flux decline for the entire time range and correspondingly better resistance to activated sludge than the NTR-7450 membrane.

However, the P84-PEI/PVS membrane showed much worse resistance to activated sludge than both the PI-PEI/SPEEK and the NTR-7450. This surprising result may be related to other surface characteristics such as hydrophilicity, surface roughness and pore structure. Since the activated sludge may consist of complicated components including salts, organics, colloidal and particles, further detailed studies are required to characterize and modify the membrane surface properties for use in MBR application.

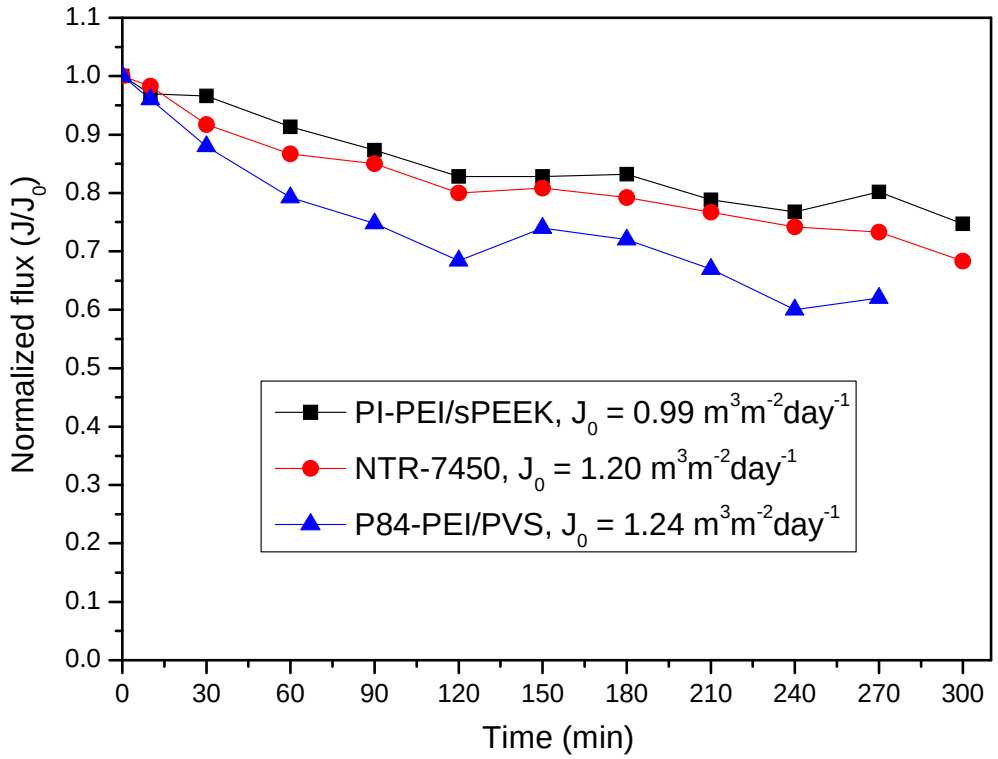

Figure 4.20 Dead-end filtration of model activate sludge solution (MLSS: 3000 – 4300 mg/L, 13.8 bar) with PI-PEI/SPEEK, NTR-7450 and P84-PEI/PVS

4.4 Conclusions

In order to prepare a fouling resistant NF membrane for potential MBR application, we designed two kinds of membrane systems. The first system consisted of a partially modified P84 polyimide membrane with PEI and a surface coating using PVS or PVA. By decreasing the extent of chemical modification which was carried

out at a low reaction temperature and controlled time, membrane brittleness was improved due to the decreased degree of cross-linking. Several initial P84 membranes were prepared from casting solutions with various concentrations from 19% to 25%. Their pore size and water permeability varied considerably. After modification with PEI and coating with PVS or PVA, the final membranes showed properties in a broad range between loose ultrafiltration to nanofiltration. These membranes may meet the needs in various industrial applications such as MBR.

Another system involved preparation of a nearly neutrally charged NF membrane developed by adsorption of a layer of negatively charged SPEEK onto the surface of a positively charged NF membrane. Still, the positively charged NF membranes were prepared by chemical modification of PMDA-ODA polyimide membranes using PEI. The modified PI-PEI membrane showed a rejection sequence of $CaCl_2 > MgSO_4 > NaCl > Na_2SO_4$, which could be explained by Donnan repulsion effect. After coating SPEEK, the PI-PEI/SPEEK membrane could remove multivalent ions more efficiently (> 95%) than monovalent ions (80%) due to the size effect; a rejection sequence of $CaCl_2 \approx MgSO_4 \approx Na_2SO_4 > NaCl$ was observed. When using bovine serum albumin (BSA), humic acid and sodium alginate as the model foulants, the neutrally charged membrane exhibited much better fouling resistance than both the positively charged and negatively charged membranes. This result suggests that the foulants would be less likely to deposit onto a neutral membrane due to the elimination of the charge interaction between the membrane and the foulants.

In an attempt to apply these two systems in an MBR process, it was found that the second membrane system PI-PEI/SPEEK showed much better resistance to activated sludge than the first membrane system P84-PEI/PVS. Although these two membranes had similar surface chemistry and surface charging, they may have other

differences in surface properties such as hydrophilicity, roughness and pore structure, which needs further detailed studies in the future.

4.5 References

[1] A.I. Schäfer, A.G. Fane, T.D. Waite (Eds.), Nanofiltration - Principles and Applications, Elsevier Ltd., 2005.

[2] R.W. Baker (Ed.), Membrane technology and applications, John Wiley & Sons, Ltd., Chichester, 2004.

[3] Bailey, B.; Lamsal, R.; Farzana, N.; Walsh, M. E.; Gagnon, G. A. Water reclamation and reuse. *Water Environment Research* 80(10) (2008) 1281.

[4] R.J. Petersen, Composite reverse osmosis and nanofiltration membranes, *J. Membr. Sci.,* 83 (1993) 81.

[5] Pabby, A. K.; Rizvi, S. S. H.; Sastre, A. M. Membrane bioreactors for wastewater treatment in Handbook of Membrane Separations Casey, E., Eds 2009, 1007.

[6] K. Kimura, Y. Hane, Y. Watanabe, G. Amy, N. Ohkuma, Irreversible membrane fouling during ultrafiltration of surface water, *Water Research* 38 (14-15) (2004) 3431.

[7] M.F.A. Goosen, S.S. Sablani, H. Al-Hinai, S. Al-Obeidani, R. Al-Belushi, D. Jackson, Fouling of reverse osmosis and ultrafiltration membranes: A critical review, *Sep. Sci. Technol.* 39 (10) (2004) 2261.

[8] N. Hilal, O.O. Ogunbiyi, N.J. Miles, R. Nigmatullin, Methods employed for control of fouling in MF and UF membranes: a comprehensive review, *Sep. Sci. Technol*. 40 (2005) 1957.

[9] A. Bhattacharya, P. Ghosh, Nanofiltration and reverse osmosis membranes: Theory and application in separation of electrolytes, *Reviews in chemical Engineering*, 20 (2004) 111.

[10] M. Elimelech, X. Zhu, A.E. Childress, S. Hong, Role of membrane surface morphology in colloidal fouling of cellulose acetate and composite aromatic polyamide reverse osmosis membranes, *J. Membr. Sci.* 127 (1997) 101.

[11] X. Zhu, M. Elimelech, Colloidal fouling of reverse osmosis membranes: measurements and fouling mechanisms, *Environ. Sci. Technol.* 31 (1997) 3654.

[12] E.M. Vrijenhoek, S. Hong, M. Elimelech, Influence of membrane surface properties on initial rate of colloidal fouling of reverse osmosis and nanofiltration membranes, *J. Membr. Sci.* 188 (2001) 115.

[13] E.M.V. Hoek, S. Bhattacharjee, M. Elimelech, Effect of membrane surface roughness on colloid-membrane DLVO interactions, *Langmuir* 19 (2003) 4836.

[14] C.R. Reiss, J.S. Taylor, C. Robert, Surface water treatment using nanofiltration -- pilot testing results and design considerations, *Desalination* 125 (1999) 97.

[15] M. Kabsch-Korbutowicz, K. Majewska-Nowak, T. Winnicki, Analysis of membrane fouling in the treatment of water solutions containing humic acids and mineral salts, *Desalination* 126 (1999) 179.

[16] A.G. Fane, C.J.D. Fell, A review of fouling and fouling control in ultrafiltration, *Desalination* 62 (1987) 117.

[17] P.J. Evans, M.R. Bird, A. Pihlajamäki, M. Nyström, The influence of hydrophobicity, roughness and charge upon ultrafiltration membranes for black tea liquor clarification, *J. Membr. Sci.* 313 (2008) 250.

[18] A. Weis, M.R. Bird, M. Nyström, C. Wright, The influence of morphology, hydrophobicity and charge upon the long-term performance of ultrafiltration membranes fouled with spent sulphite liquor, *Desalination* 175 (2005) 73.

[19] B. Van der Bruggen, M. Mänttäri, M. Nyström, Drawbacks of applying nanofiltration and how to avoid them: A review, *Sep. Purif. Technol.* 63 (2008) 251.

[20] M. Mänttäri, L. Puro, J. Nuortila-Jokinen, M. Nyström, Fouling effects of polysaccharides and humic acid in nanofiltration, *J. Membr. Sci.* 165 (2000) 1.

[21] A. Al-Amoudi, R.W. Lovitt, Fouling strategies and the cleaning system of NF membranes and factors affecting cleaning efficiency, *J. Membr. Sci.* 303 (2007) 4.

[22] J. Gilron, S. Belfer, P. Väisänen, M. Nyström, Effects of surface modification on antifouling and performance properties of reverse osmosis membranes, *Desalination* 140 (2001) 167.

[23] I. Pinnau, J.H. Ly, R.W. Baker, Reverse osmosis membrane and process, US patent 7,490,725 B2 (2009).

[24] C. Bartels, M. Wilf, W. Casey, J. Campbell, New generation of low fouling nanofiltration membranes, *Desalination* 221 (2008) 158.

[25] J.-H. Choi, K. Fukushi, K. Yamamoto, Comparison of treatment efficiency of submerged nanofiltration membrane bioreactors using cellulose triacetate and polyamide membrane, *Water Science & Technology* 51 (2005) 305.

[26] J.-H. Choi, K. Fukushi, K. Yamamoto, A submerged nanofiltration membrane bioreactor for domestic wastewater treatment: the performance of cellulose acetate nanofiltration membranes for long-term operation, *Sep. Purif. Technol*., 52 (2007) 470.

[27] S. Liang, Y. Zhao, C. Liu, L. Song, Effect of solution chemistry on the fouling potential of dissolved organic matter in membrane bioreactor systems, *J. Membr. Sci.,* 310 (2008) 503.

[28] R. Valadez-Blanco, F.C. Ferreira, R.F. Jorge, A.G. Livingston, A membrane bioreactor for biotransformations of hydrophobic molecules using organic solvent nanofiltration (OSN) membranes, *J. Membr. Sci.,* 317 (2008) 50.

[29] B.N. Tsai, C.H. Chang, D.J. Lee, J.Y. Lai, Fractionation of organic matters in sludge rejected by NF membrane, *Desalination*, 234 (2008) 386.

[30] P. Le-Clech, V. Chen, A.G. Fane, Fouling in membrane bioreactors used in wastewater treatment, *J. Membr. Sci.,* 284 (2006) 17.

[31] S. Judd (Editor), The MBR Book: Principles and Applications of Membrane Bioreactors for Water and Wastewater Treatment, Elsevier Ltd., 2006.

[32] F. Meng, S.-R. Chae, A. Drews, M. Kraume, H.-S. Shin, F. Yang, Recent advances in membrane bioreactors (MBRs): Membrane fouling and membrane material, *Water Research*, 43 (2009) 1489.

[33] C. Ba, J. Langer, J. Economy, Chemical modification of P84 copolyimide membranes by polyethylenimine for nanofiltration, *J. Membrane Sci.* (2009), 327(1-2), 49.

[34] J. Economy, J. Wang, C. Ba, Design of advanced membranes and substrates for water purification and desalination, Nanotechnology Applications for Clean Water, D. Mamadou, J. S. Duncan, N. Savage, A. Street, R. C. Sustich (Eds.), Elsevier Ltd., 2008.

[35] C. Ba, D.A. Ladner, J. Economy, Using protective polyelectrolyte films to improve fouling resistance of a positively charged NF membrane, *J. Membr. Sci.* 347 (2010) 250.

[36] W. Yuan, A.L. Zydney, Humic acid fouling during microfiltration, *J. Membr. Sci.* 157 (1999) 1.

[37] J. Wang, Y. Yao, Z. Yue, J. Economy, Preparation of polyelectrolyte multilayer films consisting of sulfonated poly(ether ether ketone) alternating with selected anionic layers, *J. Membr. Sci.* 337 (2009) 200.

[38] A. Lui, F.D.F. Talbot, A. Fouda, T. Matsuura and S. Sourirajan, Studies on the solvent exchange technique for making dry cellulose acetate membranes for the separation of gaseous mixtures, *J. Appl. Polym. Sci.* 36 (1988) 1809.

[39] B.V.d. Bruggen, J. Schaep, D. Wilms, C. Vandecasteele, Influence of molecular size, polarity and charge on the retention of organic molecules by nanofiltration, *J. Membr. Sci.* 156 (1999) 29.

[40] M. Dubois, K.A. Gilles, J.K. Hamilton, P.A. Rebers, F. Smith, Colorimetric method for determination of sugars and related substances, *Anal. Chem.* 28 (1956) 350.

[41] K. Boussu, C. Vandecasteele, B. Van der Bruggen, Study of the characteristics and the performance of self-made nanoporous polyethersulfone membranes, *Polymer*, 47 (2006) 3464.

[42] C. Ba, J. Economy, Preparation of polyimide for use as substrate in a thermally stable composite membrane, *J. Membr. Sci.* Submitted.

[43] H. Ohya, V.V. Kudryavtsev, S.I. Semenova, Polyimide Membranes: Applications, Fabrications, and Properties, Gordon and Breach, Tokyo, 1996.

[44] R.E. Kesting, A.K. Fritzsche, M.K. Murphy, A.C. Handermann, C.A. Cruse, R.F. Malon, U.S. Pat. 4,880,441, 1989.

[45] M. Mulder, Basic Principles of Membrane Technology, Kluwer, London, 1996.

[46] K. Boussu, C. Vandecasteele, B. Van der Bruggen, Study of the characteristics and the performance of self-made nanoporous polyethersulfone membranes, *Polymer*, 47 (2006) 3464.

[47] L. Ouyang, R. Malaisamy, M.L. Bruening, Multilayer polyelectrolyte films as nanofiltration membranes for separating monovalent and divalent cations, *J. Membr. Sci.* 310 (2008) 76.

[48] J.M.M. Peeters, J.P. Boom, M.H.V. Mulder, H. Strathmann, Retention measurements of nanofiltration membranes with electrolyte solutions, *J. Membr. Sci.* 145 (1998) 199.

[49] K.H. Yu, Y.H. Yoo, J.M. Rhee, M.-H. Lee, S.-C. Yu, Synthesis of poly[(amic acid)-co-(amic ester)] precursors and studies of their imidization using FT-IR and FT-Raman spectroscopy, *Mat. Res. Innovat.* 7 (2003) 51.

[50] J. Yang, M.-H. Lee, A water-soluble polyimide precursor: synthesis and characterization of poly(amic acid) salt, *Macromol. Res.* 12 (2004) 263.

[51] Y. J. Kimt, J.S. Kim, K.-Y. Choi, Studies of the formation of polyisoimides and their imidization in solution state, *J. Ind. Eng. Chem.* 7 (2001) 400.

[52] X. Qiao, T.-S. Chung, Diamine modification of P84 polyimide membranes for pervaporation dehydration of isopropanol, *AIChE*, 52 (2006) 3462.

[53] C.Y. Tang, Y.-N. Kwon, J.O. Leckie, Fouling of reverse osmosis and nanofiltration membranes by humic acid – Effects of solution composition and hydrodynamic conditions, *J. Membr. Sci.* 290 (2007) 86.

CHAPTER 5

PREPARATION OF PMDA-ODA POLYIMIDE MEMBRANE FOR USE AS SUBSTRATE IN A THERMALLY STABLE COMPOSITE MEMBRANE

5.1 Introduction

Today, thin-film-composite (TFC) membranes, prepared by coating a very thin layer of aromatic polyamide onto a polysulfone substrate, are well accepted for water desalination because of their high rejection rate and high water permeability [1]. However, it is still a challenge to develop chemically and thermally stable polymeric membranes which can withstand harsh environments including pH extremes, oxidants like chlorine, organic solvents, and very low or high temperatures, etc. while maintaining or even enhancing the separation capacity of the commercial TFC membranes [1, 2]. Such membranes are highly desired for many industrial processes. For example, in the sugar industry, a temperature of around 95 ˚C is desired to avoid repeated cooling and heating in the sugar production process, and to reduce microbial growth [3]. The pulp and paper industry also needs membranes which can resist high temperatures of 70 - 90 ˚C and alkaline conditions [3]. Therefore it is of interest to develop thermally stable membranes to overcome the limitation of 45 ˚C for the commercial membranes [4, 5, 6, 7]. For this purpose, high performance polymers like polyimides (PIs) may be considered for developing a new generation of membranes for water purification and desalination [8].

Due to their unique properties, polyimides have been developed into membranes for separation of gases, vapors and liquids [9]. Polyimide membranes exhibit excellent resistance to almost all chemical agents. Their thermal resistance

allows separations to be performed for a long time at elevated temperatures [10]. Specifically, poly(pyromellitic dianhydride-*co*-4,4'-oxydianiline) (PMDA/ODA PI) has a very high glass transition temperature of approximately 400 ˚C and excellent resistance to most non-oxidizing acids at room temperature and almost all organic solvents [11]. However, because the PMDA/ODA PI is both insoluble and infusible, any products, including membranes, can only be processed from its precursor, polyamic acid (PAA), which requires an additional step to transform the PAA into PI by either thermal or chemical treatments. So far, studies have focused on its fabrication into symmetric membranes or composite membranes for separation of gases and organics [8, 12, 13, 14, 15]. A dense symmetric membrane, prepared from PAA solution via solvent evaporation followed by chemical imidization, has also been applied for water desalination. Although the salt rejection was high, the water flux was very low [16].

There are several problems with developing PMDA/ODA PI asymmetric membranes from PAA using the phase inversion method. Firstly, because of the hydrophilic carboxylic groups, PAA has strong interaction with water, which makes the phase inversion slow. The resultant PAA membranes usually contain large amounts of macrovoids, which make the membranes mechanically very weak [17]. Secondly, PAA is known to be thermally unstable even at room temperature and tends to hydrolysis with water [18]. Thirdly, when transforming the PAA into PI by the thermal process, the pores of the membranes tend to collapse, which results in a shrinking of the PI membranes. Consequently, dense membranes are obtained with

very low permeability [19]. To solve these problems, several approaches have been reported to modify the PAA to decrease its hydrophilicity and improve its hydrolytic stability as well. For example, partially imidized PAA was used for membrane development and the effect of PAA imidization on solution characteristics and membrane morphology was studied [20]. With a benzimidazole additive, the carboxylic groups of PAA were blocked so as to decrease the hydrophilicity of PAA [19]. PAA amine salts, prepared by reaction with tertiary amines like triethylamine, have shown improved hydrolytic stability [21]. However, the PAA amine salt polymers are soluble in water and thus may not be suitable for developing asymmetric membranes by the phase inversion method. In order to prevent membrane shrinking during the thermal imidization process, a chemical process using acetic anhydride as dehydration agent and triethylamine as catalyst provides an alternative option [9].

Because of their strong coordination with the transition metal ions, the carboxylic groups of PAA can be neutralized by cations, such as Zn^{2+}, Ni^{2+} and Cu^{2+}, to form ionomers. These divalent cations may act as cross-linkers so that these ionomers behave as thermoplastic elastomers [22]. Immersion of PAA films or fibers into aqueous solutions of transition metal salts leads to chelation of a certain amount of metals onto the PAA, confirming the strong interaction between the PAA and the metal ions [23]. The improvements in physical properties and chemical stability after coordination with metal ions may benefit the development of asymmetric PMDA/ODA PI membranes. To the best of our knowledge, no related studies have been reported on preparation of PI membranes using this method.

In this study, we added predetermined amounts of zinc chloride ($ZnCl_2$) into a PAA solution to modulate the physical properties of the casting dope. We selected $ZnCl_2$ instead of zinc acetate ($ZnAc_2$) as an additive because $ZnCl_2$ could be readily dissolved in PAA/NMP solution while even small amounts of $ZnAc_2$ would precipitate the polymer. The change in viscosity of the polymer solution was measured with increasing amounts of the $ZnCl_2$ added. Then the $ZnCl_2$-containing casting dope was cast onto a polyester support followed by immersing into a water bath to prepare an asymmetric porous PAA membrane. The effect of $ZnCl_2$ on the morphology of PI membrane was then investigated. By chemical imidization, the PAA membrane was transformed into PI membrane which could then be used as substrate for depositing a thin layer of cross-linked aromatic polyamide by interfacial polymerization. This composite membrane could be used for water desalination with much better thermal stability than the commercial composite membranes based on polysulfone substrate.

5.2 Experimental

5.2.1 Chemicals

Poly(pyromellitic dianhydride-*co*-4,4'-oxydianiline) amic acid solution (PAA) was purchased from Aldrich as a 15% solution in N-methyl-2-pyrrolidone (NMP) and stored in a freezer. Trimesoyl chloride (TMC; Aldrich, 98%) was distilled under reduced pressure and stored in a desiccator to prevent hydrolysis of the acyl chloride groups. *m*-Phenylenediamine (MPDA; Aldrich, ≥ 99%) and anhydrous zinc chloride

($ZnCl_2$; Aldrich, ≥ 98%) were used as received. All the other reagents and solvents were of analytical grade and used as received.

5.2.2 Preparation of the polyimide membranes

Three casting solutions were prepared by adding 0%, 6% and 24% $ZnCl_2$ into the 15% PAA/NMP solution. With more than 24% $ZnCl_2$, the polymer solution was so highly viscous that membrane processing became difficult. The percentage of added $ZnCl_2$ was based on the polymer solution not on the polymer itself. For example, to make a casting solution with 6% $ZnCl_2$, 6 g of anhydrous $ZnCl_2$ was added to 100 g of the 15% PAA/NMP solution. The mixture was then stirred by a mechanical stirrer until the zinc chloride was totally dissolved. After that, the solution was degassed under vacuum to remove all the bubbles. The casting solution was then cast onto a polyester support (Calendered PET from Crane Nonwovens) and immersed immediately into a water coagulation bath at room temperature. The membrane thickness was controlled at roughly 100 micron. After 30 min, the membrane was removed from the water bath and washed thoroughly with deionized (DI) water. Then the PAA membrane was dried by an isopropanol-hexane displacement sequence [24]: the membrane was immersed in the isopropanol for 90 min during which the isopropanol was refreshed 3 times. Subsequently, the isopropanol was replaced by hexane using the same procedure. Chemical imidization was performed by immersing the PAA membranes into a mixture of acetic anhydride (Ac_2O) and triethylamine (TEA) (volume 4:1) at 100 ˚C for 36 hours, as shown in

Scheme 5.1. The resultant PI membranes were then washed using isopropanol several times and stored in isopropanol.

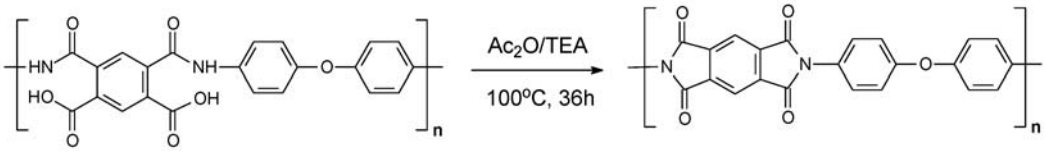

Scheme 5.1 Synthesis of polyimide from polyamic acid precursor via chemical treatment.

5.2.3 Preparation of the composite membranes

The composite membranes were prepared by the interfacial polymerization of MPDA with TMC on the surface of the PI membrane support. The PI membrane was dipped into an aqueous solution of MPDA. After removing excess liquid on the membrane surface using soft paper tissues, the membrane was immersed into a hexane solution of TMC, which resulted in an in-situ formation of a barrier layer over the surface of the polyimide substrate. The resulting composite membrane was dried at room temperature in air for two minutes to evaporate hexane and then stored in DI water prior to characterization. The preparation parameters including the monomer concentrations, immersion times, and post annealing were evaluated in order to obtain optimal desalination performance. For each data point, a minimum of two membrane samples were tested and averaged.

5.2.4 Membrane desalination performance measurements

Desalination performance of the composite membranes was examined using a dead-end filtration cell (Sterlitech HP4750) and 300 mL of a 2.0 g/L NaCl aqueous feed solution under 55.2 bar (800 psig). The feed solution was stirred at a rate of 1100 rpm in the cell using a standard magnetic stirrer (Corning Stirrer/Hot Plate, Model

PC-420) to minimize concentration polarization. Each membrane was compacted at a pressure of 55.2 bar for nine hours prior to measurements to ensure a steady state was obtained. The permeated solution was then refilled into the feed and permeate samples were collected as appropriate. The permeation flux F was determined by measuring the permeation volume V (20 mL, 6.7% recovery) flowing across the membrane of area A (14.6 cm^2) in the time period Δt, F ($m^3m^{-2}day^{-1}$) = $V/(A \times \Delta t)$. The salt rejection was calculated as $R = (1 - \sigma_p/\sigma_f) \times 100\%$, where σ_p and σ_f were the conductivity of the permeate and the feed respectively. The conductivity of the NaCl solution was measured with a bench-top conductivity meter (Oakton CON 510).

5.2.5 Membrane thermal stability measurements

The thermal stability of the TFC membrane was evaluated by measuring the change of water flux and salt rejection with temperature increasing from 25 ˚C to 95 ˚C under a constant pressure of 27.6 bar (400 psi) and a 2.0 g/L NaCl solution. Heating of the testing solution was performed by immersing the dead-end filtration cell in a temperature controlled water bath.

5.2.6 Characterization techniques

The viscosities of the casting solutions containing various amounts of $ZnCl_2$ were measured using an Ubbelohde capillary viscometer in a thermostated water bath at 29.0 ± 0.1 ˚C. The relative viscosity value of each $ZnCl_2$-containing casting solution was determined by normalizing its efflux time with respect to that of $ZnCl_2$-free polymer solution.

Characterization of membrane chemistry and morphology was conducted by attenuated total reflectance Fourier transform infrared spectroscopy (ATR-FTIR), X-ray photoelectron spectroscopy (XPS), scanning electron microscopy (SEM) and atomic force microscopy (AFM). All membrane samples were dried using the solvent exchange method to prevent the porous structure from collapsing upon drying [25].

ATR-FTIR spectra were collected at room temperature over a scanning range of 600 - 4000 cm^{-1} with a resolution of 4.0 cm^{-1}, using a Nexus 670 FT-IR (Thermo Electron Corporation, Madison, WI) with a Golden Gate™ MKII Single Reflectance ATR (Specac Inc., Woodstock, GA). The spectrometer was installed with a deuterated triglycine sulfate-potassium bromide (DTGS-KBr) detector and KBr beam splitter. Spectra collection was performed using FT-IR software (OMNIC, Thermo Electron Corporation, Madison, WI).

XPS experiments were performed on a Physical Electronics PHI Model 5400 surface analysis system using an achromatic Mg K_α (1253.6 eV) X-ray source operated at 300 W.

SEM images were obtained using a Hitachi S-4700 with 15.0 kV accelerating voltage. For cross-sectional observations the polyimide layer was peeled off of the polyester support and fractured after immersion in liquid nitrogen. All samples were coated by sputtering with gold and palladium before testing.

AFM was performed in air using a Veeco / Digital Instruments Dimension 3100 AFM. Surface roughness of the membranes was obtained by surface image analysis.

5.3 Results and discussion

5.3.1 Effect of $ZnCl_2$ additive on viscosities of the casting solutions

Figure 5.1 shows the change of viscosities of the polymer solutions by adding up to 10% $ZnCl_2$. With more $ZnCl_2$, the solution became too viscous to be measured by the viscometer. It can be seen that initially the solution viscosity increased linearly until 6% $ZnCl_2$ was added. With more $ZnCl_2$ from 6% to 10%, the solution viscosity increased more rapidly. An intersection at 6% can be clearly observed, at which point the molar ratio of Zn^{2+} to 2COOH can be calculated to be 1.2, close to equality.

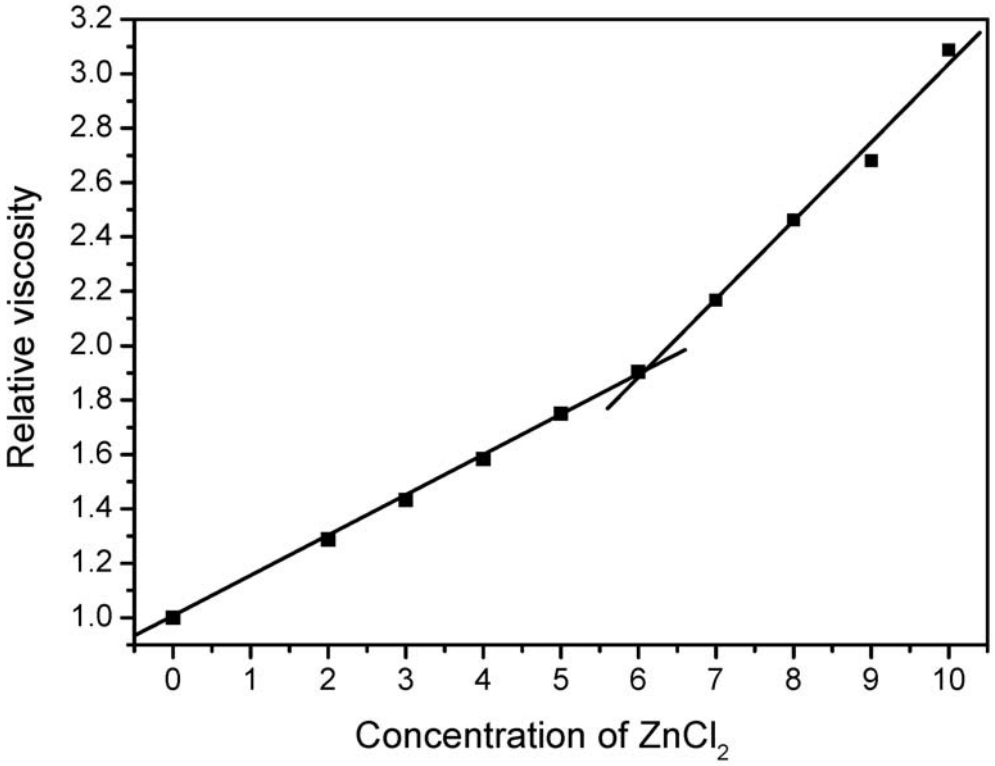

Figure 5.1 Change of viscosities of the PAA solutions by adding $ZnCl_2$. Viscosity was measured using an Ubbelohde Capillary Viscometer in a thermostated water bath at 29.0 ± 0.1 ˚C.

These results may be explained by the interaction between Zn^{2+} and both the polymer PAA [23] and the solvent NMP [26]. Due to the strong coordination

interaction between Zn^{2+} ion and carboxylic groups [27], initially each Zn^{2+} ion preferably binds to two PAA carboxylic groups in an intermolecular manner forming an ionic cross-linking network, as shown in Figure 5.2. The ionic cross-linking would decrease the mobility of the polymer chains resulting in enhanced viscosity. In addition, in the presence of zinc ions, the charge of the PAA is reduced due to the charge screening effect as well as the complex formation. This ionic cross-linking and charge decrease can reduce the hydrophilicity of the PAA and thus are favorable for membrane formation. At the point of 6% $ZnCl_2$ added, however, the complexation reaches a maximum value. With more $ZnCl_2$, a stable complex can be formed between $Zn^{2+}$and the NMP, which would reduce the solvating power of NMP for the polymer and increase the solution viscosity further.

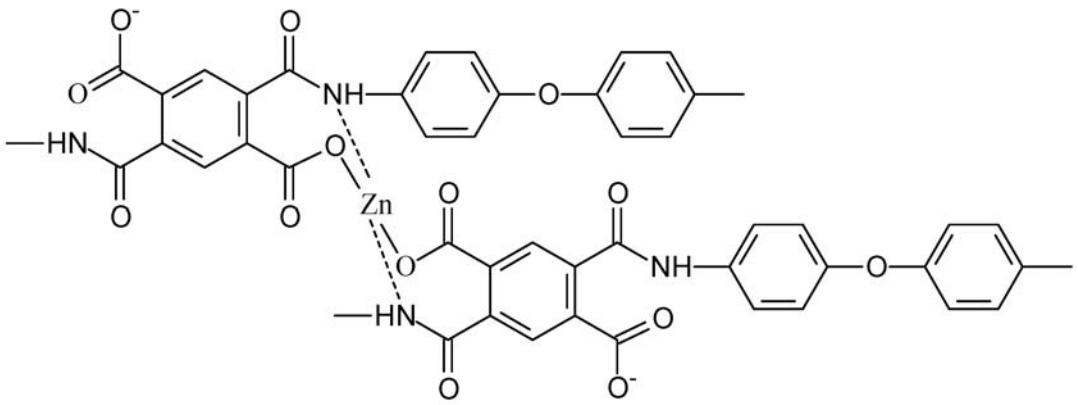

Figure 5.2 Possible intermolecular cross-linking structure formed by the interaction between Zn^{2+} and polyamic acid.

5.3.2 Preparation and characterization of the polyimide substrate membranes

5.3.2.1 Effect of $ZnCl_2$ additive on membrane morphologies

In this study, we prepared three kinds of membranes from polyamic acid solution containing 0%, 6% and 24% $ZnCl_2$ respectively and then imidized the polyamic acid into polyimide. These PI membranes will be referred to as PI-0%, PI-6% and PI-24% membranes. Figure 5.3 presents SEM images of the membrane cross-sections and surfaces. The PI-0% membrane shows a highly porous structure containing a large amount of macrovoids. Most of the macrovoids extend deeply to the bottom of the membrane. Consequently, these macrovoids lead to mechanical weakness and the membrane easily ruptured in high pressure operations. When 6% $ZnCl_2$ was added to the casting solution, the macrovoids become smaller showing a parallel finger-like structure. Meanwhile, a sponge-like structure formed at the membrane bottom. When the $ZnCl_2$ content in the solution was raised to 24%, the content of the sponge-like structure increased significantly while the number of the macrovoids decreased. While the PI-0% membrane contains a lot of micropores on the surface with the diameter ranging from 10 to 20 nm, at 6% $ZnCl_2$ additive the pore diameter decreased to 5 - 8 nm, and at 24% $ZnCl_2$ additive no pores were detected. Therefore, the $ZnCl_2$ additive played an important role to suppress the macrovoid formation in the membranes, which made the membranes mechanically stronger. Meanwhile, the membrane surface became less porous after adding $ZnCl_2$ to the casting solution.

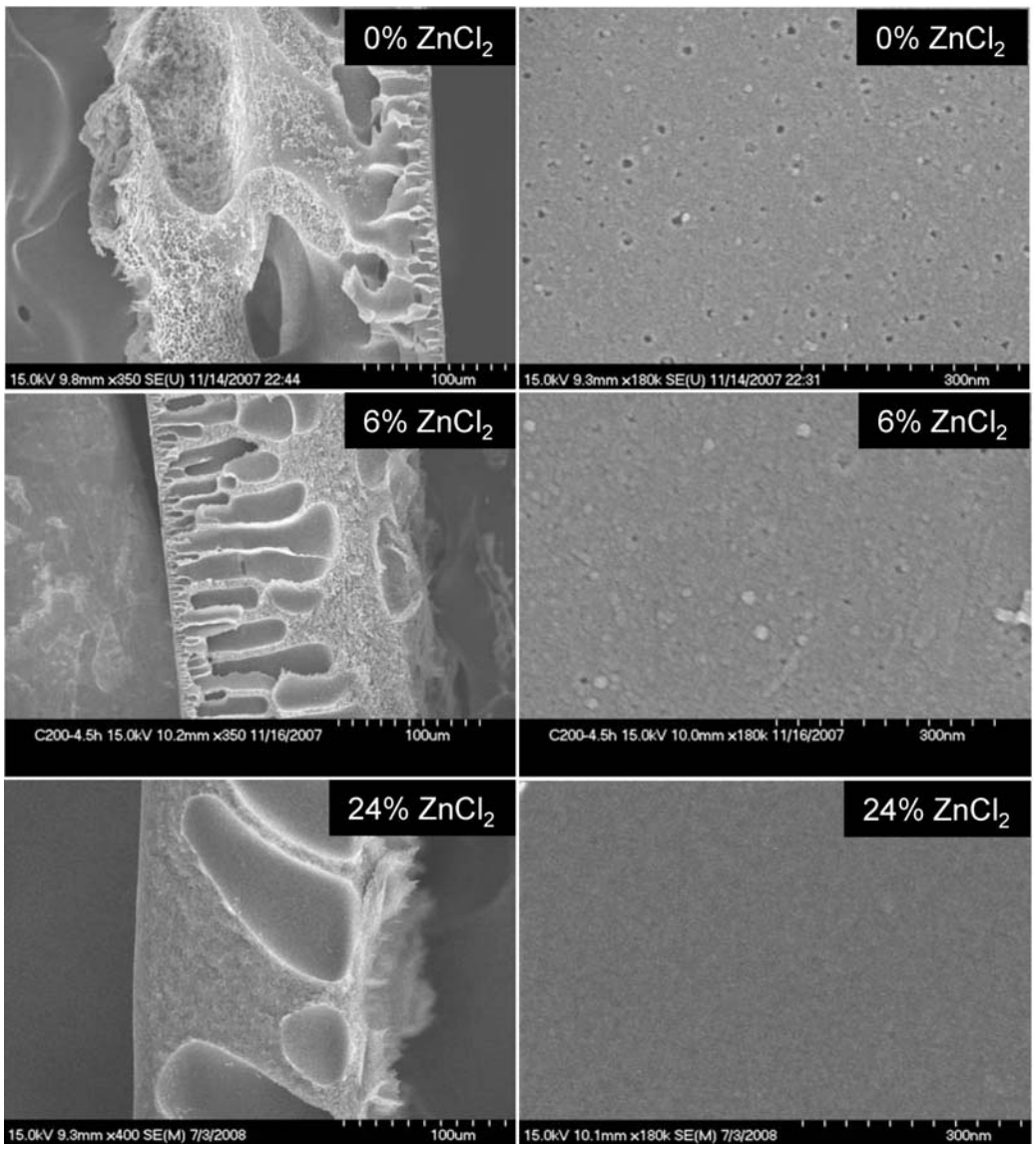

Figure 5.3 Cross-sectional (left) and surface (right) morphologies of the polyimide substrate membranes developed from polyamic acid solutions with different amount of $ZnCl_2$ additive.

Morphological changes of these membranes may be closely related to the properties of the casting solutions. Before adding $ZnCl_2$, the PAA/NMP solution had low viscosity. Due to the strong mutual affinity between water and NMP, rapid solvent/nonsolvent exchange occurred during the quench step. This process, so-called instantaneous phase separation, can commonly result in membranes having a microporous skin layer and a finger-like substructure [28, 29]. The addition of 6%

$ZnCl_2$ could facilitate polymer precipitation during quenching in water through the formation of a cross-linked structure as mentioned before. Consequently, the resultant membrane has a relatively dense surface which can hinder the exchange diffusion between the solvent and the nonsolvent. This decreased diffusion rate could delay the phase separation process so that the growth of the macrovoids was suppressed [30]. This effect became more evident when 24% $ZnCl_2$ was added to the casting solution. The diffusion between the solvent and the nonsolvent became even more difficult due to the denser membrane surface as a result of very high viscosity of the casting solution [31]. Similar effects on membrane structure have been observed when using inorganic salt additives in various polymer-solvent systems [17, 32, 33].

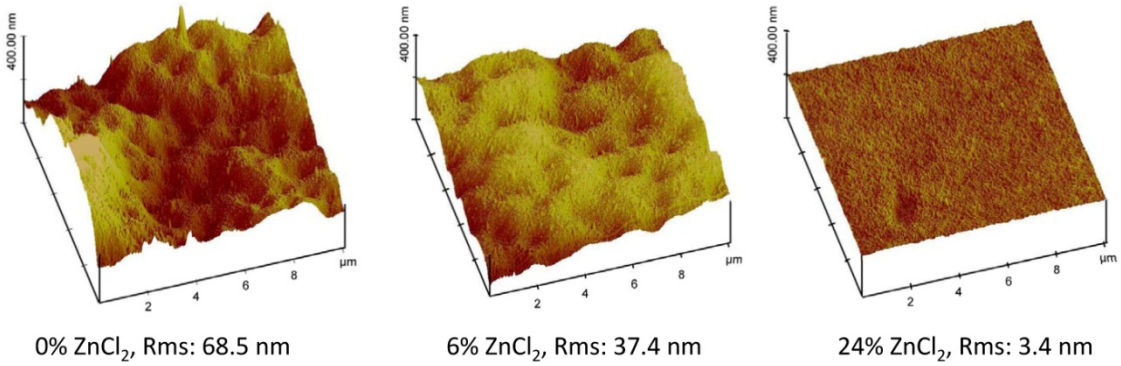

Figure 5.4 AFM images of the surface morphologies of the polyimide substrate membranes developed from polyamic acid solutions with different amount of $ZnCl_2$ additive. Scanning area: 10 µm×10 µm.

Figure 5.4 shows the three-dimensional AFM images of the three membrane surfaces. The PI-0%, PI-6% and PI-24% membranes have surface roughness of 68.5 nm, 37.4 nm and 3.4 nm (root mean square RMS roughness), respectively. The reduction in surface roughness by adding $ZnCl_2$ may be attributed, in part, to the reduction of the surface pore size as illustrated by SEM. Moreover, it can be seen

from Figure 5.3 that there are some spherical protuberances in PI-0% and PI-6% membrane surfaces, which may also contribute to the membrane roughness. However, there is no such structure in the PI-24% membrane surface. It is likely that such spherical globules were induced by polymer aggregation during the phase inversion process. By coordinating with Zn^{2+} ions the polymer chains may exist in a gel-like structure which could restrain the polymer aggregation and make the membrane smooth.

5.3.2.2 Effect of $ZnCl_2$ additive on membrane permeability

Permeability of the three polyimide membranes was tested at 13.8 bar and room temperature using tap water as the feed. The results are shown in Figure 5.5. Clearly, the permeate flux decreased with the increase of operating time, indicating membrane compaction happened. It is of interest to compare the initial fluxes of the three membranes prepared with 0%, 6% and 24% $ZnCl_2$. These values are 29.4 ± 16.8, 8.8 ± 2.8 and 17.3 ± 0.81 $m^3m^{-2}day^{-1}$ respectively. The PI-6% membrane is less permeable than the PI-0% membrane, which may be explained by the fact that the PI-6% membrane has a smaller pore size than the PI-0% membrane. However, surprisingly, the PI-24% membrane shows higher permeability than the PI-6% membrane. It is likely that by using 24% $ZnCl_2$ a large number of fine pores were formed so that the overall membrane porosity was increased [17]. On the other hand, it can be observed that the more $ZnCl_2$ was used, the less flux variation from membrane to membrane was found, which suggests that the membrane properties became more stable and uniform by using $ZnCl_2$ as additive.

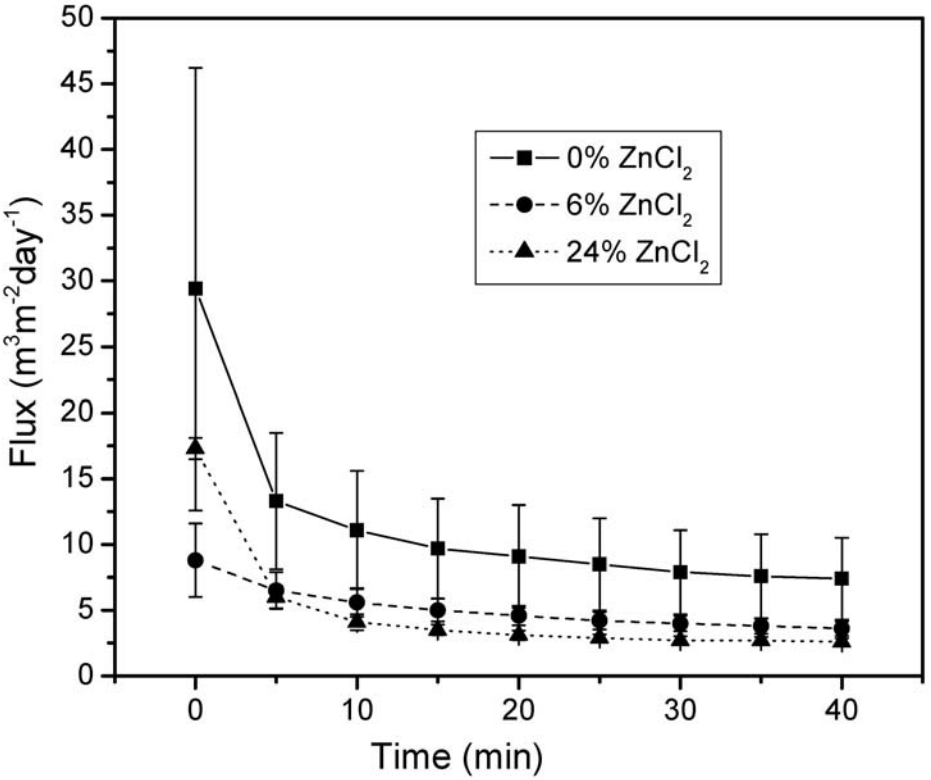

Figure 5.5 Pure water permeability of the polyimide substrate membranes developed from polyamic acid solutions with different amount of $ZnCl_2$ additive. Experiments were conducted at 13.8 bar and room temperature.

5.3.2.3 Characterization of the chemical composition of the polyimide membrane

It is of interest to investigate the chemical composition of the membranes after imidization. ATR-FTIR and XPS were used to characterize the conversion of polyamic acid to polyimide and the presence of Zn^{2+} after imidization, respectively. The membrane sample was prepared with 24% $ZnCl_2$ and the results are displayed in Figure 5.6 and Figure 5.7, respectively.

The ATR-FTIR spectrum exhibits a few characteristic bands of PMDA/ODA polyimide as follows: 1778 cm^{-1} (symmetric C=O stretching, imide I), 1722 cm^{-1} (asymmetric C=O stretching, imide I), and 1378 cm^{-1} (C-N-C stretching, imide II). The peaks at 1500 cm^{-1} and 1245 cm^{-1} are from the C-C stretching of benzene ring and the C-O-C stretching of ODA, respectively [34]. On the other hand, the typical

polyamic acid absorption bands at 1660 cm^{-1} (C=O stretching, amide I) and 1550 cm^{-1} (C-N stretching, amide II) [35], and typical isoimide bands at 1800 cm^{-1} [36] are totally absent. Therefore, this membrane has identical infrared spectrum to the polyimide film cured by thermal process [49, 50, 51], indicating the polyamic acid was completely transformed to polyimide under these reaction conditions.

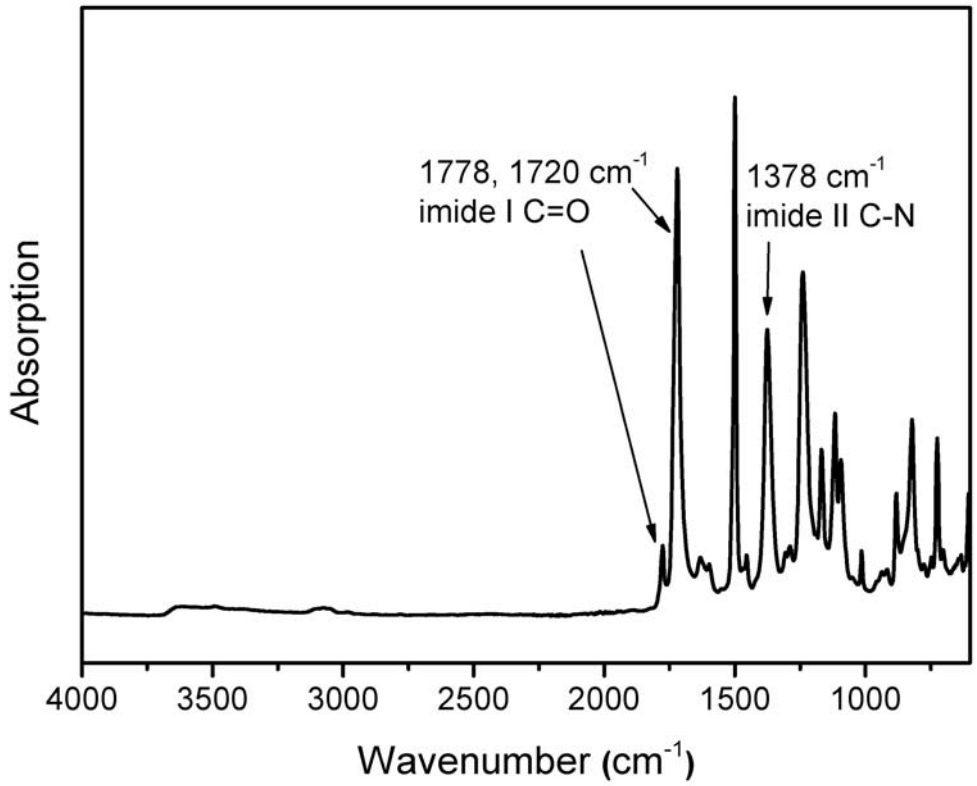

Figure 5.6 ATR-FTIR spectrum of the polyimide membrane after chemical imidization. The membrane was prepared with 24% $ZnCl_2$ additive.

From the XPS survey spectrum, one can see that only carbon, oxygen and nitrogen atoms are present on the membrane surface. No zinc atoms (Zn 2p at 1021 eV) could be detected. This result is in good agreement with the ATR-FTIR result. It is likely that the Zn^{2+} ions were dissolved into the reagent mixture of Ac_2O/TEA during the imidization process. Therefore, it can be concluded that the only role of

$ZnCl_2$ was to regulate membrane morphology and permeability and it can be completely removed during membrane preparation process.

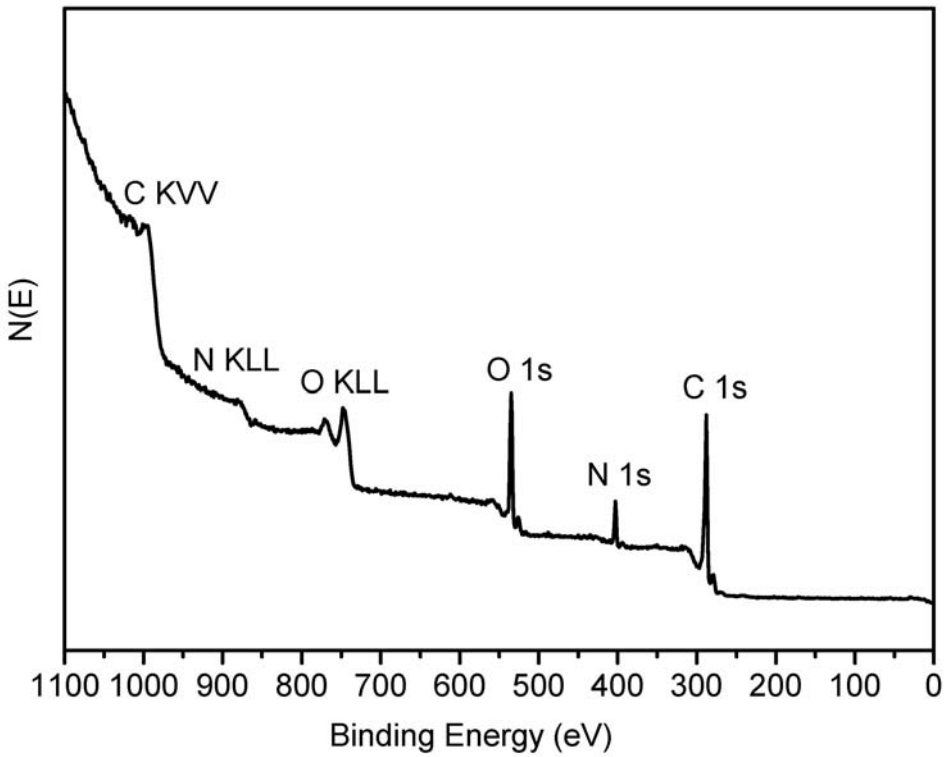

Figure 5.7 XPS survey spectrum of the polyimide membrane after chemical imidization. The membrane was prepared with 24% $ZnCl_2$ additive.

5.3.3 Preparation and characterization of the composite membranes using polyimide membranes as substrates

5.3.3.1 Effect of the PI substrate membranes on desalination performance

The three polyimide membranes PI-0%, PI-6% and PI-24% were employed as substrates for fabrication of composite RO membranes. The polyamide thin films were prepared by immersing the polyimide substrate membranes in a 1.0% MPDA/H_2O solution for 30 s and then in a 0.02% TMC/hexane solution for 5 s. These preparation parameters were optimized using the PI-24% membrane as

substrate, and these will be shown in detail in the following parts. The membrane performance data in terms of water flux and salt rejection are shown in Table 5.1.

Table 5.1 Effect of different substrate membranes on desalination performance[a].

Membrane samples	Flux[b] ($m^3m^{-2}day^{-1}$)	Rejection[b] (%)
PI-0%	0.80 ± 0.04	61.4 ± 15.1
PI-6%	0.60 ± 0.01	95.3 ± 0.4

Notes: [a]Thin film preparation conditions: 1.0% MPDA/H_2O, 30 s; 0.02% TMC/hexane, 5 s. [b]Test conditions: 2.0 g/L NaCl solution, 55.2 bar and room temperature, 9 h compaction at 55.2 bar.

It can be seen that the PI-0% membrane is not a good support for the composite membrane because the salt rejection is low. It is likely that this substrate membrane could be ruptured at high pressure, which could induce defects to the top polyamide film. By using the PI-6% membrane as a substrate, the composite membrane shows better salt rejection but less water flux. In this case, the substrate membrane may have additional resistance to water transport. Therefore, we used the PI-24% membrane as substrate for further parametric studies because of its good mechanical stability. In addition, its smooth surface may facilitate the formation of a uniform thin film.

5.3.3.2 Effect of concentration of the monomers on desalination performance

In Table 5.2 are presented the desalination data of a given thin film composite membrane prepared by interfacial polymerization of MPDA and TMC at various concentrations. At a constant concentration of TMC (0.15%), permeate flux was found to decline with an increase of the MPDA concentration. However, best salt rejection was obtained with 1% MPDA/H_2O solution. Therefore, the concentration of MPDA was fixed at 1% and various concentrations of TMC were studied. Generally,

by decreasing the concentration of TMC, the permeate flux was improved while the salt rejection did not show significant change. Comparatively, a low concentration of 0.02% TMC gave the best membrane performance. With a high TMC content of 4%, the membrane showed high permeate flux but low salt rejection.

Table 5.2 Effect of monomer concentration on desalination performance[a].

C_{MPDA} (w/v)	C_{TMC} (w/v)	Flux[b] ($m^3m^{-2}day^{-1}$)	Rejection[b] (%)
0.5%	0.15%	0.81	95.7 ± 0.2
1.0%	0.15%	0.71	98.1
2.0%	0.15%	0.67 ± 0.02	96.8 ± 0.9
4.0%	0.15%	0.62 ± 0.07	95.9 ± 0.6
1.0%	0.01%	1.06	96.9
1.0%	0.02%	1.13 ± 0.04	97.8 ± 0.7
1.0%	0.05%	1.15 ± 0.09	96.8 ± 0.8
1.0%	0.1%	0.96 ± 0.04	96.9 ± 0.7
1.0%	0.2%	0.83 ± 0.03	96.2 ± 0.8
1.0%	0.4%	1.13 ± 0.32	93.8 ± 1.3

Notes: [a]Thin film preparation conditions: using PI-24% membrane as substrate, 60 s in MPDA/H_2O, 10 s in TMC/hexane. [b]Test conditions: 2.0 g/L NaCl solution, 55.2 bar and room temperature, 9 h compaction at 55.2 bar.

The effect of TMC on membrane surface morphology was studied by SEM. The result is shown in Figure 5.8. The membrane prepared with 0.02% TMC shows the typical ridge-and-valley structure with some polymer strands on the surface [37]. When TMC concentration increases to 0.15%, the membrane shows a dense surface, which may explain the membrane performance of low permeate flux and high salt rejection. However, when TMC concentration increases to 4%, some porous defects appear on the membrane surface, which likely result in the observed high permeate flux and low salt rejection.

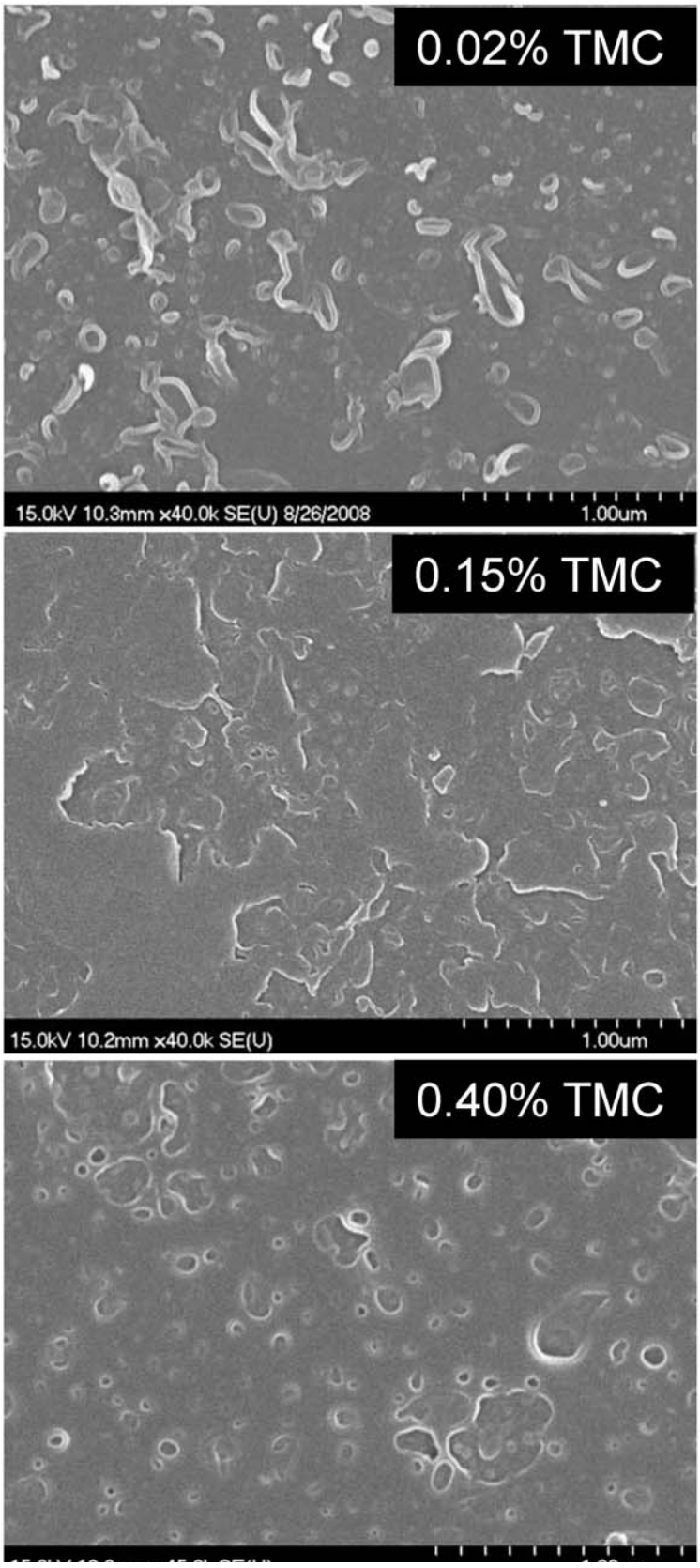

Figure 5.8 SEM images of polyamide thin films prepared with various concentration of TMC.

The relationship between preparation conditions of the polyamide thin film and membrane performance has been studied by many others in recent years [38, 39, 40]. Generally, the permeate flux depends primarily on the film thickness and surface hydrophilicity while salt rejection is mainly governed by surface chemistry, pore size and charge [38, 40]. With different concentrations and ratios of the two monomers, the reaction rate and degree of polymerization were different. Therefore, the polyamide may contain various amounts of functional groups such as carboxylic acid and amine groups, which, in turn, may induce various changes in pore size and charge density [39]. Nevertheless, most studies on the optimization of preparation conditions of the polyamide thin films are usually based on trial-and-error procedures.

5.3.3.3 Effect of immersion time on desalination performance

With fixed concentrations of the two monomers, various immersion times in both of them were studied. Table 5.3 shows the desalination performance of the resultant membranes. With 10 s immersion in MPDA and 10 s immersion in TMC, the membrane shows high permeate flux but low salt rejection. It is likely that the loading of MPDA in the membrane was not sufficient to prepare a uniform thin film. The MPDA loading became sufficient with an immersion time of 30 s because the resultant membranes show consistently good desalination performance. However, with a greater immersion time of 120 min, membrane performance decreased slightly. Similarly, the optimal reaction time in TMC solution was observed to be 5 - 10 s. More or less reaction time decreased the desalination performance of the resultant membranes.

Table 5.3 Effect of immersion time in MPDA and TMC on desalination performance.

Immersion time in MPDA (s)	Immersion time in TMC (s)	Flux ($m^3m^{-2}day^{-1}$)	Rejection (%)
10	10	1.40 ± 0.13	94.5 ± 2.4
30	10	1.13 ± 0.02	97.5 ± 0.1
120	10	1.10 ± 0.12	96.0 ± 0.9
30	3	1.31 ± 0.14	91.0 ± 2.3
30	5	1.13 ± 0.04	97.4 ± 0.1
30	20	1.10 ± 0.16	97.3 ± 1.2

Notes: Membrane prepared with 1% MPDA/H_2O and 0.02% TMC/hexane. Test conditions: 2.0 g/L NaCl solution, 55.2 bar and room temperature, 9 h compaction at 55.2 bar.

5.3.3.4 Effect of post annealing on desalination performance

We also studied the effect of annealing on the desalination performance of the membranes. The results are shown in Table 5.4. Although annealing has been commonly used for improving membrane selectivity due to the densification of the selective skins [41], this treatment afforded no apparent improvement for this system. For example, after annealing at 50 ˚C for 5 min, the water flux decreased slightly while the salt rejection remained constant. By annealing at 80 ˚C for 5 min, however, membrane curling became noticeable and defects were likely induced in the membrane active layer. Therefore, salt rejection was reduced significantly.

Table 5.4 Effect of post thermal treatment on desalination performance.

Annealing temperature (^oC)	Annealing time (min)	Flux ($m^3m^{-2}day^{-1}$)	Rejection (%)
50	5	1.07 ± 0.02	97.6 ± 0.4
80	5	1.10 ± 0.08	94.8 ± 0.7

Notes: Membrane preparation conditions: 1% MPDA/H_2O, 30 s and 0.02% TMC/hexane, 5 s. Test conditions: 2.0 g/L NaCl solution, 55.2 bar and room temperature, 9 h compaction at 55.2 bar.

Based on these studies, it can be concluded that the optimal conditions for obtaining good composite membranes of polyamide were achieved by immersion in

1.0% MPDA/H_2O solution for 30 - 60 s and then immersion in 0.02% TMC/hexane solution for 5 - 10 s without any annealing treatment. The rejection of the membrane prepared under such conditions for 2.0 g/L NaCl aqueous solution is about 98%, and the flux is about 1.1 $m^3m^{-2}day^{-1}$ when tested at 55.2 bar and room temperature.

5.3.4 Thermal stability of the composite membranes

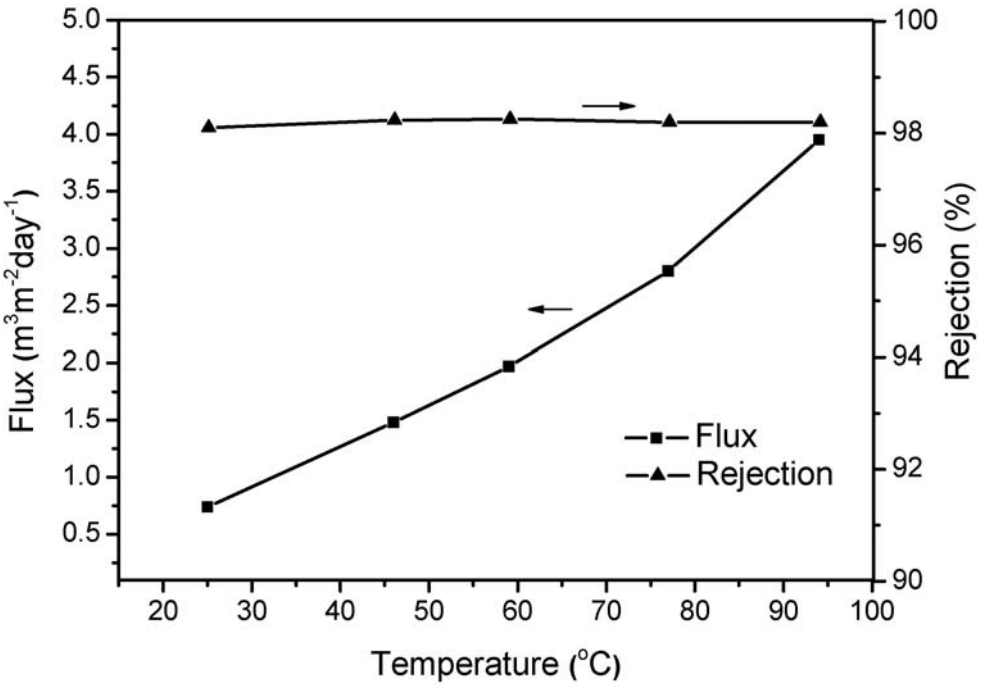

Figure 5.9 Effect of operating temperature on membrane performance. Test conditions: 27.6 bar, 2.0 g/L NaCl aqueous solution.

Thermal stability of the composite membrane was tested by measuring its permeation characteristics under various solution temperatures. The results are shown in Figure 5.9. The testing pressure was 27.6 bar (400 psi) instead of 55.2 bar (800 psi) because at elevated temperatures permeate flux will increase rapidly. For this reason, low pressure was required to measure the flux in a controlled manner. As the feed temperature increases from 25 ˚C to 95 ˚C, the water flux increases 5 - 6 times from

0.74 $m^3m^{-2}day^{-1}$ to 3.95 $m^3m^{-2}day^{-1}$, while the salt rejection stays roughly constant. The thermal stability of this membrane may be attributed to the high mechanical strength of the polyimide substrate, which can resist pore expansion as temperature increases. Therefore, these results suggest that this membrane provides a unique solution for hot water desalination. In addition, this membrane provides a feasible way to improve water flux by increasing the operating temperature without any drop in salt rejection.

5.4 Conclusions

Thermally stable RO membranes were developed using PMDA/ODA PI membranes as substrate and MPDA/TMC polyamide as the top thin film. We prepared the PI substrate membranes from PAA and then imidized the PAA into a PI substrate membrane. Zinc chloride was introduced into the PAA solution where an ionic cross-linking structure was formed by coordination of Zn^{2+} ions with carboxylic groups of PAA. As a result, membrane structure and permeability were effectively regulated. By using 24% $ZnCl_2$, the resultant PI membranes show a smooth surface with good permeability and mechanical strength. These properties are favorable for preparation of a stable and high performance composite membrane. In addition, chemical imidization by AC_2O/TEA at 100 ˚C was found to convert the PAA to PI completely and the $ZnCl_2$ additive was totally removed after membrane preparation.

Composite RO membranes were prepared by coating a thin layer of aromatic polyamide via interfacial polymerization. Detailed parametric studies were conducted and the optimized RO membranes based on polyimide showed a salt rejection of 98%

with a permeate flux of 1.1 $m^3m^{-2}day^{-1}$ when tested with a 2.0 g/L NaCl solution at 55.2 bar and room temperature. The key advantage of the polyimide-based membrane is its high thermal stability. As the feed temperature increases from 25 ˚C to 95 ˚C, the water flux increases 5 - 6 times while the salt rejection remains almost constant.

5.5 References

[1] R.J. Petersen, Composite reverse osmosis and nanofiltration membranes, *J. Membr. Sci.* 83 (1993) 81.

[2] N. Vainrot, M.S. Eisen, and R. Semiat, Membranes in desalination and water treatment, *MRS Bulletin*, 33 (2008), 16.

[3] A.I. Schäfer, A.G. Fane, T.D. Waite (Eds.), Nanofiltration - Principles and Applications, Elsevier Ltd., 2005.

[4] M. Manttari,A. Pihlajamaki, E. Kaipainen, M.Nystrom, Effect of temperature and membrane pre-treatment by pressure on the filtration properties of nanofiltration membranes, *Desalination* 145 (2002) 81.

[5] C. Wu, S. Zhang, D. Yang, J. Wei, C. Yan, X. Jian, Preparation, characterization and application in wastewater treatment of a novel thermal stable composite membrane, *J. Membr. Sci.* 279 (2006) 238.

[6] J. Wei, X. Jian, C. Wu, S. Zhang, C. Yan, Influence of polymer structure on thermal stability of composite membranes, *J. Membr. Sci.* 256 (2005) 116.

[7] M.J.H. Snow, D. de Winter, R. Buckingham, J. Campbell, J. Wagner, New techniques for extreme conditions: high temperature reverse osmosis and nanofiltration, *Desalination* 105 (1996) 57.

[8] U. Razdan, S.V. Joshi and V.J. Shah, Novel membrane processes for separation of organics, *Current Science*, 85 (2003) 761.

[9] H. Ohya, V.V. Kudryavtsev, S.I. Semenova, Polyimide Membranes: Applications, Fabrications, and Properties, Gordon and Breach, Tokyo, 1996.

[10] Y.N. Sazanov, Applied significance of polyimides, *Russ. J. Appl. Chem.,* 74 (2001) 1253.

[11] T. Takekoshi, Polyimides - Fundamentals and Applications, Ed. M. K. Ghosh and K. L. Mittal, Marcel Dekker, New York, 1996.

[12] S.I. Semenova, H. Ohya, T. Higashijima and Y. Negshi, Dependence of permeability through polyimide membranes on state of gas, vapor, liquid and supercritical fluid at high temperature, *J. Membr. Sci.* 67 (1992) 29.

[13] H. Yanagishita, D. Kitamoto, K. Haraya, T. Nakane, T. Okadab, H. Matsuda, Y. Idemoto, N. Koura, Separation performance of polyimide composite membrane prepared by dip coating process, *J. Membr. Sci.* 188 (2001) 165.

[14] H. Yanagishita, J. Arai, T. Sandoh, H. Negishi, D. Kitamoto, T. Ikegami, K. Haraya, Y. Idemoto, N. Koura, Preparation of polyimide composite membranes grafted by electron beam irradiation, *J. Membr. Sci.* 232 (2004) 93.

[15] S. Niyogi, B. Adhikari, Preparation and characterization of a polyimide membrane, *Eur. Polym. J.* 38 (2002) 1237.

[16] A. Walch, H. Lukas, A. Klimmek, W. Pusch, Structure and hyperfiltration properties of polyimide membranes, *J. Polym. Sci. Polym. Letters Ed.* 12 (1974) 697.

[17] H.J. Lee, J. Won, H. Lee, H. Lee, and Y.S. Kang, Solution properties of poly(amic acid)-NMP containing LiCl and their effects on membrane morphologies, *J. Membr. Sci.* 196 (2002) 267.

[18] J.A. Kreuz, Hydrolyses of polyamic acid solutions, *J. Polym. Sci. Polym. Chem.* 28 (1990) 3787.

[19] A. Polotskya, V. Cherkasovaa, I. Potokina, G. Polotskayab and T. Meleshkob, Chemically and thermally resistant polyimide ultrafiltration membranes prepared from polyamic acid, *Desalination* 200 (2006) 341.

[20] H.J. Lee, J. Won, H.C. Park, H. Lee, and Y.S. Kang, Effect of poly(amic acid) imidization on solution characteristics and membrane morphology, *J. Membr. Sci.* 178 (2000) 35.

[21] Y. Ding, B. Bikson and J.K. Nelson, Polyimide membranes derived from poly(amic acid) salt precursor polymers. 1. Synthesis and characterization, *Macromolecules,* 35 (2002) 905.

[22] X. Yu, B. P. Grady, R. S. Reiner and S. L. Cooper, Properties of polyamic acid ionomers, *J. Appl. Polym. Sci.* 47(1993) 1673.

[23] B.A. Zhubanov, I.A. Arkhipova and I.D. Shalabaeva, Interaction of carboxyl-containing polyimides and polyamides with metals, *Acta Polymerica* 39 (1988) 443.

[24] A. Lui, F.D.F. Talbot, A. Fouda, T. Matsuura and S. Sourirajan, Studies on the solvent exchange technique for making dry cellulose acetate membranes for the separation of gaseous mixtures, *J. Appl. Polym. Sci.* 36 (1988) 1809.

[25] C. Ba, J. Langer, J. Economy, Chemical modification of P84 copolyimide membranes by polyethylenimine for nanofiltration, *J. Membr. Sci.* 327 (2009) 49.

[26] S.K. Madan, Amides as ligands. VII. Complexes of N-methyl-y-butyrolactam with nontransition metals, *Inorganic Chemistry*, 6 (1967) 421.

[27] K. Koh, A.G. Wong-Foy, A.J. Matzger, A crystalline mesoporous coordination copolymer with high microporosity, *Angew. Chem. Int. Ed.* 46 (2007) 1.

[28] A.J. Reuvers, J.W.A. van den Berg, C.A. Smolders, Formation of membranes by means of immersion precipitation. Part IA. Model to describe mass transfer during immersion precipitation, *J. Membr. Sci.* 34 (1987) 45.

[29] W. Albrecht, Th. Weigel, M. Schossig-Tiedemann, K. Kneifel, K.-V. Peinemann, D. Paul, Formation of hollow fiber membranes from poly(ether imide) at wet phase inversion using binary mixtures of solvents for the preparation of the dope, *J. Membr. Sci.* 192 (2001) 217.

[30] F.G. Paulsen, S.S. Shojaie, W.B. Krantz, Effect of evaporation step on macrovoid formation in wet-cast polymeric membranes, *J. Membr. Sci.* 91 (1994) 265.

[31] M.A. Frommer, R.M. Messalem, Mechanism of membrane formation. VI. Convective flows and large void formation during membrane precipitation, *Ind. Eng. Chem. Prod. Res. Dev.* 12 (1973) 328.

[32] J.-S. Park, S.-K. Kim, K.-H. Lee, Effect of ZnCl2 on formation of asymmetric PEI membrane by phase inversion process, *J. Ind. Eng. Chem.* 6 (2000) 93.

[33] S.R. Kim, K.H. Lee, M.S. Jhon, The effect of ZnC12 on the formation of polysulfone membrane, *J. Membr. Sci.* 119 (1996) 59.

[34] K.H. Yu, Y.H. Yoo, J.M. Rhee, M.-H. Lee, S.-C. Yu, Synthesis of poly[(amic acid)-co-(amic ester)] precursors and studies of their imidization using FT-IR and FT-Raman spectroscopy, *Mat. Res. Innovat.* 7 (2003) 51.

[35] J. Yang, M.-H. Lee, A water-soluble polyimide precursor: synthesis and characterization of poly(amic acid) salt, *Macromol. Res.* 12 (2004) 263.

[36] Y. J. Kimt, J.S. Kim, K.-Y. Choi, Studies of the formation of polyisoimides and their imidization in solution state, *J. Ind. Eng. Chem.* 7 (2001) 400.

[37] S.-Y. Kwak, S.G. Jung, Y.S. Yoon, D.W. Ihm, Details of surface features in aromatic polyamide reverse osmosis membranes characterized by scanning electron and atomic force microscopy, *J. Polym. Sci. part B: Polym. Phys.* 37 (1999) 1429.

[38] I.J. Roh, A.R. Greenberg, V.P. Khare, Synthesis and characterization of interfacially polymerized polyamide thin films, *Desalination* 191 (2006) 279.

[39] A.L. Ahmad, B.S. Ooi, Properties - performance of thin film composites membrane: study on trimesoyl chloride content and polymerization time, *J. Membr. Sci.* 255 (2005) 67.

[40] A.P. Rao, S.V. Joshi, J.J Trivedi, C.V. Devmurari, V.J. Shah, Structure – performance correlation of polyamide thin film composite membranes: effect of coating conditions on film formation. *J. Membr. Sci.* 211 (2003) 13.

[41] A.P. Rao, N.V. Desai, R. Rangarajan, Interfacially synthesized thin film composite RO membranes for seawater desalination, *J. Membr. Sci.* 124 (1997) 263.

AUTHOR'S BIOGRAPHY

Chaoyi Ba was born in Puyang City, Henan Province, P. R. China in 1977. In 1995, he was enrolled in the Chemistry department at Peking University. In 1999, he graduated with a Bachelor of Science degree in Chemistry. In the same year, Chaoyi was exempted from the graduate entrance examination and entered the Institute of Chemistry in the Chinese Academy of Sciences. In 2002, he got his Masters degree in Polymeric Chemistry and Physics. After that, he worked as a research associate for over one year in Shanghai Institute of Organic Chemistry in the Chinese Academy of Sciences. In August 2004, he was enrolled in the Materials Science and Engineering department at the University of Illinois at Urbana-Champaign and joined the research group of Professor James Economy. His doctoral dissertation is entitled "Design of Advanced Reverse Osmosis and Nanofiltration Membranes for Water Purification". He has authored or co-authored 9 research publications.